ISSN 1949-8470 (online)

World Journal of Radiology

World J Radiol 2010 April 28; 2(4): 113-150

A peer-reviewed, online, open-access journal of Radiology

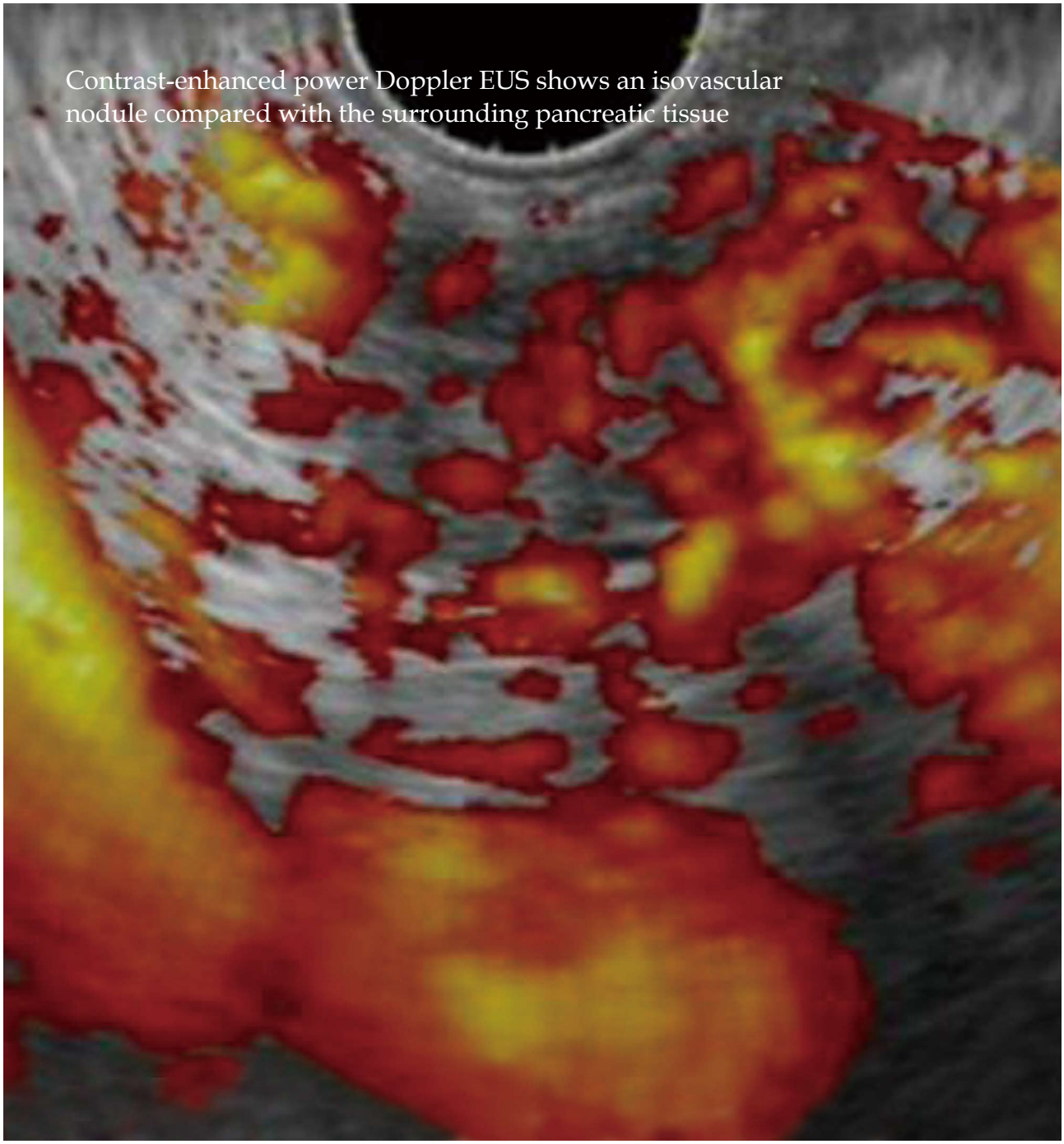

Contrast-enhanced power Doppler EUS shows an isovascular nodule compared with the surrounding pancreatic tissue

WJR World Journal of Radiology

A peer-reviewed, online, open-access journal of Radiology

Editorial Board

2009-2013

The *World Journal of Radiology* Editorial Board consists of 307 members, representing a team of worldwide experts in radiology. They are from 39 countries, including Australia (3), Austria (4), Belgium (4), Brazil (2), Canada (9), Chile (1), China (23), Denmark (1), Egypt (4), Estonia (1), Finland (1), France (6), Germany (17), Greece (8), Hungary (1), India (9), Iran (5), Ireland (1), Israel (4), Italy (28), Japan (14), Lebanon (1), Libya (1), Malaysia (2), Mexico (1), Netherlands (4), New Zealand (1), Norway (1), Saudi Arabia (3), Serbia (1), Singapore (2), Slovakia (1), South Korea (16), Spain (8), Switzerland (5), Thailand (1), Turkey (20), United Kingdom (15), and United States (76).

Nathalie Lassau, *Villejuif*
Youlia M Kirova, *Paris*
Géraldine Le Duc, *Grenoble Cedex*
Laurent Pierot, *Reims*
Frank Pilleul, *Lyon*
Pascal Pommier, *Lyon*

Germany

Ambros J Beer, *München*
Thomas Deserno, *Aachen*
Frederik L Giesel, *Heidelberg*
Ulf Jensen, *Kiel*
Markus Sebastian Juchems, *Ulm*
Kai U Juergens, *Bremen*
Melanie Kettering, *Jena*
Jennifer Linn, *Munich*
Christian Lohrmann, *Freiburg*
David Maintz, *Münster*
Henrik J Michaely, *Mannheim*
Oliver Micke, *Bielefeld*
Thoralf Niendorf, *Berlin-Buch*
Silvia Obenauer, *Duesseldorf*
Steffen Rickes, *Halberstadt*
Lars V Baron von Engelhardt, *Bochum*
Goetz H Welsch, *Erlangen*

Greece

Panagiotis Antoniou, *Alexandroupolis*
George C Kagadis, *Rion*
Dimitris Karacostas, *Thessaloniki*
George Panayiotakis, *Patras*
Alexander D Rapidis, *Athens*
C Triantopoulou, *Athens*
Ioannis Tsalafoutas, *Athens*
Virginia Tsapaki, *Anixi*
Ioannis Valais, *Athens*

Hungary

Peter Laszlo Lakatos, *Budapest*

India

Anil Kumar Anand, *New Delhi*
Surendra Babu, *Tamilnadu*
Sandip Basu, *Bombay*
Kundan Singh Chufal, *New Delhi*
Shivanand Gamanagatti, *New Delhi*
Vimoj J Nair, *Haryana*
R Prabhakar, *New Delhi*
Sanjeeb Kumar Sahoo, *Orissa*

Iran

Vahid Reza Dabbagh Kakhki, *Mashhad*
Mehran Karimi, *Shiraz*
Farideh Nejat, *Tehran*
Alireza Shirazi, *Tehran*
Hadi Rokni Yazdi, *Tehran*

Ireland

Joseph Simon Butler, *Dublin*

Israel

Amit Gefen, *Tel Aviv*
Eyal Sheiner, *Be'er-Sheva*
Jacob Sosna, *Jerusalem*
Simcha Yagel, *Jerusalem*

Italy

Mohssen Ansarin, *Milan*
Stefano Arcangeli, *Rome*
Tommaso Bartalena, *Imola*
Filippo Cademartiri, *Parma*
Sergio Casciaro, *Lecce*
Laura Crocetti, *Pisa*
Alberto Cuocolo, *Napoli*
Mirko D'Onofrio, *Verona*
Massimo Filippi, *Milan*
Claudio Fiorino, *Milano*
Alessandro Franchello, *Turin*
Roberto Grassi, *Naples*
Stefano Guerriero, *Cagliari*
Francesco Lassandro, *Napoli*
Nicola Limbucci, *L'Aquila*
Raffaele Lodi, *Bologna*
Francesca Maccioni, *Rome*
Laura Martincich, *Candiolo*
Mario Mascalchi, *Florence*
Roberto Miraglia, *Palermo*
Eugenio Picano, *Pisa*
Antonio Pinto, *Naples*
Stefania Romano, *Naples*
Luca Saba, *Cagliari*
Sergio Sartori, *Ferrara*
Mariano Scaglione, *Castel Volturno*
Lidia Strigari, *Rome*
Vincenzo Valentini, *Rome*

Japan

Shigeru Ehara, *Morioka*
Nobuyuki Hamada, *Chiba*
Takao Hiraki, *Okayama*
Akio Hiwatashi, *Fukuoka*
Masahiro Jinzaki, *Tokyo*
Hiroshi Matsuda, *Saitama*
Yasunori Minami, *Osaka*
Jun-Ichi Nishizawa, *Tokyo*
Tetsu Niwa, *Yokohama*
Kazushi Numata, *Kanagawa*
Kazuhiko Ogawa, *Okinawa*
Hitoshi Shibuya, *Tokyo*
Akira Uchino, *Saitama*
Haiquan Yang, *Kanagawa*

Lebanon

Aghiad Al-Kutoubi, *Beirut*

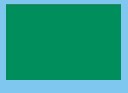

Libya

Anuj Mishra, *Tripoli*

Malaysia

R Logeswaran, *Cyberjaya*
Kwan-Hoong Ng, *Kuala Lumpur*

Mexico

Heriberto Medina-Franco, *Mexico City*

Netherlands

Jurgen J Fütterer, *Nijmegen*
Raffaella Rossin, *Eindhoven*
Paul E Sijens, *Groningen*
Willem Jan van Rooij, *Tilburg*

New Zealand

W Howell Round, *Hamilton*

Norway

Arne Sigmund Borthne, *Lørenskog*

Saudi Arabia

Mohammed Al-Omran, *Riyadh*
Ragab Hani Donkol, *Abha*
Volker Rudat, *Al Khobar*

Serbia

Djordjije Saranovic, *Belgrade*

Singapore

Uei Pua, *Singapore*
Lim CC Tchoyoson, *Singapore*

Slovakia

František Dubecký, *Bratislava*

South Korea

Bo-Young Choe, *Seoul*
Joon Koo Han, *Seoul*
Seung Jae Huh, *Seoul*
Chan Kyo Kim, *Seoul*
Myeong-Jin Kim, *Seoul*
Seung Hyup Kim, *Seoul*
Kyoung Ho Lee, *Gyeonggi-do*
Won-Jin Moon, *Seoul*
Wazir Muhammad, *Daegu*
Jai Soung Park, *Bucheon*
Noh Hyuck Park, *Kyunggi*
Sang-Hyun Park, *Daejeon*
Joon Beom Seo, *Seoul*
Ji-Hoon Shin, *Seoul*
Jin-Suck Suh, *Seoul*
Hong-Gyun Wu, *Seoul*

Spain

Eduardo J Aguilar, *Valencia*

Miguel Alcaraz, *Murcia*
Juan Luis Alcazar, *Pamplona*
Gorka Bastarrika, *Pamplona*
Rafael Martínez-Monge, *Pamplona*
Alberto Muñoz, *Madrid*
Joan C Vilanova, *Girona*

Switzerland

Nicolau Beckmann, *Basel*
Silke Grabherr, *Lausanne*
Karl-Olof Lövblad, *Geneva*
Tilo Niemann, *Basel*
Martin A Walter, *Basel*

Thailand

Sudsriluk Sampatchalit, *Bangkok*

Turkey

Olus Api, *Istanbul*
Kubilay Aydin, *İstanbul*
Işıl Bilgen, *Izmir*
Zulkif Bozgeyik, *Elazig*
Barbaros E Çil, *Ankara*
Gulgun Engin, *Istanbul*
M Fatih Evcimik, *Malatya*
Ahmet Kaan Gündüz, *Ankara*
Tayfun Hakan, *Istanbul*
Adnan Kabaalioglu, *Antalya*
Fehmi Kaçmaz, *Ankara*
Musturay Karcaaltincaba, *Ankara*
Osman Kizilkilic, *Istanbul*
Zafer Koc, *Adana*
Cem Onal, *Adana*
Yahya Paksoy, *Konya*
Bunyamin Sahin, *Samsun*
Ercument Unlu, *Edirne*
Ahmet Tuncay Turgut, *Ankara*
Ender Uysal, *Istanbul*

United Kingdom

K Faulkner, *Wallsend*
Peter Gaines, *Sheffield*
Balaji Ganeshan, *Brighton*
Nagy Habib, *London*
Alan Jackson, *Manchester*
Pradesh Kumar, *Portsmouth*
Tarik F Massoud, *Cambridge*
Igor Meglinski, *Bedfordshire*
Ian Negus, *Bristol*
Georgios A Plataniotis, *Aberdeen*
N J Raine-Fenning, *Nottingham*
Manuchehr Soleimani, *Bath*
MY Tseng, *Nottingham*
Edwin JR van Beek, *Edinburgh*
Feng Wu, *Oxford*

United States

Athanassios Argiris, *Pittsburgh*
Stephen R Baker, *Newark*
Lia Bartella, *New York*
Charles Bellows, *New Orleans*
Walter L Biffl, *Denver*
Homer S Black, *Houston*
Wessam Bou-Assaly, *Ann Arbor*
Owen Carmichael, *Davis*
Shelton D Caruthers, *St Louis*
Yuhchyau Chen, *Rochester*
Melvin E Clouse, *Boston*
Ezra Eddy Wyssam Cohen, *Chicago*
Aaron Cohen-Gadol, *Indianapolis*
Patrick M Colletti, *Los Angeles*
Kassa Darge, *Philadelphia*
Abhijit P Datir, *Miami*
Delia C DeBuc, *Miami*
Russell L Deter, *Houston*
Adam P Dicker, *Phil*
Khaled M Elsayes, *Ann Arbor*
Steven Feigenberg, *Baltimore*
Christopher G Filippi, *Burlington*
Victor Frenkel, *Bethesda*
Thomas J George Jr, *Gainesville*
Patrick K Ha, *Baltimore*
Robert I Haddad, *Boston*
Walter A Hall, *Syracuse*
Mary S Hammes, *Chicago*
John Hart Jr, *Dallas*
Randall T Higashida, *San Francisco*
Juebin Huang, *Jackson*
Andrei Iagaru, *Stanford*
Craig Johnson, *Milwaukee*
Ella F Jones, *San Francisco*
Csaba Juhasz, *Detroit*
Mannudeep K Kalra, *Boston*
Riyad Karmy-Jones, *Vancouver*
Daniel J Kelley, *Madison*
Amir Khan, *Longview*
Vikas Kundra, *Houston*
Kennith F Layton, *Dallas*
Rui Liao, *Princeton*
CM Charlie Ma, *Philadelphia*
Nina A Mayr, *Columbus*
Thomas J Meade, *Evanston*
Steven R Messé, *Philadelphia*
Feroze B Mohamed, *Philadelphia*
Koenraad J Mortele, *Boston*
Mohan Natarajan, *San Antonio*
John L Nosher, *New Brunswick*
Chong-Xian Pan, *Sacramento*
Dipanjan Pan, *St Louis*
Martin R Prince, *New York*
Reza Rahbar, *Boston*
Carlos S Restrepo, *San Antonio*
Veronica Rooks, *Honolulu*
Maythem Saeed, *San Francisco*
Edgar A Samaniego, *Palo Alto*
Jason P Sheehan, *Charlottesville*
William P Sheehan, *Willmar*
Charles Jeffrey Smith, *Columbia*
Dan Stoianovici, *Baltimore*
Dian Wang, *Milwaukee*
Jian Z Wang, *Columbus*
Liang Wang, *New York*
Shougang Wang, *Santa Clara*
Wenbao Wang, *New York*
Aaron H Wolfson, *Miami*
Ying Xiao, *Philadelphia*
Juan Xu, *Pittsburgh*
Benjamin M Yeh, *San Francisco*
Terry T Yoshizumi, *Durham*
Jinxing Yu, *Richmond*
Jianhui Zhong, *Rochester*

WJR World Journal of Radiology

Contents

Monthly Volume 2 Number 4 April 28, 2010

World Journal of Radiology
Volume 2 Number 4 April 28, 2010

Contents

NAME OF JOURNAL
World Journal of Radiology

LAUNCH DATE
December 31, 2009

SPONSOR
Beijing Baishideng BioMed Scientific Co., Ltd.,
Room 903, Building D, Ocean International Center,
No. 62 Dongsihuan Zhonglu, Chaoyang District,
Beijing 100025, China
Telephone: 0086-10-8538-1892
Fax: 0086-10-8538-1893
E-mail: baishideng@wjgnet.com
http://www.wjgnet.com

EDITING
Editorial Board of *World Journal of Radiology*,
Room 903, Building D, Ocean International Center,
No. 62 Dongsihuan Zhonglu, Chaoyang District,
Beijing 100025, China
Telephone: 0086-10-5908-0036
Fax: 0086-10-8538-1893
E-mail: wjr@wjgnet.com
http://www.wjgnet.com

PUBLISHING
Beijing Baishideng BioMed Scientific Co., Ltd.,
Room 903, Building D, Ocean International Center,
No. 62 Dongsihuan Zhonglu, Chaoyang District,
Beijing 100025, China
Telephone: 0086-10-8538-1892
Fax: 0086-10-8538-1893
E-mail: baishideng@wjgnet.com
http://www.wjgnet.com

SUBSCRIPTION
Beijing Baishideng BioMed Scientific Co., Ltd.,
Room 903, Building D, Ocean International Center,
No. 62 Dongsihuan Zhonglu, Chaoyang District,
Beijing 100025, China
Telephone: 0086-10-8538-1892
Fax: 0086-10-8538-1893
E-mail: baishideng@wjgnet.com
http://www.wjgnet.com

ONLINE SUBSCRIPTION
One-Year Price 216.00 USD

PUBLICATION DATE
April 28, 2010

CSSN
ISSN 1949-8470 (online)

EDITORIAL OFFICE
Na Ma, Director
World Journal of Radiology
Room 903, Building D, Ocean International Center,
No. 62 Dongsihuan Zhonglu, Chaoyang District,
Beijing 100025, China
Telephone: 0086-10-5908-0036
Fax: 0086-10-8538-1893
E-mail: wjr@wjgnet.com
http://www.wjgnet.com

INSTRUCTIONS TO AUTHORS
Full instructions are available online at http://www.wjgnet.com/1949-8470/g_info_20100316162358.htm. If you do not have web access please contact the editorial office.

ONLINE SUBMISSION
http://www.wjgnet.com/1949-8470office

World Journal of Radiology

Online Submissions: http://www.wjgnet.com/1949-8470office
wjr@wjgnet.com
doi:10.4329/wjr.v2.i4.113

World J Radiol 2010 April 28; 2(4): 113-121
ISSN 1949-8470 (online)

EDITORIAL

Magnetic resonance enterography in Crohn's disease: Standard and advanced techniques

Arda Kayhan, Jacob Oommen, Farid Dahi, Aytekin Oto

Arda Kayhan, Jacob Oommen, Farid Dahi, Aytekin Oto, Department of Radiology, University of Chicago, Chicago, IL 60637, United States
Author contributions: Kayhan A wrote the article; Oommen J and Oto A collected the patients in clinics (data collection); Oommen J organized the figures; Dahi F searched and organized the references; Oto A revised the article.
Correspondence to: Arda Kayhan, MD, Department of Radiology, University of Chicago, 5841 S. Maryland Ave, Chicago, IL 60637, United States. arda_kayhan@yahoo.com
Telephone: +1-773-7028553 Fax: +1-773-7021161
Received: March 4, 2010 Revised: March 30, 2010
Accepted: April 12, 2010
Published online: April 28, 2010

Abstract

Crohn's disease (CD) is a chronic autoimmune disorder that affects mainly young people. The clinical management is based on the Crohn's Disease Activity Index and especially on biologic parameters with or without additional endoscopic and imaging procedures, such as barium and computed tomography examinations. Recently, magnetic resonance (MR) imaging has been a promising diagnostic radiologic technique with lack of ionizing radiation, enabling superior tissue contrast resolution due to new pulse-sequence developments. Therefore, MR enterography has the potential to become the modality of choice for imaging the small bowel in CD patients.

Key words: Crohn's disease; Magnetic resonance enterography; Advantages; Pulse sequences; Advanced techniques

Peer reviewers: Joon Koo Han, MD, PhD, Professor, Department of Radiology, Seoul National University College of Medicine, 103, Daehangno, Jongno-gu, Seoul 110-744, South Korea; Arne S Borthne, MD, PhD, Associate Professor, Diagnostic Imaging Center, Akershus University Hospital, Sykehusveien 27, Nordbyhagen, NO-1478 Lørenskog, Norway

Kayhan A, Oommen J, Dahi F, Oto A. Magnetic resonance enterography in Crohn's disease: Standard and advanced techniques. *World J Radiol* 2010; 2(4): 113-121 Available from: URL: http://www.wjgnet.com/1949-8470/full/v2/i4/113.htm
DOI: http://dx.doi.org/10.4329/wjr.v2.i4.113

INTRODUCTION

The small bowel (SB) has been a challenging organ for clinical and radiological evaluation. Crohn's disease (CD) is the most common SB disease. Detection of disease and its extent are the two clinically important questions. Moreover, there is increasing interest in determining the degree of inflammatory activity of the disease. For symptomatic patients, it is also important to determine whether the symptoms are functional or due to active inflammatory activity *vs* fibrotic stenosis. In recent years, magnetic resonance imaging (MRI) has emerged as a promising technique in patients with CD. In this article, we are going to review the role of MRI in the diagnosis of CD.

CROHN'S DISEASE

CD is a chronic, transmural inflammatory disorder of the entire gastrointestinal tract. It is the most common SB disease in United States and Europe (3.1 to 14.6/100 000 in North America and 0.7 to 9.8/100 000 in Europe)[1]. The etiology of CD is unknown. It has been proposed that the condition is immune-mediated, with an abnormal mucosal response to unknown luminal antigens[2]. It commonly involves the SB, in particular the terminal ileum. The initial lesion starts as a focal inflammatory infiltrate in mucosa and submucosa leading to hyperemia and edema. As the disease progresses, superficial ulcers develop. In severe cases, transmural inflammation and even serosal involvement is present. In long-standing cases, chronic

obstruction due to scarring, luminal narrowing, and stricture formation may arise. Extramural manifestations are fistulae, abscesses, adhesions, creeping fat, malabsorption and enlargement of lymph nodes.

DIAGNOSTIC MODALITIES

More than 70% of CD patients develop disease in the SB. Since endoscopic techniques are often limited to more proximal segments of the SB, either enteroclysis or SB follow-through (SBFT) has been the gold standard for the diagnosis of CD[3,4]. SB enteroclysis has been shown to be more reliable when compared to SBFT in demonstrating early mucosal changes[5,6]. It has been claimed that SBFT is inaccurate in detecting active CD of the SB[7-9]. Both methods give limited and indirect information about the bowel wall and extraluminal extension of disease and their diagnostic accuracy is dependent on examiner experience. Additionally, these techniques require an extensive bowel preparation, and their indication is limited in young patients due to the amount of ionizing radiation exposure. Newer techniques, such as video capsule endoscopy (VCE), push endoscopy and double-balloon endoscopy (DBE), have been developed to compensate for the above-mentioned disadvantages. VCE demonstrates the mucosal surface of the SB wall. However, tissue sampling and therapeutic interventions are not possible and it is contraindicated in patients with obstruction. In a recent study comparing VCE and magnetic resonance enterography (MRE), it has been claimed that VCE can depict and characterize subtle mucosal lesions missed at MRE, whereas MRE gives additional information about mural, perienteric and extraenteric involvement[10]. DBE provides visualization of the entire SB and endoscopic therapy and, moreover, it allows obtaining tissue sample for analysis[11]. Ileocolonoscopy has been a most valuable tool for diagnosis and follow-up of CD in the colon and terminal ileum, but inspection of the terminal ileum fails in up to 27.8% of examinations[12].

CROSS-SECTIONAL IMAGING MODALITIES

Transmural and extramural extent of disease cannot be visualized with SB barium examinations (enteroclysis or SBFT), VCE, DBE or ileocolonoscopy. Recent advances in computer technology have furthered the usefulness of cross-sectional imaging, leading to improved spatial and temporal resolution to obtain high-resolution imaging.

Ultrasonography, computed tomography (CT) and MRI are the three techniques often used in abdominal examination. While CT is the modality of choice in the USA, in Europe MRI and US are preferred[11]. US is mostly performed without using enteric contrast medium. However, there are some studies reporting a higher sensitivity following the enteric contrast medium administration[13,14]. Although US can be used to assess both small and large bowel, diseases of the duodenum and jejunum are often missed. Moreover, the rectum and distal sigmoid cannot be visualized accurately. As the spatial resolution is insufficient to detect superficial pathology, it is less suitable for early diagnosis. Doppler US is useful only to assess whether the disease is in active phase or remission, however, it cannot give information about the severity of active disease[15]. In a recent study, evaluating the role of US and MRI to assess extension and inflammatory activity of CD, Martínez *et al*[16] reported that both US and MRI are sensitive to localize the affected bowel segments and to detect transmural complications. They found a significant correlation between color Doppler flow and bowel wall enhancement on MRI.

CT is not as sensitive as barium studies in detecting mucosal lesions but it is valuable in demonstrating intramural and extraluminal findings. CT enterography (CTE) is a fast, noninvasive technique that uses thin sections and large volumes of enteric contrast material to better delineate the wall and lumen of the SB[17,18]. The use of neutral enteric contrast agents, such as water, combined with intravenous (IV) contrast material allows excellent visualization of hypervascular lesions and hyperenhancing segments[7,8,19]. However, due to repetitive use for follow-up in young CD patients, its role is limited by the amount of ionizing radiation. CTE is less suitable for detecting mild disease, as superficial lesions are not accurately visualized[9]. Extramural complications are well demonstrated on CTE[20] but exposure to ionizing radiation with repeated tests in a relatively young patient population is a matter of concern. MRI has been introduced as an alternative method to detect CD, and it can be performed as either MRE or enteroclysis[21-23]. MRE has been shown to be useful to detect active ileitis, to assess disease activity and to identify extraenteric complications[21,23,24]. In a recent series, which systematically reviewed the evidence on the accuracy of MRI for grading CD activity, MRI was found to correctly grade 91% of patients with frank disease, 62% of patients with mild disease and 62% of patients in remission. Thus, it was concluded that MRI correctly graded disease activity in a large proportion of patients with frank disease[25].

ADVANTAGES OF MRE

MRE is currently used as an alternative modality to CTE due to its potential advantages. Lack of ionizing radiation is an important feature of MRE. MRE has improved soft tissue contrast, which is important for detecting subtle pathologic areas. It is particularly helpful for detection, staging and follow-up of perianal fistulae. MRE also enables static and dynamic studies that provide real-time and functional imaging. By using multiphase imaging techniques, bowel peristalsis and distensibility can be evaluated. MRE helps to determine the cause of bowel narrowings, i.e. whether they are due to contractions or to fixed strictures. Due to the safety profile of gadolinium contrast agents, the technique may be preferred in patients who are allergic to iodine contrast medium.

FACTORS ASSOCIATED WITH EXPOSURE TO DIAGNOSTIC RADIATION

Mean cumulative exposure dose (CED) to significant levels of ionizing radiation is of particular concern in patients with CD, as the disease presents in adolescence and has a life-long duration. The United States National Research Council estimates that for every 1000 patients undergoing a 10 mSv CT examination of the abdomen, one patient will develop a radiation-induced cancer in their lifetime[26]. In a population-based cohort, CTE was shown to deliver approximately 1.5-2 times the effective dose of conventional abdominopelvic CT scanning. It was found that CD patients received a CED of 36.9 mSv over a follow-up of 10.9 years[27]. Desmond *et al*[28] measured a mean CED value of 36.1 mSv and the value exceeded 75 mSv in 15.5% of patients followed between 1992 and 2007. As there is an increased time-life risk of developing intestinal malignancies, especially SB lymphoma and liver and biliary tract tumors[29], imaging modalities which impart no radiation dose have a definite advantage in imaging CD patients.

WHAT CLINICIANS EXPECT FROM RADIOLOGISTS REGARDING CD

Diagnosis of CD still remains a clinical challenge. A combination of clinical information is required, with radiologic imaging playing a key role. The radiologic information is sought for two purposes. One is to noninvasively and accurately diagnose CD, so that gastroenterologists may avoid treating patients who do not have true CD with intensive medical therapies, which have a potential for morbidity. The other role of radiologic examinations is to evaluate the extent, activity and severity of disease, and to exclude penetrating disease. The extent of the disease influences the medical and surgical approach. The presence of perienteric inflammation, fistulae and partial SB obstruction may also alter the management decision. A standardized reporting system and radiologic activity index may be achieved by a detailed radiologic imaging, and this may help assessing the disease activity[30].

PATIENT PREPARATION PROTOCOLS

As a collapsed bowel loop may obscure lesions or mimic pathologic wall thickening, bowel distension is the single most important factor for any method of choice. For this purpose, a large amount of orally administered enteric contrast material is used in MRI examination, to achieve SB luminal distension. Oral contrast agents not only distend the lumen but also decrease the susceptibility to develop artifacts by displacing intraluminal air. Positive contrast agents increase intraluminal signal [hyperintense on both T1-weighted (T1W) and T2- weighted (T2W) images]. They consist of paramagnetic substances such as gadolinium chelates, ferrous and manganic ions and manganese ions[31-33]. They reduce T1 relaxation time, while T2 relaxation time is usually not affected. Due to water content of the solutions, they will also be seen as hyperintense on T2W images. Wall thickening is well delineated on T1W images but, due to the increased intensity of the bowel lumen, they may hinder evaluation of inflammatory enhancement or intraluminal lesions. Negative contrast agents reduce intraluminal signal (hypointense on both T1W and T2W images). They include superparamagnetic particles such as perfluorooctyl bromide, iron oxides and oral magnetic particles[31,34-36]. Barium sulfate can also be used as a negative contrast agent, when administered at high concentrations. These agents induce local dishomogeneity in the magnetic field affecting both T1 and T2 relaxation time. They are helpful in the detection of bowel wall thickening on T1W images and, due to their decreased signal intensity, bowel wall enhancement will be more remarkable on T1W images. These agents are preferred for the visualization of inflamed bowel wall and surrounding fat on T2W images. In fact, since the bowel lumen will be seen as hypointense, the hyperintense inflammation will be more conspicuous. Biphasic contrast agents demonstrate different signal intensities on different sequences[37,38]. Water, hyperosmolar (mannitol-based solutions) and iso-osmolar watery solutions and barium sulfate are seen as low intensity signal on T1W and high intensity signal on T2W images[31]. Following IV contrast administration, the low signal intensity on T1W images provide a better resolution between bowel lumen and hyperenhancing wall inflammation or masses. Water is readily available, better accepted by the patients and cheap, but it is rapidly absorbed from distal bowel. Therefore, adequate distension may not be obtained. Potential limitations of these agents are gas formation and osmotic effects. For this reason, nonosmotic agents such as methylcellulose, polyethylene glycol and locust bean gum have also been used[37,39,40]. Manganese and gadolinium chelates are also biphasic agents seen as low intensity signal on T2W and high intensity signal on T1W images when they are administered at high concentrations[31,33]. In a recent study, alternative oral contrast agents, such as rose hip syrup, black current extract, iron-deferoxamine and cocoa, were investigated as oral contrast agents for MRI. Cocoa, with its differing relaxation and signal enhancement, provided good contrast between lumen and water, and between fat and gadolinium enhancement, and it was found to be a promising oral contrast agent[41]. Currently, there is no universal consensus on an optimal oral contrast agent or ingestion protocol and none of them can be considered ideal. After the appropriate administration of oral contrast, the patient should be placed on the MRI table. The preferred scanning position is prone, in order to separate bowel loops and to enable maximal bowel coverage in coronal planes[42,43]. However, for comfort reasons, MRI is usually performed in the supine position. An antispasmodic agent is given immediately before the examination, either by intramuscular or IV route. Gadolinium is infused IV as soon as noncontrast enhanced sequences are completed. It has been shown that IV contrast contributes to the delineation of active inflammation in CD[44]. There have also been various series evaluating the role of rectal contrast administration in assessing the

active inflammation of the colon. It has been claimed that rectal contrast can improve reader agreement[45,46].

PULSE SEQUENCES

Although there is no consensus on a universal protocol, an appropriate SB examination should consist of fast and ultrafast T1W and T2W sequences in both axial and coronal planes. Contrast enhanced T1W sequences are obtained by using gradient echo technique with fat saturation. The most commonly used sequence in SB imaging is fast low-angle shot using both 2D and 3D acquisitions. These are routinely used to identify increased enhancement in inflamed bowel wall[47,48]. 3D imaging provides better spatial resolution and SNR than 2D imaging and the volumetric data can be reconstructed in any planes. But it is more susceptible to motion which may cause blurring in the abdominal wall. Fast T1W gradient echo sequences without fat supression or T1W fast spin echo sequences may also be applied before IV contrast administration. T2W sequences are generated by rapid acquisition and relaxation enhancement with ultrafast acquisition time. They are known as half-acquisition single-shot fast spin echo (SSFSE) or SSFSE sequences, depending on the manufacturers. They are heavily T2W sequences, complementary to gadolinium-enhanced gradient echo sequences, and produce high contrast between the lumen and the bowel wall. As these sequences are highly resistant to magnetic susceptibility or chemical shift artifacts, the wall thickness may be evaluated accurately. Moreover, the sinus tracts and fistulas are well visualized. These sequences are sensitive to intraluminal motion and there may be intraluminal low intensity signal artifacts. Visualization of the mesenteric structures is impaired on these sequences due to k-space filtering effects. In recent years, high resolution, ultra-fast sequences based on steady-state free precession have emerged as the predominant technique for imaging of SB. These sequences are called true fast imaging with steady state precession, balanced fast field echo or fast imaging employing steady-state acquisition (FIESTA) sequences, depending on the manufacturer. They are relatively insensitive to motion artifacts, provide uniform intraluminal signal and lead to a high contrast between the bowel wall, lumen and mesentery. Mesenteric vessels and lymph nodes are better visualized on these sequences than on the single-shot sequences. The disadvantage of the sequence is a black-boundary artifact at the interface of the bowel wall and mesenteric fat that may hinder small lesions[49]. Although it is claimed that this artifact is also a potential limitation for bowel wall thickness assessment, Fidler[50] reported that it did not represent a significant limitation in their routine practice. There is still not a consensus on the scan delay: it has been reported that, in normal volunteers, peak wall enhancement for MRI was at 60-70 s (portal venous phase)[51].

MRE *VS* MR ENTEROCLYSIS

MR enteroclysis is an emerging technique for SB imaging that combines the advantages of conventional enteroclysis with those of cross-sectional imaging. It enables visualization of luminal, mural and extramural abnormalities. It is performed with intubation of the duodenum or proximal SB by subsequently administering enteric contrast agents. It provides superior distension and improves depiction of mucosal abnormalities. However, as placement and positioning of an intestinal tube are still necessary for the examination, it is not well tolerated by the patient. MRE is performed by ingestion of a large volume of enteric contrast. It obviates the need for a nasoenteric intubation, so the technique is well tolerated by the patients. As yet, there is no consensus about the modality of choice in the radiologic community. In a recent prospective study performed with 40 CD patients, the two techniques were compared and luminal distension and visualization of superficial mucosal, mural and mesenteric abnormalities were evaluated. No statistically significant differences were found in assessing the diagnostic efficacy as to the visualization of mural stenoses and fistulae. The number of detected mesenteric findings was very high with both techniques[42]. The study concluded that MRE might have a role in patients who refuse or have failed intubation and also during follow-up.

MRE *VS* OTHER DIAGNOSTIC MODALITIES

Various studies have been performed to compare MRE with other techniques as a diagnostic modality in CD patients. Lee *et al*[52] compared the usefulness of CTE, MRE and SBFT in 30 patients to detect active terminal ileitis and extraenteric complications. Differences in areas under the ROC curves for three modalities were not significant. Sensitivity values for detection of extraenteric complications were significantly higher for CTE and MRE. In another recent series, MRE and CTE were compared in follow-up of CD patients, in which polyethylene glycol was used as oral contrast medium. MRE showed a good sensitivity in detection of CD activity and it was suggested as an accurate method in monitoring the activity of CD compared to CT[39]. Siddiki *et al*[53] compared, in a prospective study, MRE and CTE in 33 CD patients and found similar sensitivities for MRE and CTE (90.5% *vs* 95.2%, respectively). Horsthuis *et al*[54] performed a meta-analysis on the accuracy of US, MR, scintigraphy, CT and positron emission tomography (PET) in the diagnosis of inflammatory bowel disease. They found no significant differences in the diagnostic accuracy among the imaging techniques. Tillack *et al*[55] compared the diagnostic performance of MRE and wireless VCE in detecting and classifying SB CD proximal to the terminal ileum. As for the presence or absence of pathology, results of MRE and VCE were in total agreement for the evaluated segments (85%). In judging lesion severity, both yielded identical results. The researchers concluded that both modalities were complementary and MRE should be used in more severe cases of CD and in patients who might have involvement beyond the

mucosa of the SB. In a pilot study, performed to compare double-balloon enteroscopy and MR enteroclysis in diagnosing suspected CD, the presence of pathology and its localization, degree and extent of involvement were evaluated. Both techniques had the potential to become diagnostic standards that complement each other in patients with suspected complex SB CD[56].

SAMPLE PROTOCOL

At our institution, MRI examinations are performed with a 1.5-T GE Signa MR scanner (GE Healthcare, Milwaukee, WI). Patients fast for 6 h before the MRI examination. A total of 1350 mL of Volumen (E-Z-EM Inc.) is administered orally over the course of 45 min prior to scanning. Immediately prior to starting the examination, when the patient is being placed in the scanner, 1 mg of intramuscular glucagon (Glucagen; Bedford Laboratories, Bedford, Ohio) is administered. After acquiring a standard three-plane scout image, the following sequences are obtained through the abdomen and pelvis using a 4-channel phased array body coil: (1) Axial and coronal FIESTA with and without fat suppression (TR/TE 3.4/1.4, matrix 224 × 224, flip angle 45, slice thickness/gap: 7 mm/0 mm); (2) Axial and coronal T2W SSFSE with and without fat suppression (TR/TE infinite/90, matrix 256 × 256, slice thickness/gap: 6 mm/0 mm); (3) Pre- and post-contrast T1W LAVA with additional dynamic post-contrast images (TR/TE 3.5-3.9/1.6-1.9, matrix 192 × 256, flip angle 10, interpolated slice thickness 2.2 mm); and (4) Axial and/or coronal diffusion-weighted images (*b* values, 0 and 600 s/mm^2; TR, 8000 ms; TE, 75 ms; matrix, 128 × 128-224; slice thickness, 7 mm; gap, 0 mm). A number of signals are acquired. For each sequence, the upper abdomen and pelvis are scanned separately. Gadodiamide (Omniscan; Nycomed-Amersham, Princeton, NJ) is administered IV at a dose of 0.1 mmol/kg, followed by a 20-mL saline flush at the rate of 2.0 mL/s. For the dynamic-contrast enhanced MRI (DCE-MRI) examinations, T1W, three-dimensional, gradient-echo, and free-breathing coronal DCE-MR images covering the entire abdomen are acquired (repetition time, 3.5-3.9 ms; echo time, 1.6-1.9 ms; matrix size, 160 × 256; flip angle, 10°; interpolated slice thickness, 3 mm) with temporal resolution of 5 to 12 s for approximately 4 to 7 min. The dynamic scans are started immediately with the injection of contrast without delay. Post-contrast high resolution T1W images are obtained after completion of the DCE-MRI sequence acquisition. Acquisition time for each sequence ranges from 5 to 8 min. Field of view ranges between 32 and 40 cm and ASSET factor of 2 is used in all sequences. Total scan time is between 35-50 min.

MR FINDINGS IN CD

There have been various MR imaging findings proposed as imaging biomarkers of CD activity[48,57,58]. Bowel wall thickening is a significant but yet not entirely specific feature of CD. Mural thickness increases with acute inflammation, given the associated histologic findings of edema and inflammatory infiltrate. A wall thickness of greater than 3 mm in an appropriately distended segment should be considered abnormal (Figures 1 and 2). Increased enhancement of bowel wall is also an important finding of active inflammation, which is associated with mucosal hyperemia (Figure 2). The degree of bowel wall thickening and enhancement has also a high degree of correlation with the CD activity index and the histologic grading. Many investigators[59,60] have suggested that a greater degree of mural enhancement is seen when inflammatory activity increases but Punwani *et al*[61], in their recent series performed with 18 CD patients, failed to find this correlation in their study group. The enhancement pattern of the inflamed bowel has also been evaluated[24]. A layered pattern (mural stratification) of bowel enhancement has been reported to have good correlation with active inflammation[62,63]. Mural stratification is the abnormal separation of the contrast-enhancing outer gut margin (serosa/muscularis propria) from the contrast-enhancing inner gut margin (mucosa/muscularis mucosa). The layered appearance consists of an inner enhancing ring produced by the hyperemic mucosa and an outer ring by enhancing muscle and serosa with an intermediate low-density ring is produced by submucosal edema. A similar target sign may be seen due to a low intensity sig-

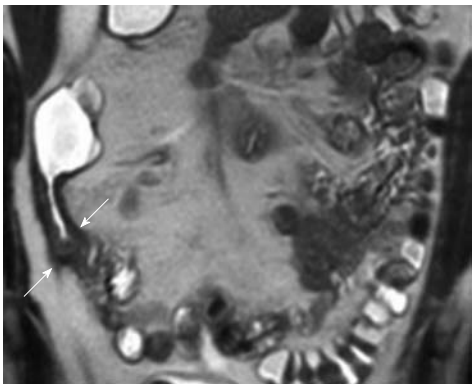

Figure 1 Coronal T2-weighted single-shot fast spin echo (SSFSE) image shows wall thickening and increased mural T2-signal intensity in the terminal ileum wall (arrows).

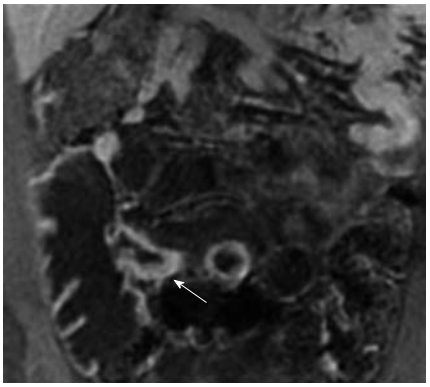

Figure 2 Coronal contrast-enhanced 3D GRE T1-weighted image shows wall thickening and increased enhancement of TI wall (arrow).

nal ring formed by hypertrophied fat and fibrosis of the submucosa. This sign is seen in chronic stage, and thus it is important to distinguish between spasms and strictures of active inflammation from fat-halo sign, as seen in the chronic stage. There is also a strong association between mural signal intensity on T2W images and inflammatory activity[59,61] (Figure 1). Low signal wall thickening on T2W images with lack of increased enhancement is indicative of chronic or inactive CD. Comb sign is another finding of CD which is produced by distended, enhancing, mesenteric vessels supplying the inflamed bowel segment. Fibro-fatty proliferation (fat-wrapping) of the mesentery around the inflamed bowel is a secondary finding, which leads to separation of bowel loops. Fat stranding adjacent to thickened bowel wall may also be present in CD patients. Introduction of ultrafast pulse sequences in MR examination protocols has significantly improved the identification of mesenteric lymph nodes in patients with CD. Some investigators state that enhancement of lymph nodes is indicative of CD activity[59]. Gourtsoyianni *et al*[64] studied mesenteric lymph nodes in patients with different subtypes of CD and they concluded that enhancement ratio of lymph nodes identified on MR may vary across different subtypes of CD. Such differences may be valuable in clinical practice. CD may lead to some complications such as fistulae, phlegmon, abscesses and bowel obstruction. CD may be subgrouped into 3 categories: fistula-forming/perforating, fibrostenotic and perianal. In fistula-forming/perforating disease, the large sinus tracks or fistulae may be visualized by enteric contrast agent and they are seen as linear hyperintense tracks. Fibrostenotic CD is seen as a fixed narrowing of the affected segment without any bowel wall thickening or inflammation on MRI. Chronic strictures are seen as hypointense on both T1 and T2W images and may show minimal enhancement. In perineal CD, MRI helps in diagnosis and demonstrating the anatomy of perineal fistulae.

ADVANCED MR TECHNIQUES IN CD

New MR applications have been applied to obtain additional information about the structural organization of tissues on bowel imaging. Diffusion-weighted imaging (DWI) and DCE-MRI techniques are still being studied for their potential to provide more quantitative and accurate assessment of fibrosis and active inflammation in the bowel wall.

DWI reflects the changes in the mobility of water molecules and yields qualitative and quantitative information reflecting tissue cellularity and cell membrane integrity. It complements morphological information obtained by conventional MRI. There are some studies on the role of DWI in detection of bowel inflammation in CD. The apparent diffusion coefficient (ADC) may facilitate quantitative analysis of disease activity. Visual assessment of DWI may provide higher accuracy, and the calculation of the ADC may facilitate the quantitative analysis of disease activity (Figure 3). Considering its relatively light patient burden, DWI may contribute to the follow-up of CD patients. Oto *et al*[65] reviewed DWI images of 11 CD patients and measured ADC values in a pilot study. They concluded that inflamed bowel segments showed higher signal and decreased ADC values compared to normal segments on DWI sequence. Kiryu *et al*[66] found an accuracy of 93.3% in the SB, based on visual evaluation and lower ADC values in the disease-active than that in disease-inactive area in CD patients.

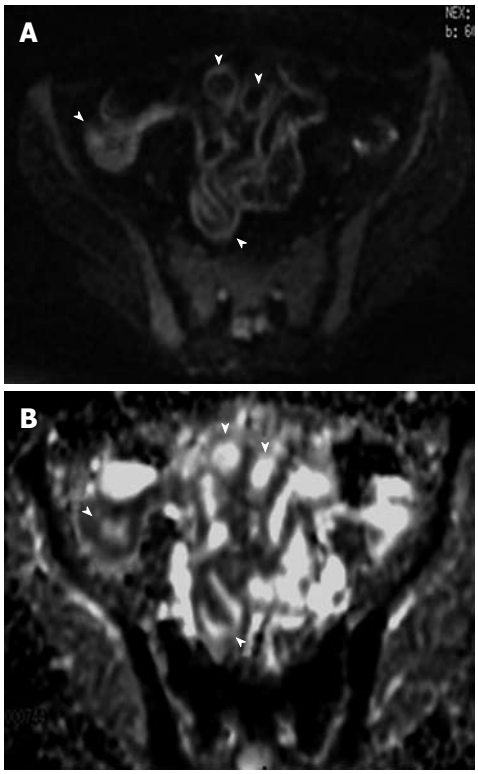

Figure 3 DWI and apparent diffusion coefficient (ADC) map of inflamed bowel wall. A: Thickened inflamed bowel wall with high signal on DWI image (arrowheads); B: On ADC map, inflamed bowel wall presents a dark signal (arrowheads).

DCE-MRI is a method useful to investigate microvascular structure and function by tracking the pharmacokinetics of injected low-molecular weight contrast agents. It is sensitive to alterations in vascular permeability, extracellular, extravascular and vascular volumes and blood flow[67]. The microvasculature neoangiogenesis has been introduced as a recent component of inflammatory bowel disease pathogenesis[68] and local vascularization is known to increase with the activity of the disease[23]. In clinical DCE-MRI, T1W image signals are repeatedly measured after the IV injection of a contrast agent, typically a low-molecular weight gadolinium chelate. When the tissue is highly permeable, the contrast agent will rapidly leak from the vasculature into the extravascular space and result in fast enhancement in the DCE-MRI images. Therefore; the evaluation of the increased enhancement in the pathologic bowel wall can be useful in determining the site and the degree of activity of CD (Figure 4). There are some initial qualitative and semi-quantitative studies on the ability of DC-MRI in assessing CD activity[60,63,23,69-71]. Horsthuis *et al*[72] assessed the

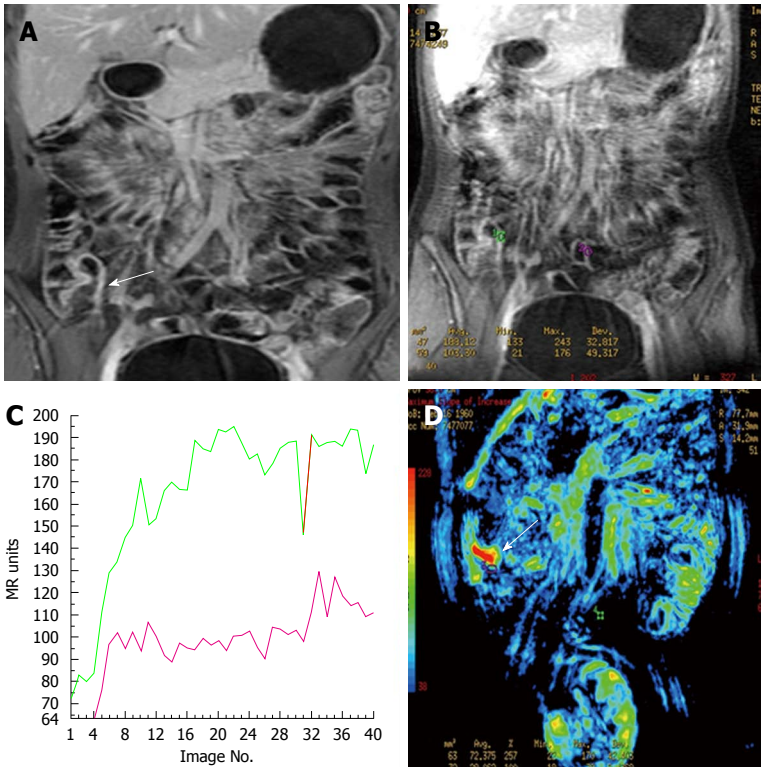

Figure 4 Dynamic-contrast enhanced magnetic resonance imaging (DCE-MRI) findings in inflamed terminal ileum and in a normal segment. A: Coronal contrast-enhanced 3D GRE T1-weighted image shows wall thickening and increased enhancement of TI wall (arrow); B: Dynamic contrast-enhanced image showing ROI placed on inflamed terminal ileum (green ROI) wall and normal ileal segment (purple ROI); C: The time-intensity curves plotted as a function of time for terminal ileum and normal ileal segment. Perfusion parameters of TI (green curve) is higher than the normal ileal segments (purple curve); D: Color map generated from dynamic contrast enhanced study shows increased perfusion in terminal ileum (arrow).

efficacy of DCE-MRI in perianal CD in 33 patients and found a significant correlation between time intensity curves and perianal activity disease index.

The assessment of stenoses in CD is an important clinical problem and observation of intestinal motility has been of prime importance for an accurate diagnosis for both the gastroenterologist and the radiologist. Yet, there is no established technique that can reliably distinguish inflammatory from scarred stenoses. The physician needs to decide whether anti-inflammatory or surgical therapy should be carried out. Cinematographic techniques have recently been evaluated for this purpose[73,74]. A continuous liquid infusion through a nasojejunal probe during data acquisition provides optimal distension of the intestinal loops and makes it possible to differentiate between functional and scarred stenoses, even on static images.

CONCLUSION

Cross-sectional imaging techniques have a crucial role in SB imaging. MRI has many advantages over CT, including lack of ionizing radiation, improved soft tissue contrast, ability to provide real-time and functional imaging and the safety profile of utilized contrast agents. Limitations of MRI are inferior temporal and spatial resolution, difficulty in access to the scanners and cost. With increasing awareness of radiation exposure caused by CT examinations, and improvements in MRI techniques, MRE will emerge as a diagnostic modality of choice in CD patients.

REFERENCES

1 **Loftus EV Jr**. Clinical epidemiology of inflammatory bowel disease: Incidence, prevalence, and environmental influences. *Gastroenterology* 2004; **126**: 1504-1517
2 **Przemioslo RT**, Ciclitira PJ. Pathogenesis of Crohn's disease. *QJM* 1995; **88**: 525-527
3 **Stange EF**, Travis SP, Vermeire S, Beglinger C, Kupcinkas L, Geboes K, Barakauskiene A, Villanacci V, Von Herbay A, Warren BF, Gasche C, Tilg H, Schreiber SW, Schölmerich J, Reinisch W. European evidence based consensus on the diagnosis and management of Crohn's disease: definitions and diagnosis. *Gut* 2006; **55** Suppl 1: i1-i15
4 **Maglinte DD**, Sandrasegaran K, Tann M. Advances in alimentary tract imaging. *World J Gastroenterol* 2006; **12**: 3139-3145
5 **Wills JS**, Lobis IF, Denstman FJ. Crohn disease: state of the art. *Radiology* 1997; **202**: 597-610
6 **Maglinte DD**, Kelvin FM, O'Connor K, Lappas JC, Chernish SM. Current status of small bowel radiography. *Abdom Imaging* 1996; **21**: 247-257
7 **Wold PB**, Fletcher JG, Johnson CD, Sandborn WJ. Assessment of small bowel Crohn disease: noninvasive peroral CT enterography compared with other imaging methods and endoscopy--feasibility study. *Radiology* 2003; **229**: 275-281
8 **Hara AK**, Leighton JA, Heigh RI, Sharma VK, Silva AC, De Petris G, Hentz JG, Fleischer DE. Crohn disease of the small bowel: preliminary comparison among CT enterography, capsule endoscopy, small-bowel follow-through, and ileoscopy. *Radiology* 2006; **238**: 128-134
9 **Triester SL**, Leighton JA, Leontiadis GI, Gurudu SR, Fleischer DE, Hara AK, Heigh RI, Shiff AD, Sharma VK. A meta-analysis of the yield of capsule endoscopy compared to other diagnostic modalities in patients with non-stricturing small bowel Crohn's disease. *Am J Gastroenterol* 2006; **101**: 954-964
10 **Crook DW**, Knuesel PR, Froehlich JM, Eigenmann F, Unterweger M, Beer HJ, Kubik-Huch RA. Comparison of magnetic resonance enterography and video capsule endoscopy in evaluating small bowel disease. *Eur J Gastroenterol Hepatol* 2009; **21**: 54-65
11 **Horsthuis K**, Stokkers PC, Stoker J. Detection of inflammatory bowel disease: diagnostic performance of cross-section-

al imaging modalities. *Abdom Imaging* 2008; **33**: 407-416
12 **Kundrotas LW**, Clement DJ, Kubik CM, Robinson AB, Wolfe PA. A prospective evaluation of successful terminal ileum intubation during routine colonoscopy. *Gastrointest Endosc* 1994; **40**: 544-546
13 **Pallotta N**, Tomei E, Viscido A, Calabrese E, Marcheggiano A, Caprilli R, Corazziari E. Small intestine contrast ultrasonography: an alternative to radiology in the assessment of small bowel disease. *Inflamm Bowel Dis* 2005; **11**: 146-153
14 **Parente F**, Greco S, Molteni M, Anderloni A, Sampietro GM, Danelli PG, Bianco R, Gallus S, Bianchi Porro G. Oral contrast enhanced bowel ultrasonography in the assessment of small intestine Crohn's disease. A prospective comparison with conventional ultrasound, x ray studies, and ileocolonoscopy. *Gut* 2004; **53**: 1652-1657
15 **Spalinger J**, Patriquin H, Miron MC, Marx G, Herzog D, Dubois J, Dubinsky M, Seidman EG. Doppler US in patients with crohn disease: vessel density in the diseased bowel reflects disease activity. *Radiology* 2000; **217**: 787-791
16 **Martínez MJ**, Ripollés T, Paredes JM, Blanc E, Martí-Bonmatí L. Assessment of the extension and the inflammatory activity in Crohn's disease: comparison of ultrasound and MRI. *Abdom Imaging* 2009; **34**: 141-148
17 **Furukawa A**, Saotome T, Yamasaki M, Maeda K, Nitta N, Takahashi M, Tsujikawa T, Fujiyama Y, Murata K, Sakamoto T. Cross-sectional imaging in Crohn disease. *Radiographics* 2004; **24**: 689-702
18 **Reittner P**, Goritschnig T, Petritsch W, Doerfler O, Preidler KW, Hinterleitner T, Szolar DH. Multiplanar spiral CT enterography in patients with Crohn's disease using a negative oral contrast material: initial results of a noninvasive imaging approach. *Eur Radiol* 2002; **12**: 2253-2257
19 **Paulsen SR**, Huprich JE, Fletcher JG, Booya F, Young BM, Fidler JL, Johnson CD, Barlow JM, Earnest F 4th. CT enterography as a diagnostic tool in evaluating small bowel disorders: review of clinical experience with over 700 cases. *Radiographics* 2006; **26**: 641-657; discussion 657-662
20 **Booya F**, Fletcher JG, Huprich JE, Barlow JM, Johnson CD, Fidler JL, Solem CA, Sandborn WJ, Loftus EV Jr, Harmsen WS. Active Crohn disease: CT findings and interobserver agreement for enteric phase CT enterography. *Radiology* 2006; **241**: 787-795
21 **Maccioni F**, Bruni A, Viscido A, Colaiacomo MC, Cocco A, Montesani C, Caprilli R, Marini M. MR imaging in patients with Crohn disease: value of T2- versus T1-weighted gadolinium-enhanced MR sequences with use of an oral superparamagnetic contrast agent. *Radiology* 2006; **238**: 517-530
22 **Bernstein CN**, Greenberg H, Boult I, Chubey S, Leblanc C, Ryner L. A prospective comparison study of MRI versus small bowel follow-through in recurrent Crohn's disease. *Am J Gastroenterol* 2005; **100**: 2493-2502
23 **Florie J**, Wasser MN, Arts-Cieslik K, Akkerman EM, Siersema PD, Stoker J. Dynamic contrast-enhanced MRI of the bowel wall for assessment of disease activity in Crohn's disease. *AJR Am J Roentgenol* 2006; **186**: 1384-1392
24 **Sempere GA**, Martinez Sanjuan V, Medina Chulia E, Benages A, Tome Toyosato A, Canelles P, Bulto A, Quiles F, Puchades I, Cuquerella J, Celma J, Orti E. MRI evaluation of inflammatory activity in Crohn's disease. *AJR Am J Roentgenol* 2005; **184**: 1829-1835
25 **Horsthuis K**, Bipat S, Stokkers PC, Stoker J. Magnetic resonance imaging for evaluation of disease activity in Crohn's disease: a systematic review. *Eur Radiol* 2009; **19**: 1450-1460
26 Health Risks from Exposure to Low Levels of Ionizing Radiation: BEIR VII Phase 2. Washington: National Academies Press, 2005
27 **Peloquin JM**, Pardi DS, Sandborn WJ, Fletcher JG, McCollough CH, Schueler BA, Kofler JA, Enders FT, Achenbach SJ, Loftus EV Jr. Diagnostic ionizing radiation exposure in a population-based cohort of patients with inflammatory bowel disease. *Am J Gastroenterol* 2008; **103**: 2015-2022
28 **Desmond AN**, O'Regan K, Curran C, McWilliams S, Fitzgerald T, Maher MM, Shanahan F. Crohn's disease: factors associated with exposure to high levels of diagnostic radiation. *Gut* 2008; **57**: 1524-1529
29 **Jess T**, Loftus EV Jr, Velayos FS, Harmsen WS, Zinsmeister AR, Smyrk TC, Schleck CD, Tremaine WJ, Melton LJ 3rd, Munkholm P, Sandborn WJ. Risk of intestinal cancer in inflammatory bowel disease: a population-based study from olmsted county, Minnesota. *Gastroenterology* 2006; **130**: 1039-1046
30 **Bruining DH**, Loftus EV Jr. Crohn's disease clinical issues and treatment: what the radiologist needs to know and what the gastroenterologist wants to know. *Abdom Imaging* 2009; **34**: 297-302
31 **Rieber A**, Aschoff A, Nüssle K, Wruk D, Tomczak R, Reinshagen M, Adler G, Brambs HJ. MRI in the diagnosis of small bowel disease: use of positive and negative oral contrast media in combination with enteroclysis. *Eur Radiol* 2000; **10**: 1377-1382
32 **Rieber A**, Nüssle K, Reinshagen M, Brambs HJ, Gabelmann A. MRI of the abdomen with positive oral contrast agents for the diagnosis of inflammatory small bowel disease. *Abdom Imaging* 2002; **27**: 394-399
33 **Vlahos L**, Gouliamos A, Athanasopoulou A, Kotoulas G, Claus W, Hatziioannou A, Kalovidouris A, Papavasiliou C. A comparative study between Gd-DTPA and oral magnetic particles (OMP) as gastrointestinal (GI) contrast agents for MRI of the abdomen. *Magn Reson Imaging* 1994; **12**: 719-726
34 **Boraschi P**, Braccini G, Gigoni R, Cartei F, Perri G. MR enteroclysis using iron oxide particles (ferristene) as an endoluminal contrast agent: an open phase III trial. *Magn Reson Imaging* 2004; **22**: 1085-1095
35 **Schreyer AG**, Gölder S, Scheibl K, Völk M, Lenhart M, Timmer A, Schölmerich J, Feuerbach S, Rogler G, Herfarth H, Seitz J. Dark lumen magnetic resonance enteroclysis in combination with MRI colonography for whole bowel assessment in patients with Crohn's disease: first clinical experience. *Inflamm Bowel Dis* 2005; **11**: 388-394
36 **Anderson CM**, Brown JJ, Balfe DM, Heiken JP, Borrello JA, Clouse RE, Pilgram TK. MR imaging of Crohn disease: use of perflubron as a gastrointestinal contrast agent. *J Magn Reson Imaging* 1994; **4**: 491-496
37 **Lauenstein TC**, Schneemann H, Vogt FM, Herborn CU, Ruhm SG, Debatin JF. Optimization of oral contrast agents for MR imaging of the small bowel. *Radiology* 2003; **228**: 279-283
38 **Ajaj W**, Goehde SC, Schneemann H, Ruehm SG, Debatin JF, Lauenstein TC. Dose optimization of mannitol solution for small bowel distension in MRI. *J Magn Reson Imaging* 2004; **20**: 648-653
39 **Ippolito D**, Invernizzi F, Galimberti S, Panelli MR, Sironi S. MR enterography with polyethylene glycol as oral contrast medium in the follow-up of patients with Crohn disease: comparison with CT enterography. *Abdom Imaging* 2009; Epub ahead of print
40 **McKenna DA**, Roche CJ, Murphy JM, McCarthy PA. Polyethylene glycol solution as an oral contrast agent for MRI of the small bowel in a patient population. *Clin Radiol* 2006; **61**: 966-970
41 **Babos M**, Schwarcz A, Randhawa MS, Marton B, Kardos L, Palkó A. In vitro evaluation of alternative oral contrast agents for MRI of the gastrointestinal tract. *Eur J Radiol* 2008; **65**: 133-139
42 **Masselli G**, Casciani E, Polettini E, Gualdi G. Comparison of MR enteroclysis with MR enterography and conventional enteroclysis in patients with Crohn's disease. *Eur Radiol* 2008; **18**: 438-447
43 **Cronin CG**, Lohan DG, Mhuircheartaigh JN, McKenna D, Alhajeri N, Roche C, Murphy JM. MRI small-bowel follow-through: prone versus supine patient positioning for best small-bowel distention and lesion detection. *AJR Am J Roentgenol* 2008; **191**: 502-506
44 **Ochsenkühn T**, Herrmann K, Schoenberg SO, Reiser MF, Göke B, Sackmann M. Crohn disease of the small bowel

proximal to the terminal ileum: detection by MR-enteroclysis. *Scand J Gastroenterol* 2004; **39**: 953-960
45 **Ajaj W**, Lauenstein TC, Langhorst J, Kuehle C, Goyen M, Zoepf T, Ruehm SG, Gerken G, Debatin JF, Goehde SC. Small bowel hydro-MR imaging for optimized ileocecal distension in Crohn's disease: should an additional rectal enema filling be performed? *J Magn Reson Imaging* 2005; **22**: 92-100
46 **Narin B**, Ajaj W, Göhde S, Langhorst J, Akgöz H, Gerken G, Rühm SG, Lauenstein TC. Combined small and large bowel MR imaging in patients with Crohn's disease: a feasibility study. *Eur Radiol* 2004; **14**: 1535-1542
47 **Horsthuis K**, Lavini C, Stoker J. MRI in Crohn's disease. *J Magn Reson Imaging* 2005; **22**: 1-12
48 **Gourtsoyiannis NC**, Papanikolaou N, Karantanas A. Magnetic resonance imaging evaluation of small intestinal Crohn's disease. *Best Pract Res Clin Gastroenterol* 2006; **20**: 137-156
49 **Hohl C**, Haage P, Krombach GA, Schmidt T, Ahaus M, Günther RW, Staatz G. [Diagnostic evaluation of chronic inflammatory intestinal diseases in children and adolescents: MRI with true-FISP as new gold standard?] *Rofo* 2005; **177**: 856-863
50 **Fidler J**. MR imaging of the small bowel. *Radiol Clin North Am* 2007; **45**: 317-331
51 **Lauenstein TC**, Ajaj W, Narin B, Göhde SC, Kröger K, Debatin JF, Rühm SG. MR imaging of apparent small-bowel perfusion for diagnosing mesenteric ischemia: feasibility study. *Radiology* 2005; **234**: 569-575
52 **Lee SS**, Kim AY, Yang SK, Chung JW, Kim SY, Park SH, Ha HK. Crohn disease of the small bowel: comparison of CT enterography, MR enterography, and small-bowel follow-through as diagnostic techniques. *Radiology* 2009; **251**: 751-761
53 **Siddiki HA**, Fidler JL, Fletcher JG, Burton SS, Huprich JE, Hough DM, Johnson CD, Bruining DH, Loftus EV Jr, Sandborn WJ, Pardi DS, Mandrekar JN. Prospective comparison of state-of-the-art MR enterography and CT enterography in small-bowel Crohn's disease. *AJR Am J Roentgenol* 2009; **193**: 113-121
54 **Horsthuis K**, Bipat S, Bennink RJ, Stoker J. Inflammatory bowel disease diagnosed with US, MR, scintigraphy, and CT: meta-analysis of prospective studies. *Radiology* 2008; **247**: 64-79
55 **Tillack C**, Seiderer J, Brand S, Göke B, Reiser MF, Schaefer C, Diepolder H, Ochsenkühn T, Herrmann KA. Correlation of magnetic resonance enteroclysis (MRE) and wireless capsule endoscopy (CE) in the diagnosis of small bowel lesions in Crohn's disease. *Inflamm Bowel Dis* 2008; **14**: 1219-1228
56 **Seiderer J**, Herrmann K, Diepolder H, Schoenberg SO, Wagner AC, Göke B, Ochsenkühn T, Schäfer C. Double-balloon enteroscopy versus magnetic resonance enteroclysis in diagnosing suspected small-bowel Crohn's disease: results of a pilot study. *Scand J Gastroenterol* 2007; **42**: 1376-1385
57 **Malagò R**, Manfredi R, Benini L, D'Alpaos G, Mucelli RP. Assessment of Crohn's disease activity in the small bowel with MR-enteroclysis: clinico-radiological correlations. *Abdom Imaging* 2008; **33**: 669-675
58 **Girometti R**, Zuiani C, Toso F, Brondani G, Sorrentino D, Avellini C, Bazzocchi M. MRI scoring system including dynamic motility evaluation in assessing the activity of Crohn's disease of the terminal ileum. *Acad Radiol* 2008; **15**: 153-164
59 **Gourtsoyiannis N**, Papanikolaou N, Grammatikakis J, Papamastorakis G, Prassopoulos P, Roussomoustakaki M. Assessment of Crohn's disease activity in the small bowel with MR and conventional enteroclysis: preliminary results. *Eur Radiol* 2004; **14**: 1017-1024
60 **Pupillo VA**, Di Cesare E, Frieri G, Limbucci N, Tanga M, Masciocchi C. Assessment of inflammatory activity in Crohn's disease by means of dynamic contrast-enhanced MRI. *Radiol Med* 2007; **112**: 798-809
61 **Punwani S**, Rodriguez-Justo M, Bainbridge A, Greenhalgh R, De Vita E, Bloom S, Cohen R, Windsor A, Obichere A, Hansmann A, Novelli M, Halligan S, Taylor SA. Mural inflammation in Crohn disease: location-matched histologic validation of MR imaging features. *Radiology* 2009; **252**: 712-720
62 **Masselli G**, Casciani E, Polettini E, Lanciotti S, Bertini L, Gualdi G. Assessment of Crohn's disease in the small bowel: Prospective comparison of magnetic resonance enteroclysis with conventional enteroclysis. *Eur Radiol* 2006; **16**: 2817-2827
63 **Del Vescovo R**, Sansoni I, Caviglia R, Ribolsi M, Perrone G, Leoncini E, Grasso RF, Cicala M, Zobel BB. Dynamic contrast enhanced magnetic resonance imaging of the terminal ileum: differentiation of activity of Crohn's disease. *Abdom Imaging* 2008; **33**: 417-424
64 **Gourtsoyianni S**, Papanikolaou N, Amanakis E, Bourikas L, Roussomoustakaki M, Grammatikakis J, Gourtsoyiannis N. Crohn's disease lymphadenopathy: MR imaging findings. *Eur J Radiol* 2009; **69**: 425-428
65 **Oto A**, Zhu F, Kulkarni K, Karczmar GS, Turner JR, Rubin D. Evaluation of diffusion-weighted MR imaging for detection of bowel inflammation in patients with Crohn's disease. *Acad Radiol* 2009; **16**: 597-603
66 **Kiryu S**, Dodanuki K, Takao H, Watanabe M, Inoue Y, Takazoe M, Sahara R, Unuma K, Ohtomo K. Free-breathing diffusion-weighted imaging for the assessment of inflammatory activity in Crohn's disease. *J Magn Reson Imaging* 2009; **29**: 880-886
67 **O'Connor JP**, Jackson A, Parker GJ, Jayson GC. DCE-MRI biomarkers in the clinical evaluation of antiangiogenic and vascular disrupting agents. *Br J Cancer* 2007; **96**: 189-195
68 **Danese S**, Sans M, de la Motte C, Graziani C, West G, Phillips MH, Pola R, Rutella S, Willis J, Gasbarrini A, Fiocchi C. Angiogenesis as a novel component of inflammatory bowel disease pathogenesis. *Gastroenterology* 2006; **130**: 2060-2073
69 **Oto A**, Fan X, Mustafi D, Jansen SA, Karczmar GS, Rubin DT, Kayhan A. Quantitative analysis of dynamic contrast enhanced MRI for assessment of bowel inflammation in Crohn's disease pilot study. *Acad Radiol* 2009; **16**: 1223-1230
70 **Taylor SA**, Punwani S, Rodriguez-Justo M, Bainbridge A, Greenhalgh R, De Vita E, Forbes A, Cohen R, Windsor A, Obichere A, Hansmann A, Rajan J, Novelli M, Halligan S. Mural Crohn disease: correlation of dynamic contrast-enhanced MR imaging findings with angiogenesis and inflammation at histologic examination--pilot study. *Radiology* 2009; **251**: 369-379
71 **Knuesel PR**, Kubik RA, Crook DW, Eigenmann F, Froehlich JM. Assessment of dynamic contrast enhancement of the small bowel in active Crohn's disease using 3D MR enterography. *Eur J Radiol* 2010; **73**: 607-613
72 **Horsthuis K**, Lavini C, Bipat S, Stokkers PC, Stoker J. Perianal Crohn disease: evaluation of dynamic contrast-enhanced MR imaging as an indicator of disease activity. *Radiology* 2009; **251**: 380-387
73 **Röttgen R**, Ocran K, Lochs H, Hamm B. Cinematographic techniques in the diagnostics of intestinal diseases using MRT enteroclysma. *Clin Imaging* 2009; **33**: 25-32
74 **Torkzad MR**, Vargas R, Tanaka C, Blomqvist L. Value of cine MRI for better visualization of the proximal small bowel in normal individuals. *Eur Radiol* 2007; **17**: 2964-2968

S- Editor Cheng JX **L- Editor** Negro F **E- Editor** Zheng XM

World Journal of Radiology

Online Submissions: http://www.wjgnet.com/1949-8470office
wjr@wjgnet.com
doi:10.4329/wjr.v2.i4.122

World J Radiol 2010 April 28; 2(4): 122-134
ISSN 1949-8470 (online)

Diagnosis of pancreatic tumors by endoscopic ultrasonography

Hiroki Sakamoto, Masayuki Kitano, Ken Kamata, Muhammad El-Masry, Masatoshi Kudo

Hiroki Sakamoto, Masayuki Kitano, Ken Kamata, Masatoshi Kudo, Division of Gastroenterology and Hepatology, Department of Internal Medicine, Kinki University School of Medicine, 377-2, Ohno-Higashi, Osaka-Sayama, 589-8511, Japan
Muhammad El-Masry, Hepatogastroenterology and Endoscopy Unit, Department of Internal Medicine, Assiut University Hospitals, Assiut 71515, Egypt
Author contributions: Sakamoto H and Kitano M both contributed equally to writing this manuscript; El-Masry M searched the literature; Kudo M revised the manuscript.
Supported by The Japan Society for Promotion of Science, Research and Development Committee Program of The Japan Society of Ultrasonics in Medicine; Japan Research Foundation for Clinical Pharmacology; Japanese Foundation for Research and Promotion of Endoscopy
Correspondence to: Masayuki Kitano, MD, PhD, Division of Gastroenterology and Hepatology, Department of Internal Medicine, Kinki University School of Medicine, 377-2, Ohno-Higashi, Osaka-Sayama, 589-8511, Japan. m-kitano@med.kindai.ac.jp
Telephone: +81-72-3660221 Fax: +81-72-3672880
Received: March 8, 2010 Revised: March 29, 2010
Accepted: April 12, 2010
Published online: April 28, 2010

Abstract

Pancreatic tumors are highly diverse, as they can be solid or cystic, and benign or malignant. Since their imaging features overlap considerably, it is often difficult to characterize these tumors. In addition, small pancreatic tumors, especially those less than 2 cm in diameter, are difficult to detect and diagnose. For characterizing pancreatic tumors and detecting small pancreatic tumors, endoscopic ultrasonography (EUS) is the most sensitive of the imaging procedures currently available. This technique also provides good results in terms of the preoperative staging of pancreatic tumors. EUS-guided fine needle aspiration (EUS-FNA) has also proved to be a safe and useful method for tissue sampling of pancreatic tumors. Despite these advantages, however, it is still difficult to differentiate between benign and malignant, solid or cystic pancreatic tumors, malignant neoplasms, and chronic pancreatitis using EUS, even when EUS-FNA is performed. Recently, contrast-enhanced EUS with Doppler mode (CE-EUS) employing ultrasound contrast agents, which indicate vascularization in pancreatic lesions, has been found to be useful in the differential diagnosis of pancreatic tumors, especially small pancreatic tumors. However, Doppler ultrasonography with contrast-enhancement has several limitations, including blooming artifacts, poor spatial resolution, and low sensitivity to slow flow. Consequently, an echoendoscope was developed recently that has a broad-band transducer and an imaging mode that was designed specifically for contrast-enhanced harmonic EUS (CEH-EUS) with a second-generation ultrasound contrast agent. The CEH-EUS technique is expected to improve the differential diagnosis of pancreatic disease in the future. This review describes the EUS appearances of common solid and cystic pancreatic masses, the diagnostic accuracy of EUS-FNA, and the relative efficacies and advantages of CE-EUS and CEH-EUS along with their relative advantages and their complementary roles in clinical practice.

Key words: Contrast-enhanced endoscopic ultrasonography; Endoscopic ultrasonography; EUS-guided fine needle aspiration; Pancreas; Sonazoid

Peer reviewers: Adnan Kabaalioglu, MD, Professor, Akdeniz University Hospital, 07059, Antalya, Turkey; Wellington P Martins, PhD, Departamento de Ginecologia e, Obstetrícia da Faculdade de Medicina de Ribeirão Preto da Universidade de São Paulo, Avenida dos Bandeirantes 3900, 8º andar, Ribeirão Preto, São Paulo 14049-900, Brazil; Kenneth Coenegrachts, MD, PhD, Department of Radiology, AZ St.-Jan AV, Ruddershove 10, B-8000 Bruges, Belgium; Ragab Hani Donkol, Professor, Radiology Department, Aseer Central Hospital, 34 Abha, Saudi Arabia

Sakamoto H, Kitano M, Kamata K, El-Masry M, Kudo M. Diagnosis of pancreatic tumors by endoscopic ultrasonography.

World J Radiol 2010; 2(4): 122-134 Available from: URL: http://www.wjgnet.com/1949-8470/full/v2/i4/122.htm DOI: http://dx.doi.org/10.4329/wjr.v2.i4.122

INTRODUCTION

Although the morphology of pancreatic tumors is highly diverse, these tumors can be classified broadly into solid and cystic tumors. Solid pancreatic masses may be due to the inflammation associated with chronic pancreatitis or they may be caused by a malignancy[1,2]. Ductal pancreatic adenocarcinoma is the most common malignant pancreatic neoplasm as it accounts for more than 95% of all malignant solid pancreatic tumors[3]. Only a minority of pancreatic tumors are neuroendocrine tumors. Other pancreatic tumors such as squamous cell carcinomas and primary pancreatic lymphomas are even rarer. Cystic tumors comprise 10%-15% of all cystic masses and 1%-5% of all pancreatic malignancies[4]. The imaging features of benign and malignant cystic lesions overlap considerably. Moreover, solid pancreatic tumors with cystic degeneration can mimic primary cystic tumors. Thus, it is often difficult to differentiate benign lesions from malignant lesions, and solid tumors from cystic pancreatic tumors. Compared to other imaging techniques, endoscopic ultrasonography (EUS) has been shown to be more accurate in terms of local staging and predicting vascular invasion and tumor resectability, particularly with tumors less than 2 cm in diameter[5-7]. Furthermore, EUS permits a pancreatic mass to be aspirated and/or biopsied during an examination, which allows a histological diagnosis to be made and benign masses to be differentiated from malignant masses.

EUS has also been adapted to employ an ultrasound (US) contrast agent. This technique is termed contrast-enhanced EUS (CE-EUS), and it has been used to assess the microvascular structures of pancreatic tumors. However, because this technique is associated with several imaging limitations, contrast-enhanced harmonic EUS (CEH-EUS) was developed recently. This technique employs an echoendoscope with a broad-band transducer and an imaging mode that was designed specifically for CEH-EUS with a second generation US contrast agent. All of these non-invasive methods have improved the discrimination between malignant and benign masses and the differential diagnosis of the pancreatic masses. In this article, the EUS imaging findings of the common pancreatic solid and cystic masses are reviewed. In addition, the diagnostic accuracy of EUS-guided fine needle aspiration (EUS-FNA) is examined. Finally, the efficacies and relative advantages of CE-EUS, CEH-EUS, and other diagnostic EUS adapted procedures and their complementary role in clinical practice are discussed.

ENDOSCOPIC ULTRASONOGRAPHY

EUS was developed in the 1980s to overcome problems associated with the transabdominal US imaging of the pancreas caused by intervening gas, bone, and fat. Since the EUS high-frequency transducers can be positioned *via* the stomach and duodenum in direct proximity to the pancreas, this technique yields detailed high-resolution images of the pancreas that far surpass those achieved by computed tomography (CT) or magnetic resonance imaging (MRI). The high resolution of these images permits the detection of lesions as small as 2-3 mm in diameter and their relationship with adjacent blood vessels such as the portal vein and mesenteric vasculature to be characterized. As a result, EUS is more accurate than other imaging techniques in terms of local staging and predicting vascular invasion and tumor resectability, particularly with tumors less than 2 cm in diameter[5-7]. EUS is also useful for locating occult pancreatic tumors in patients who have liver metastases and an unknown primary tumor. For example, when EUS was applied to 33 patients whose CT images only revealed metastatic tumors derived from an unknown primary tumor, primary pancreatic tumors were detected in 17 patients[8]. The identification of these primary pancreatic tumors meant that these patients could be treated with pancreas-specific chemotherapy, which improved their outcome.

SOLID PANCREATIC LESIONS

Solid pancreatic masses include benign masses, namely focal chronic pancreatitis, and malignancies, namely ductal adenocarcinomas, neuroendocrine tumors, lymphomas, and metastases.

Focal chronic pancreatitis

Regardless of whether CT, MRI, or even EUS is used, it is very difficult to reliably distinguish between chronic pancreatitis masses, namely masses that are due to advanced inflammation or fibrosis, and malignant tumors. To diagnose chronic pancreatitis, nine EUS criteria are currently accepted. Four are parenchymal criteria: hyperechogenic foci, hyperechogenic strands, pseudocysts, and lobularity. Five are ductal criteria: dilated main pancreatic ducts (MPDs), visible side branches, and hyperechogenic walls of the MPD[9-11]. When these 4-5 diagnostic criteria are used, the diagnostic sensitivity of EUS ranges between 84% and 100%, while its specificity ranges between 60% and 95%[12-16]. In addition, Rösch *et al*[17] and Glasbrenner *et al*[18] independently proposed EUS criteria that are suggestive of an inflammatory mass, namely inhomogeneous echo pattern, calcification, peripancreatic echo-rich stranding, and cysts. Their EUS criteria of malignant masses included: signs of invasion of adjacent organs, enlargement of adjacent lymph nodes, and masses with irregular outer margins (Figure 1). While these criteria markedly improved the diagnostic specificity of EUS, the sensitivity of the technique remained rather low, which means that the B-mode images of EUS are still insufficient for discriminating between chronic pancreatitis and malignant tumors.

Figure 1 Focal chronic pancreatitis. Endoscopic ultrasonography (EUS) shows a mass with an irregular, inhomogeneous echo pattern, and calcification (arrow) at the head of the pancreas.

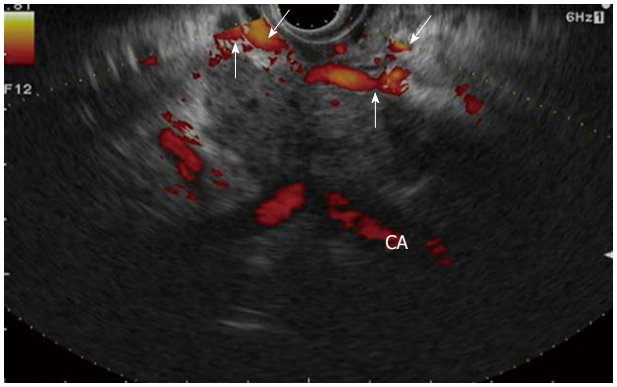

Figure 2 Pancreatic adenocarcinoma. EUS shows a heterogeneous hypoechoic mass with irregular margins at the body of the pancreas, infiltrating the celiac artery, and development of collateral vessels around the tumor (arrows). CA: Celiac artery.

Pancreatic adenocarcinoma

Pancreatic adenocarcinomas typically have the EUS appearance of a heterogeneous hypoechoic mass with irregular margins (Figure 2). However, relying on these morphological features alone only yields a diagnostic specificity of 53% since these features can also be seen in focal pancreatitis, neuroendocrine tumors, and metastases[19]. However, with a sensitivity of 89%-100%, EUS has been remarkably successful in the early detection of small adenocarcinomas[20-22]. In our institute, helical CT and EUS can detect pancreatic carcinomas 2 cm or less in diameter with a sensitivity of 50% and 94.4%, respectively. Thus EUS is significantly more sensitive than helical CT for detecting small pancreatic tumors[23].

Compared to other imaging techniques, EUS also facilitates more accurate staging, which improves the management of pancreatic cancer. Indeed, it has been suggested that EUS is most useful for assessing peripancreatic vascular and lymph node involvement. Many large series have found that when EUS is used for staging, the T stage accuracy ranges between 78%-91% and the nodal (N) stage accuracy ranges between 41%-86%[24-28]. In general, the T stage accuracy based on EUS findings

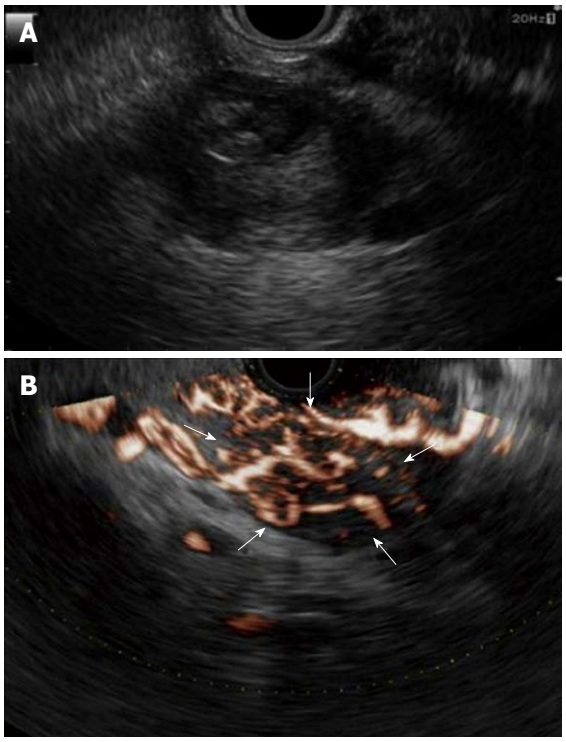

Figure 3 Neuroendocrine tumor. A: EUS shows a heterogeneous appearance; cystic, with a solid component or pure fluid 31 mm in diameter; B: EUS using Doppler mode shows a hypervascular mass at the tail of the pancreas (arrows).

is highest for patients with smaller tumors, whereas helical CT is more accurate in staging larger tumors[26-29]. When all four features that are suggestive of malignant lymph nodes, namely round shape, well-delimitated, size > 1 cm, and hypoechogenity, are present the chance of malignancy is 80%-100%[30].

Another benefit of EUS with regard to pancreatic tumors is that it can show the invasion of the great peripancreatic vessels with an accuracy of 67%-93%[17,31,32]. The splenic vein, portal vein and proximal superior mesenteric artery are easier to visualize on EUS than the other major peripancreatic vessels[33,34]. The vascular invasion criteria are as follows: irregularity of the interface with the vessels, intravascular tumor growth, and nonvisualization of the vessel, with collateral circulation growth. EUS can detect vascular invasion with a sensitivity and specificity of 42%-91% and 89%-100%, respectively[17,31,32]. While the accuracy can be rather low, this is because the staging accuracy of EUS can be influenced by several factors, including the experience of the endosonographer, the presence of imaging artifacts, and the endosonographer's knowledge of the results of previous imaging tests.

Neuroendocrine tumors

On EUS, neuroendocrine tumors usually appear as a hypoechogenic well-delimited lesion with intense vascularization; moreover, 60%-75% of all neuroendocrine tumors are less than 1.5 cm in diameter[35,36]. Lesions greater than 3 cm are likely to have an increased potential for malignancy and a heterogeneous appearance, namely cys-

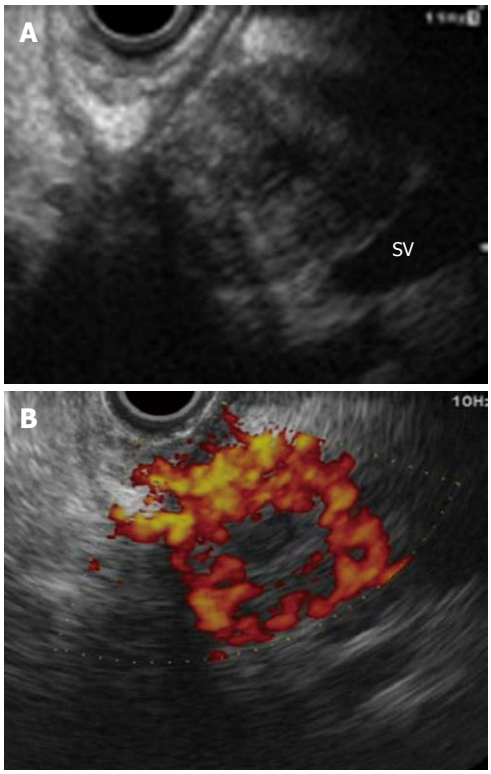

Figure 4 Metastatic pancreatic cancer from renal cell carcinoma. A: EUS shows a heterogeneous hypoechoic mass with a central necrotic area at the head of the pancreas; B: Contrast-enhanced Doppler EUS shows a hypervascular mass. SV: Splenic vein.

tic, with a solid component or pure fluid[37] (Figure 3A). The accuracy and specificity with which EUS can localize neuroendocrine tumors are 93% and 95%, respectively[38]. Since typical neuroendocrine tumors are known to be hypervascular tumors, EUS employing a Doppler mode is useful for observing the vascularity of identified neuroendocrine tumors (Figure 3B).

Primary pancreatic lymphoma

Primary pancreatic lymphoma is rare, comprising 1.3%-1.5% of all malignant pancreatic tumors. It is characterized by non-specific symptoms, laboratory tests and imaging results. Consequently, it can be very difficult to differentiate pancreatic lymphoma from pancreatic cancer on the basis of clinical and imaging data alone[39,40]. One report has described the EUS appearance of a pancreatic lymphoma as a bulky localized tumor in the pancreas without significant dilation of the MPD. Furthermore, if enlarged lymph nodes are encountered below the level of the renal veins, pancreatic lymphoma may be suspected. These EUS appearances may be useful for distinguishing between pancreatic lymphoma and other malignant pancreatic masses[41].

Metastatic pancreatic cancer

While primary pancreatic adenocarcinoma is the most common malignant tumor of the pancreas, a recent study showed that 3% of all pancreatic resections performed for malignant disease are due to pancreatic metastases of renal cell carcinomas[42]. Most pancreatic metastases develop from primary kidney, lung, breast, colon, or skin tumors[43] (Figure 4A and B). Confirming the metastatic nature of a pancreatic tumor is not an easy task, even for pathologists. However, metastatic tumors are more likely to have well-defined borders than primary pancreatic cancers[44].

CYSTIC PANCREATIC LESIONS

Cystic neoplasms of the pancreas often pose a diagnostic dilemma. They can be essentially classified according to malignant potential into mucinous and non-mucinous lesions with significant differences in the natural history and survival between the two groups. Mucinous tumors have recently been classified into mucinous cystic neoplasms (MCN) and intraductal papillary mucinous neoplasms (IPMN). Non-mucinous cysts include neoplastic cysts [serous cyst adenomas (SCAs) and solid pseudopapillary tumors], inflammatory cysts (pseudocysts), and epithelial cysts (adult polycystic disease and cystic fibrosis). Mucinous lesions are premalignant or malignant tumors, and surgical resection is generally recommended on operative candidates. Of the non-mucinous lesions, SCAs, whose potential for malignancy is low, and pseudocysts, which are always benign, are generally only resected if they are causing symptoms or complications[45-47].

The morphological features of cystic pancreatic lesions that can be determined by EUS include the presence of a wall, septa, solid component, the number and size of cysts, and the dilatation and thickening of the MPD. The presence of intracystic mucin or floating debris, pancreatic duct dilation, echogenic ductal wall thickening, and focal cyst wall nodularity or thickening are distinctly usual and suggestive of a mucinous tumor. These EUS features are thus useful for the differential diagnosis of cystic pancreatic lesions[48-53], although the accuracy with which they can be used to diagnose malignant cystic pancreatic tumors is rather low (51%-82%). Their usefulness is particularly limited in the case of large lesions (> 5-6 cm) that escape the focal field of the transducer[18,54-56].

Pseudocysts

The diagnosis of pseudocysts is generally not a clinical dilemma if there is a history of pancreatitis. However, cysts occurring in the setting of pancreatitis are not always pseudocysts; IPMN, for example may present with pancreatitis. Mature pseudocysts often have a thick wall surrounding a round collection of fluid, whereas early pseudocysts have a thin wall containing a collection of complex fluids[48] (Figure 5). To differentiate pseudocysts from cystic malignancies, it is useful to know that internal cyst debris and pancreatic parenchymal changes are observed more frequently in pseudocysts, and that mural nodules and septa are present more frequently in cystic

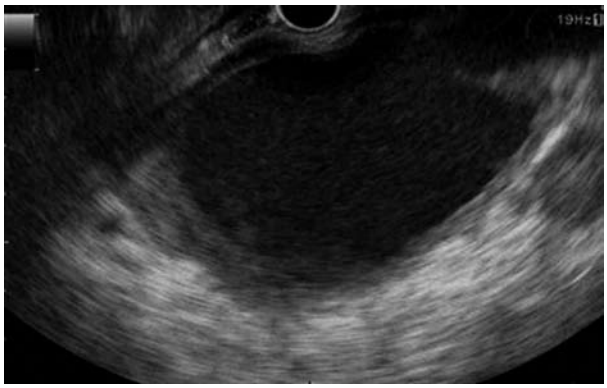

Figure 5 Pseudocyst. EUS shows a cystic lesion with a thick wall surrounding a round fluid collection at the body of the pancreas.

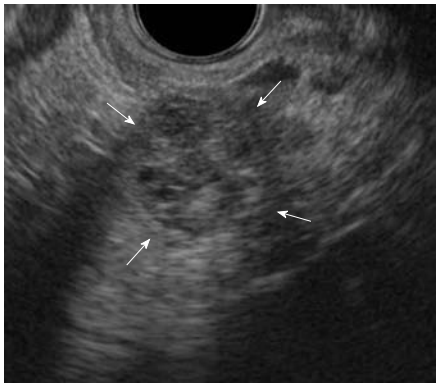

Figure 6 Serous cyst adenoma. EUS shows a mass with a "honeycomb appearance" at the body of the pancreas 13 mm in diameter (arrows).

malignancies[57]. However, several studies have concluded that when used in isolation, morphological features cannot reliably differentiate between malignancies and cystic lesions including pseudocysts[58,59].

SCAs

SCAs occur predominantly in young females. Although several reports have found that 50% to 70% are located in the pancreatic body or tail, other studies have found them more commonly in the head or neck region (63%). Although there are case reports of the malignant transformation of SCAs, they are largely benign cystic lesions and as such are often managed non-surgically[59,60]. SCAs usually appear as focal, well-demarcated lesions that contain multiple, and small (less than 1-2 cm in diameter) fluid-filled microcysts. The microcysts are separated by dense fibrous septa, producing a honeycomb appearance (Figure 6). Central fibrosis or calcification may be seen, particularly in large lesions, and can result in sunburst calcification. While this is a pathognomonic feature, it is present in only about 10% of patients with SCAs. A less common macrocystic variant contains larger (greater than 2 cm) cysts. They are typically microcystic. A solid variant contains numerous tiny cysts, each 1-2 mm in diameter, and appears as a homogeneous hypoechoic mass that can be mistaken for a ductal carcinoma.

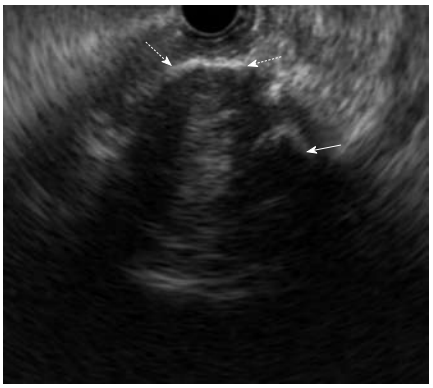

Figure 7 Solid pseudopapillary tumor. EUS shows a tumor in part of the calcified wall (dashed arrows) with acoustic shadow and inner calcifications (arrow) at the body of the pancreas 12 mm in diameter.

Solid pseudopapillary tumors

These tumors have a fairly well-defined behavior and malignant risk and are often managed surgically. In these cases, EUS plays a limited role because of the large size of the lesions and the resulting limitation of the examination field. However, typical EUS images of these tumors reveal well-delimited tumors with inner cystic formations and calcification (Figure 7). The atypical pure fluid forms are difficult to differentiate from the MCNs.

IPMN

IPMNs are more common in the elderly and are located more frequently in the head of the pancreas. IPMNs are characterized by the papillary proliferation of the ductal epithelium that is responsible for mucus production, which leads to the dilatation of the excretory pancreatic ducts. In a minority of cases, an endoscopic diagnosis of an IPMN can be established if a papulous papilla with mucin extrusion, also sometimes referred to as a "fish-eye" ampulla, is seen[61] (Figure 8A). These lesions can progress from hyperplasia to dysplasia, then to carcinoma *in situ*, and finally to invasive carcinoma. Macroscopically, IPMN is characterized by the mucinous dilatation of the pancreatic ducts, with involvement of either the MPD alone (main duct type), the side branch ducts alone (side branch type), or both (combined type)[62-64] (Figure 8B-D). Although communication with the MPD is a feature of side branch type IPMN and helps to exclude MCN, the absence of communication does not exclude IPMN because the mucus can block the flow of contrast into the abnormal side branch. EUS can: (1) visualize the communication between the MPD and a dilated side pancreatic duct; (2) help to make a differential diagnosis between an intraductal mucus deposit (as filaments or hyperechogenic round structures surrounded by a hyperechogenic ring) and a hypoechogenic intraductal polypoid lesion; and (3) visualize the thickening of the pancreatic duct wall or mural nodes. The diagnostic accuracy of EUS for IPMN is 92%, which is higher than that provided by US (82%) or endoscopic retrograde cholangiopancreatography (89%). Although not specific, an underlying malignancy

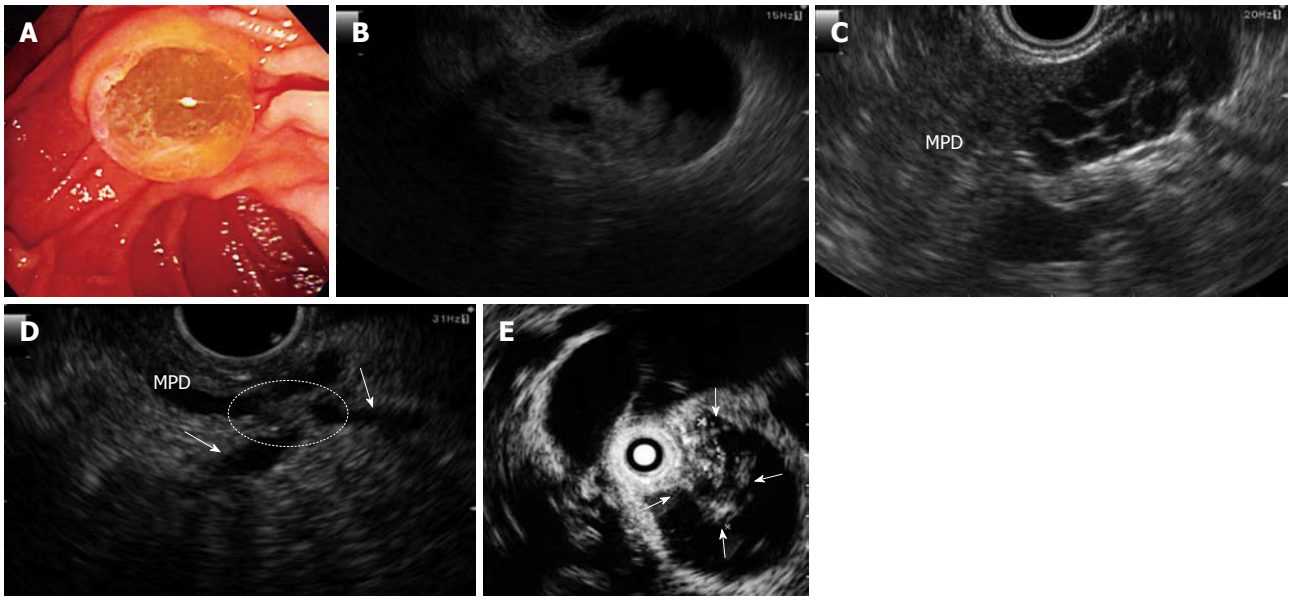

Figure 8 Intraductal papillary mucinous neoplasms (IPMN). A: An endoscopic diagnosis of an IPMN can be established if the "fish-eye" ampulla is visualized in minority cases; B: IPMN of main duct type. EUS shows a mural nodule within by the mucinous dilatation of the pancreatic ducts, with involvement of the main duct at the tail of the pancreas; C: IPMN of side branch type. EUS shows a multiple dilatation of the side branch at the neck of the pancreas; D: IPMN of the combined type. EUS show a mural nodule stretching (circle) over the main pancreatic duct and side branches (arrows) at the body of the pancreas. E: IPMN of main duct type. Intraductal ultrasonography (IDUS) can identify tumor nodule development into the main pancreatic duct (arrows). MPD: Main pancreatic duct.

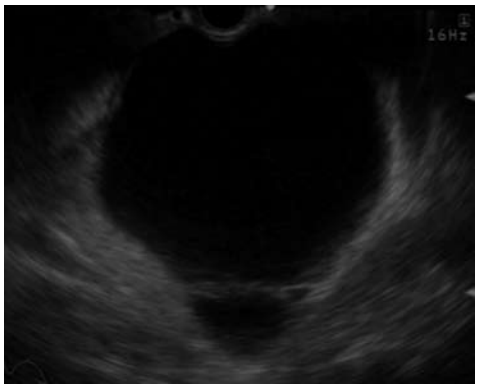

Figure 9 Mucinous cystic neoplasms (MCN). EUS shows a separated macrocyst 40 mm in diameter.

is suggested by an MPD diameter greater than 10 mm, branch-duct type IPMNs that have a cystic lesion diameter greater than 40 mm and a thick, irregular septum, and the presence of mural nodules that exceed 10 mm in diameter[49].

In cases where the pancreatic duct is sufficiently dilated, intraductal ultrasonography (IDUS) that utilizes a thin caliber (approximately 2 mm in diameter) ultrasonic probe with high-frequency ultrasound (12-30 MHz) can be useful. This technique results in images that have a high spatial resolution and can be used to determine the extent of a tumor along the MPD or the progression of a tumor from a branch duct into the MPD. Thus, it provides critical information for surgical candidates with IPMN. It can also detect flat lesions that are less than 500 μm in height[65], but the depth of image penetration is limited (Figure 8E).

MCN

MCNs are more common in middle-aged women and are located more frequently in the body and tail of the pancreas. Although MCNs are typically macrocystic tumors that are > 2 cm in diameter, there are also small MCNS that are only a few, millimeters in diameter (Figure 9). Peripheral calcifications are found in 15% of patients but can also occur in other cystic lesions, as well as in mural nodes or vegetations[66]. Pancreatic duct communication is seldom seen because MCNs originate within the peripheral ductal system. Angiography, although rarely performed on these lesions, shows that most MCNs are hypervascular. Evidence of malignancy includes the presence of cyst wall irregularity and thickening, intracystic solid regions, or an adjacent solid mass. The presence of "ovarian type stroma" is strongly suggestive of an MCN lesion, although MCNs with "non-ovarian type stroma" have also been reported[67,68].

EUS-FNA

EUS-FNA has proved to be a safe and useful method for tissue sampling of pancreatic masses. The safety of EUS-FNA for evaluating pancreatic lesions is now well established[69-71]. Several studies have reported that the rate of complications, which include pancreatitis, infection, and bleeding, is 0%-2%[69,72,73]. In addition, a multicenter study evaluating the safety of EUS-FNA of solid pancreatic masses found that, 14 of 4958 patients developed pancreatitis[69]. The accuracy of EUS-FNA for the diagnosis of pancreatic carcinoma and neuroendocrine tumors is reported to be 80%-95%[72-75] and 46%-83%[75,76], respectively. The low accuracy for endo-

crine tumors may be because inadequate hemorrhagic samples are often obtained: this reflects the vascular nature of these tumors. In terms of the diagnostic sensitivity of EUS-FNA, a study of 282 patients with pancreatic solid tumors with and without chronic pancreatitis found that the diagnostic sensitivity of EUS-FNA was significantly lower for chronic pancreatitis cases (73.9% *vs* 91.3%, $P = 0.02$)[36]. Another study of 69 patients with chronic pancreatitis showed that compared to EUS alone, EUS-FNA of the patients' masses improved the sensitivity, specificity and overall accuracy with which inflammatory conditions could be differentiated from pancreatic adenocarcinomas (63.6% *vs* 72.7%, 75.9% *vs* 100%, 73.9% *vs* 95.7%, respectively)[77]. However, the relatively poor sensitivity of EUS-FNA means that even this technique is insufficient for distinguishing between inflammatory and malignant masses. If the EUS-FNA data are suggestive of pancreatitis but other diagnostic modalities, including EUS, point to pancreatic cancer, close follow-up tests must be performed.

EUS-FNA of a cystic lesion may improve the accuracy of EUS since it permits the cystic fluid to be analyzed and a cytological diagnosis to be made. The cytological analyses include specific testing for the presence of columnar epithelial cells that stain for mucin (which is suggestive of MCNs or IPMNs), or cuboidal epithelial cells that stain for glycogen (which is suggestive of SCAs). In relation to this, a recent cooperative, multicenter trial in the United States studied 112 patients with cystic lesions of the pancreas who first underwent EUS-FNA and then surgical resection of their masses (which provided a histological diagnosis)[54]. The accuracy with which EUS, cystic fluid cytology, and staining of the cyst fluid for tumor markers such as carcinoembryonic antigen (CEA) provided the correct diagnosis was assessed. Of the 112 patients, 68, 7, 25, 5 and 5 were found to have mucinous, serous, inflammatory, endocrine, and other cystic lesions, respectively. Immunostaining for CEA differentiated between mucinous and non-mucinous cystic lesions with significantly greater accuracy (79%) than EUS morphology (51%) or cytology (59%). The investigators concluded that cystic lesions should be aspirated and that the fluid should be analyzed for CEA to differentiate between mucinous and non-mucinous lesions. In contrast, another study found that cystic fluid aspiration and CEA analysis did not improve diagnoses made on the basis of EUS[78]. In this study, 34 patients with a cystic lesion underwent EUS-FNA followed by resection of the lesion. The abilities of EUS, cytology, and cystic fluid analysis to provide a diagnosis were compared. Histological analysis revealed that the lesions were benign (simple cysts, pseudocysts, or SCAs) or malignant/potentially malignant (MCAs, IPMNs, cystic islet cell tumors, or cystic adenocarcinomas). The diagnostic sensitivities of EUS, cytology and CEA were 91%, 27%, and 28%, respectively ($P = 0.01$), their specificities were 60%, 100%, and 25%, respectively, and their accuracies were 82%, 55%, and 27%, respectively. If EUS was combined with cytopathology and CEA, its diagnostic accuracy did not improve further. It was concluded that cystic fluid cytology and CEA analysis does not improve the diagnostic ability of EUS.

Table 1 Pancreatic cyst fluid levels of amylase and tumor markers

	Serous cystadenoma	Mucinous cystic neoplasm	IPMN	Pseudocyst
Amylase	Low	Low	High	High
CEA	Low	High	High	Low
CA 72-4	Low	High	High	Low
CA 19-9	Variable	Variable	Variable	High
CA 125	Low	Variable	Low	Low

IPMN: Intraductal papillary mucinous neoplasia; CEA: Carcinoembryonic antigen; CA: Carbohydrate antigen.

Tumor markers other than CEA have also been used to analyze pancreatic cystic fluids sampled by EUS-FNA. These include CA19-9, CA125, and CA 72-4. The largest study to date that has examined the ability of multiple tumor markers in cystic fluid to detect benign and malignant mucinous cystic lesions in pancreatic cystic lesions found that mucinous cystic tumors had significant CA 72-4 levels and that this marker could detect mucinous or malignant cysts with a specificity and sensitivity of 95% and 80%, respectively[79].

Fluid obtained during FNA of pancreatic cysts could be sent for biochemical and cytological analysis, and tumor marker levels, which often determines the cyst type and the presence of malignancy[80-84]. A combined analysis of 11 studies[85,86] found that cytology from cyst fluid was diagnostic in 38% to 48% of cystic pancreatic neoplasms, and the Cooperative Pancreatic Cyst Study[84] determined the diagnostic accuracy to be 59% in this setting. When tumor markers, amylase testing and mucin staining are combined with cytological testing, the diagnostic accuracy increases to 80% or 90%[80-84] (Table 1). High levels of cyst fluid amylase are more often found in cysts that communicate with pancreatic ducts (pseudocysts and IPMN); a cyst fluid amylase level greater than 5000 U/L has a sensitivity and specificity of 61% and 58%, respectively, for distinguishing pseudocysts from other cystic neoplasms[86,87].

With regard to the complications associated with EUS-FNA of pancreatic cystic lesions, it has been reported that in 81 patients subjected to EUS-FNA, one developed an infected cystadenoma[88]. This patient did not receive prophylactic antibiotics before the procedure. The current standard of care for patients undergoing FNA of a pancreatic cystic lesion includes routine administration of antibiotics.

CONTRAST-ENHANCED EUS

While EUS is a diagnostic method that can detect small pancreatic lesions with high sensitivity, it remains difficult to differentially diagnose pancreatic lesions, especially malignant neoplasms in patients with chronic pancre-

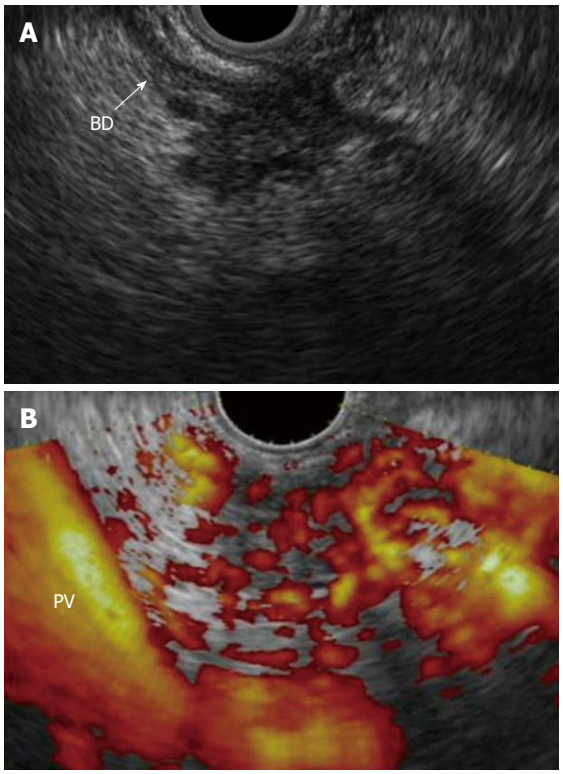

Figure 10 Focal chronic pancreatitis. A: EUS shows a mass with an irregular and inhomogeneous echo pattern at the head of the pancreas; B: Contrast-enhanced power Doppler EUS shows an isovascular nodule compared with the surrounding pancreatic tissue. BD: Bile duct; PV: Portal vein.

atitis[89]. The introduction of EUS-FNA has made this task easier, however, there are cases where the diagnosis is still difficult using EUS-FNA. These include cases where the EUS-FNA aspirant contains insufficient tumor material because the pancreatic tumor is small, and cases with severe chronic pancreatitis that make it difficult to see the borders of the lesion, thereby hampering the accurate insertion of the needle. Moreover, there are cases where a non-invasive diagnostic technique is needed because the patient is using anticoagulants. For these reasons, CE-EUS was developed.

Contrast-enhanced techniques provide information on vascularity and blood flow in normal and pathological tissues. CE-US has played an important role in clinical practice by aiding the differential diagnosis of diseases in a wide array of organs, including the liver, gallbladder, bile duct, pancreas, kidney, thyroid, and prostate. It has also helped to guide interventional procedures and to evaluate treatment responses after local therapies and chemotherapy[90-95].

Several studies that assessed the utility of CE-EUS for diagnosing pancreatic tumors were reported recently[23,96-100]. One of these was our study comparing the ability of power Doppler EUS (PD-EUS), CE-EUS with power Doppler mode using first generation US contrast agent (Levovist), and contrast-enhanced helical CT (CE-CT) to diagnose small pancreatic tumors[23]. PD-EUS and CE-EUS allowed the pancreatic tumors to be classified according to their density of vessels relative to the vascularity of the surrounding pancreatic tissue, namely as, hypovascular, isovascular, and hypervascular (Figures 10 and 11): For small pancreatic tumors that were ≤ 2 cm, the sensitivity with which PD-EUS, CE-EUS and CE-CT differentiated ductal carcinoma from other tumors was 50%, 83.3% and 11%, respectively. Thus, CE-EUS was significantly more sensitive than PD-EUS and CE-CT, which suggests that CE-EUS is particularly useful for differentially diagnosing, pancreatic tumors, especially small pancreatic tumors. However, such Doppler ultrasonography with contrast enhancement has several limitations, including blooming artifacts, poor spatial resolution, and low sensitivity to slow flow[96-99]. Indeed, in our study, these limitations

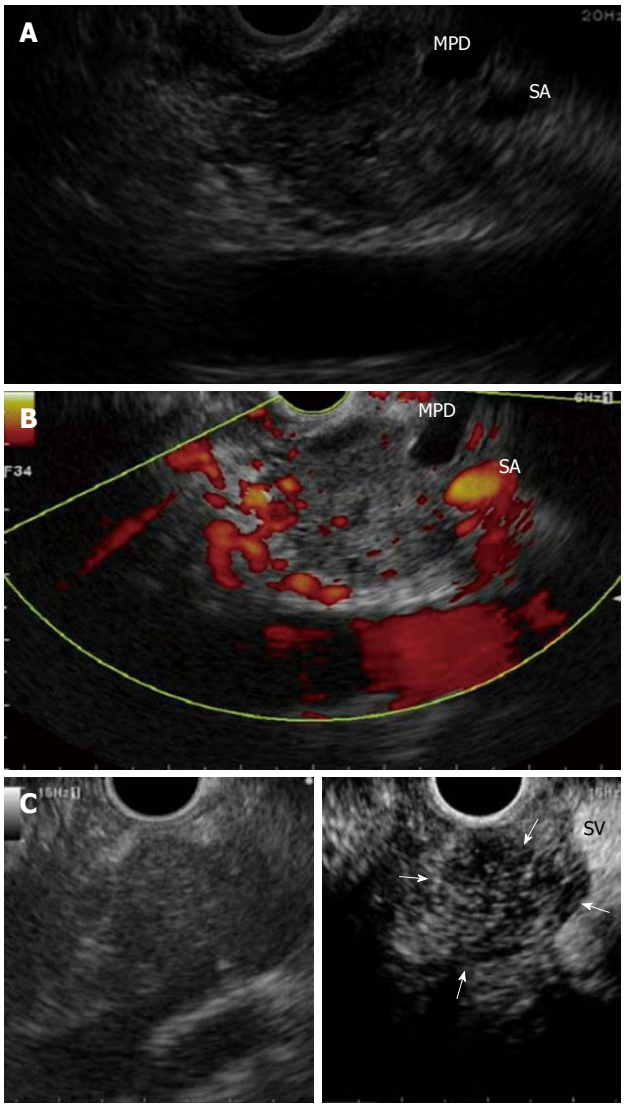

Figure 11 Pancreatic adenocarcinoma. A: EUS shows a heterogeneous hypoechoic mass with irregular margins at the body of the pancreas and tail side main pancreatic duct enlarged due to the infiltrating mass; B: Contrast-enhanced power Doppler EUS shows a hypovascular nodule compared with the surrounding pancreatic tissue; C: Contrast-enhanced harmonic EUS showing a clear margin and hypovascular nodule compared with surrounding pancreatic tissue (arrows) without blooming artifact such as that found with Doppler imaging. Left: B-mode imaging; Right: Contrast imaging. MPD: Main pancreatic duct; SA: Splenic artery.

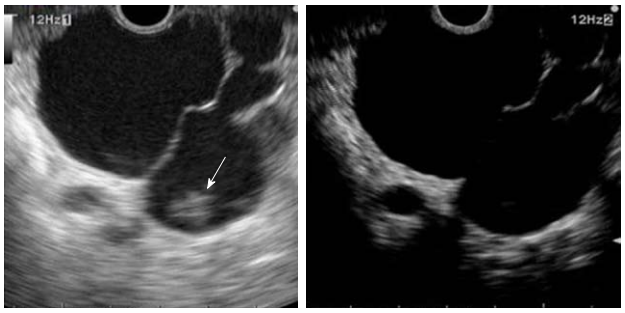

Figure 12 IPMN of side branch type. Left (B-mode image): The nodule (arrow) in dilatation of the side branch cannot be distinguished between sediment and tumor by B-EUS; Right (contrast image): Contrast-enhanced harmonic EUS reveals that this nodule is sediment.

prevented vascularity from benign evaluated in 7.8% of all patients, of whom 22.2% had carcinomas that were ≤ 2 cm in diameter.

Hocke *et al*[100] evaluated the ability of CE-EUS with power Doppler mode using SonoVue, a second generation US contrast agent, to differentiate inflammation from pancreatic carcinoma on the basis of the perfusion characteristics of the microvessels. For this study, chronic pancreatitis without neoplasm was defined as the lack of detectable vascularization or the regular appearance of vessels both before and after the injection of SonoVue, and the detection of both arterial and venous vessels in the contrast-enhanced phase. Malignancy was defined as the lack of detectable vascularization before the injection of SonoVue, the irregular appearance of arterial vessels after the injection of SonoVue, and the absence of venous vessels in the lesion. In patients with chronic pancreatitis, combined conventional B-mode and power Doppler EUS diagnosed pancreatic cancer with a sensitivity and specificity of 73.2% and 83.3%, respectively, whereas CE-EUS with power Doppler had a sensitivity and specificity of 91.1% and 93.3%, respectively. Thus, CE-EUS is highly useful for the differential diagnosis of pancreatic cancer.

CONTRAST-ENHANCED HARMONIC EUS

Kitano *et al*[101] recently developed an echoendoscope with a broad-band transducer and an imaging mode specifically for CEH-EUS. This technology can detect signals from microbubbles in vessels with a very slow flow without Doppler-related artifacts and can be used to characterize tumor vascularity in the pancreas (Figure 11C). Second-generation US contrast agents such as SonoVue and Sonazoid, harmonic signals at low acoustic powers and thus are suitable for EUS imaging at low acoustic powers[102,103]. CEH-EUS successfully creates novel perfusion images and the vascular structures of pancreatic lesions (Figure 12). This CEH-EUS mediated evaluation of the microvasculature of pancreas lesions is expected to improve the differential diagnosis of pancreatic disease in the near future.

OTHER DIAGNOSTIC EUS ADAPTED PROCEDURES

IDUS

The list of indications of EUS is growing, which has forced gastroenterologists to think outside the lumen. Technological advances in EUS imaging has led to the development of IDUS mini propes for the evaluation of the pancreatobiliary tree and periductal structures. In the evaluation of patients with pancreatic duct stenosis, IDUS can be used to distinguish malignant strictures, allow for the early detection of small pancreatic adenocarcinomas, assist in local staging and to determine resectability[104,105]. IDUS may also be useful for the localization of pancreatic neuroendocrine tumors not visualized by other imaging modalities[104-106]. In the evaluation of IPMN, IDUS is used to determine malignant disease and disease extent before surgery. IDUS and pancreatoscopy had a reported combined sensitivity, specificity and accuracy of 91%, 82% and 88%, respectively[107].

EUS-elastography

EUS-elastography can assess tissue hardness by measuring its elasticity which might provide clinical utility in the diagnosis of pancreatic disorders. Tissue elasticity studies can provide information on both its pattern and distribution. EUS-elastography has introduced a new form of pathologic analysis, that is, tissue elasticity. This parameter appears to correlate with the malignant potential of the lesions. Importantly, the image of EUS elastography indicates the relative value in a region of interest (ROI), so the same lesion might display different colors in a different ROI. This is a limitation of EUS-elastography. The other is the distribution of tissue elasticity. With the prototype image analysis software, we can now capture and analyze features of real-time tissue elastography by using computer software. Theoretically, this will limit interpretation bias and provide a measure of pattern distribution that is constant and independent, regardless of ROIs[108]. More studies and greater experience are needed before it has a place in our diagnostic armamentarium.

Tridimensional-EUS

Tridimensional (3D)-EUS certainly facilitates anatomical interpretation of the images in the pancreatobiliary area, as well as vascular landmarks used for staging and assessment of resectability. The method might be feasible for the assessment of venous invasion and venous compression in focal pancreatic masses, in both chronic pancreatitis and pancreatic cancer[109]. The acquisition of 3D volume allows a retrospective assessment and slicing of the reconstructed cube, with accurate depiction of focal masses, even if missed on the initial real-time evaluation. However, further progress of the technology is still necessary.

CONCLUSION

EUS is established as a most accurate method for stag-

ing malignancies of the pancreas, particularly small pancreatic lesions. EUS-FNA also allows safe tissue sampling of pancreatic tumors. EUS and EUS-FNA are now indispensable for the management of pancreatic tumors. In addition, we have recently been able to use various new EUS adapted technologies such as CE-EUS and CEH-EUS in clinical practice, which are helpful in the differential diagnosis of pancreatic tumors, especially small pancreatic tumors. Further improvements in EUS technology are expected to provide more useful modalities for the detection and diagnosis of pancreatic tumors.

REFERENCES

1 **Kamisawa T**, Egawa N, Nakajima H, Tsuruta K, Okamoto A, Kamata N. Clinical difficulties in the differentiation of autoimmune pancreatitis and pancreatic carcinoma. *Am J Gastroenterol* 2003; **98**: 2694-2699

2 **Yadav D**, Notahara K, Smyrk TC, Clain JE, Pearson RK, Farnell MB, Chari ST. Idiopathic tumefactive chronic pancreatitis: clinical profile, histology, and natural history after resection. *Clin Gastroenterol Hepatol* 2003; **1**: 129-135

3 **Kalra MK**, Maher MM, Mueller PR, Saini S. State-of-the-art imaging of pancreatic neoplasms. *Br J Radiol* 2003; **76**: 857-865

4 **Visser BC**, Muthusamay VR, Mulvihill SJ, Coakley F. Diagnostic imaging of cystic pancreatic neoplasms. *Surg Oncol* 2004; **13**: 27-39

5 **Buscail L**, Pagès P, Berthélemy P, Fourtanier G, Frexinos J, Escourrou J. Role of EUS in the management of pancreatic and ampullary carcinoma: a prospective study assessing resectability and prognosis. *Gastrointest Endosc* 1999; **50**: 34-40

6 **Hunt GC**, Faigel DO. Assessment of EUS for diagnosing, staging, and determining resectability of pancreatic cancer: a review. *Gastrointest Endosc* 2002; **55**: 232-237

7 **Mertz HR**, Sechopoulos P, Delbeke D, Leach SD. EUS, PET, and CT scanning for evaluation of pancreatic adenocarcinoma. *Gastrointest Endosc* 2000; **52**: 367-371

8 **tenBerge J**, Hoffman BJ, Hawes RH, Van Enckevort C, Giovannini M, Erickson RA, Catalano MF, Fogel R, Mallery S, Faigel DO, Ferrari AP, Waxman I, Palazzo L, Ben-Menachem T, Jowell PS, McGrath KM, Kowalski TE, Nguyen CC, Wassef WY, Yamao K, Chak A, Greenwald BD, Woodward TA, Vilmann P, Sabbagh L, Wallace MB. EUS-guided fine needle aspiration of the liver: indications, yield, and safety based on an international survey of 167 cases. *Gastrointest Endosc* 2002; **55**: 859-862

9 **Sahai AV**, Zimmerman M, Aabakken L, Tarnasky PR, Cunningham JT, van Velse A, Hawes RH, Hoffman BJ. Prospective assessment of the ability of endoscopic ultrasound to diagnose, exclude, or establish the severity of chronic pancreatitis found by endoscopic retrograde cholangiopancreatography. *Gastrointest Endosc* 1998; **48**: 18-25

10 **Sahai AV**. EUS and chronic pancreatitis. *Gastrointest Endosc* 2002; **56**: S76-S81

11 Reproduction of minimal standard terminology in Gastrointestinal Endosonography. *Dig Endosc* 1998; **10**: 158-185

12 **Wiersema MJ**, Hawes RH, Lehman GA, Kochman ML, Sherman S, Kopecky KK. Prospective evaluation of endoscopic ultrasonography and endoscopic retrograde cholangiopancreatography in patients with chronic abdominal pain of suspected pancreatic origin. *Endoscopy* 1993; **25**: 555-564

13 **Wallace MB**, Hawes RH, Durkalski V, Chak A, Mallery S, Catalano MF, Wiersema MJ, Bhutani MS, Ciaccia D, Kochman ML, Gress FG, Van Velse A, Hoffman BJ. The reliability of EUS for the diagnosis of chronic pancreatitis: interobserver agreement among experienced endosonographers. *Gastrointest Endosc* 2001; **53**: 294-299

14 **Buscail L**, Escourrou J, Moreau J, Delvaux M, Louvel D, Lapeyre F, Tregant P, Frexinos J. Endoscopic ultrasonography in chronic pancreatitis: a comparative prospective study with conventional ultrasonography, computed tomography, and ERCP. *Pancreas* 1995; **10**: 251-257

15 **Catalano MF**, Lahoti S, Geenen JE, Hogan WJ. Prospective evaluation of endoscopic ultrasonography, endoscopic retrograde pancreatography, and secretin test in the diagnosis of chronic pancreatitis. *Gastrointest Endosc* 1998; **48**: 11-17

16 **Hollerbach S**, Klamann A, Topalidis T, Schmiegel WH. Endoscopic ultrasonography (EUS) and fine-needle aspiration (FNA) cytology for diagnosis of chronic pancreatitis. *Endoscopy* 2001; **33**: 824-831

17 **Rösch T**, Lorenz R, Braig C, Feuerbach S, Siewert JR, Schusdziarra V, Classen M. Endoscopic ultrasound in pancreatic tumor diagnosis. *Gastrointest Endosc* 1991; **37**: 347-352

18 **Glasbrenner B**, Schwarz M, Pauls S, Preclik G, Beger HG, Adler G. Prospective comparison of endoscopic ultrasound and endoscopic retrograde cholangiopancreatography in the preoperative assessment of masses in the pancreatic head. *Dig Surg* 2000; **17**: 468-474

19 **Brand B**, Pfaff T, Binmoeller KF, Sriram PV, Fritscher-Ravens A, Knöfel WT, Jäckle S, Soehendra N. Endoscopic ultrasound for differential diagnosis of focal pancreatic lesions, confirmed by surgery. *Scand J Gastroenterol* 2000; **35**: 1221-1228

20 **Bhutani MS**, Gress FG, Giovannini M, Erickson RA, Catalano MF, Chak A, Deprez PH, Faigel DO, Nguyen CC. The No Endosonographic Detection of Tumor (NEST) Study: a case series of pancreatic cancers missed on endoscopic ultrasonography. *Endoscopy* 2004; **36**: 385-389

21 **DeWitt J**, Devereaux B, Chriswell M, McGreevy K, Howard T, Imperiale TF, Ciaccia D, Lane KA, Maglinte D, Kopecky K, LeBlanc J, McHenry L, Madura J, Aisen A, Cramer H, Cummings O, Sherman S. Comparison of endoscopic ultrasonography and multidetector computed tomography for detecting and staging pancreatic cancer. *Ann Intern Med* 2004; **141**: 753-763

22 **Maguchi H**, Takahashi K, Osanai M, Katanuma A. Small pancreatic lesions: is there need for EUS-FNA preoperatively? What to do with the incidental lesions? *Endoscopy* 2006; **38** Suppl 1: S53-S56

23 **Sakamoto H**, Kitano M, Suetomi Y, Maekawa K, Takeyama Y, Kudo M. Utility of contrast-enhanced endoscopic ultrasonography for diagnosis of small pancreatic carcinomas. *Ultrasound Med Biol* 2008; **34**: 525-532

24 **Gress FG**, Hawes RH, Savides TJ, Ikenberry SO, Cummings O, Kopecky K, Sherman S, Wiersema M, Lehman GA. Role of EUS in the preoperative staging of pancreatic cancer: a large single-center experience. *Gastrointest Endosc* 1999; **50**: 786-791

25 **Palazzo L**, Roseau G, Gayet B, Vilgrain V, Belghiti J, Fékéte F, Paolaggi JA. Endoscopic ultrasonography in the diagnosis and staging of pancreatic adenocarcinoma. Results of a prospective study with comparison to ultrasonography and CT scan. *Endoscopy* 1993; **25**: 143-150

26 **Yasuda K**, Mukai H, Nakajima M, Kawai K. Staging of pancreatic carcinoma by endoscopic ultrasonography. *Endoscopy* 1993; **25**: 151-155

27 **DeWitt J**, Devereaux B, Chriswell M, McGreevy K, Howard T, Imperiale TF, Ciaccia D, Lane KA, Maglinte D, Kopecky K, LeBlanc J, McHenry L, Madura J, Aisen A, Cramer H, Cummings O, Sherman S. Comparison of endoscopic ultrasonography and multidetector computed tomography for detecting and staging pancreatic cancer. *Ann Intern Med* 2004; **141**: 753-763

28 **Legmann P**, Vignaux O, Dousset B, Baraza AJ, Palazzo L, Dumontier I, Coste J, Louvel A, Roseau G, Couturier D,

Bonnin A. Pancreatic tumors: comparison of dual-phase helical CT and endoscopic sonography. *AJR Am J Roentgenol* 1998; **170**: 1315-1322
29 **Nakaizumi A**, Uehara H, Iishi H, Tatsuta M, Kitamura T, Kuroda C, Ohigashi H, Ishikawa O, Okuda S. Endoscopic ultrasonography in diagnosis and staging of pancreatic cancer. *Dig Dis Sci* 1995; **40**: 696-700
30 **Bhutani MS**, Hawes RH, Hoffman BJ. A comparison of the accuracy of echo features during endoscopic ultrasound (EUS) and EUS-guided fine-needle aspiration for diagnosis of malignant lymph node invasion. *Gastrointest Endosc* 1997; **45**: 474-479
31 **Soriano A**, Castells A, Ayuso C, Ayuso JR, de Caralt MT, Ginès MA, Real MI, Gilabert R, Quintó L, Trilla A, Feu F, Montanyà X, Fernández-Cruz L, Navarro S. Preoperative staging and tumor resectability assessment of pancreatic cancer: prospective study comparing endoscopic ultrasonography, helical computed tomography, magnetic resonance imaging, and angiography. *Am J Gastroenterol* 2004; **99**: 492-501
32 **Ramsay D**, Marshall M, Song S, Zimmerman M, Edmunds S, Yusoff I, Cullingford G, Fletcher D, Mendelson R. Identification and staging of pancreatic tumours using computed tomography, endoscopic ultrasound and mangafodipir trisodium-enhanced magnetic resonance imaging. *Australas Radiol* 2004; **48**: 154-161
33 **Rösch T**, Dittler HJ, Strobel K, Meining A, Schusdziarra V, Lorenz R, Allescher HD, Kassem AM, Gerhardt P, Siewert JR, Höfler H, Classen M. Endoscopic ultrasound criteria for vascular invasion in the staging of cancer of the head of the pancreas: a blind reevaluation of videotapes. *Gastrointest Endosc* 2000; **52**: 469-477
34 **Brugge WR**, Lee MJ, Kelsey PB, Schapiro RH, Warshaw AL. The use of EUS to diagnose malignant portal venous system invasion by pancreatic cancer. *Gastrointest Endosc* 1996; **43**: 561-567
35 **Zimmer T**, Scherübl H, Faiss S, Stölzel U, Riecken EO, Wiedenmann B. Endoscopic ultrasonography of neuroendocrine tumours. *Digestion* 2000; **62** Suppl 1: 45-50
36 **King CM**, Reznek RH, Dacie JE, Wass JA. Imaging islet cell tumours. *Clin Radiol* 1994; **49**: 295-303
37 **McLean AM**, Fairclough PD. Endoscopic ultrasound in the localisation of pancreatic islet cell tumours. *Best Pract Res Clin Endocrinol Metab* 2005; **19**: 177-193
38 **Anderson MA**, Carpenter S, Thompson NW, Nostrant TT, Elta GH, Scheiman JM. Endoscopic ultrasound is highly accurate and directs management in patients with neuroendocrine tumors of the pancreas. *Am J Gastroenterol* 2000; **95**: 2271-2277
39 **Reed K**, Vose PC, Jarstfer BS. Pancreatic cancer: 30 year review (1947 to 1977). *Am J Surg* 1979; **138**: 929-933
40 **Volmar KE**, Routbort MJ, Jones CK, Xie HB. Primary pancreatic lymphoma evaluated by fine-needle aspiration: findings in 14 cases. *Am J Clin Pathol* 2004; **121**: 898-903
41 **Merkle EM**, Bender GN, Brambs HJ. Imaging findings in pancreatic lymphoma: differential aspects. *AJR Am J Roentgenol* 2000; **174**: 671-675
42 **Faure JP**, Tuech JJ, Richer JP, Pessaux P, Arnaud JP, Carretier M. Pancreatic metastasis of renal cell carcinoma: presentation, treatment and survival. *J Urol* 2001; **165**: 20-22
43 **Matsukuma S**, Suda K, Abe H, Ogata S, Wada R. Metastatic cancer involving pancreatic duct epithelium and its mimicry of primary pancreatic cancer. *Histopathology* 1997; **30**: 208-213
44 **DeWitt J**, Jowell P, Leblanc J, McHenry L, McGreevy K, Cramer H, Volmar K, Sherman S, Gress F. EUS-guided FNA of pancreatic metastases: a multicenter experience. *Gastrointest Endosc* 2005; **61**: 689-696
45 **Sarr MG**, Carpenter HA, Prabhakar LP, Orchard TF, Hughes S, van Heerden JA, DiMagno EP. Clinical and pathologic correlation of 84 mucinous cystic neoplasms of the pancreas: can one reliably differentiate benign from malignant (or pre-malignant) neoplasms? *Ann Surg* 2000; **231**: 205-212
46 **Wilentz RE**, Albores-Saavedra J, Zahurak M, Talamini MA, Yeo CJ, Cameron JL, Hruban RH. Pathologic examination accurately predicts prognosis in mucinous cystic neoplasms of the pancreas. *Am J Surg Pathol* 1999; **23**: 1320-1327
47 **Siech M**, Tripp K, Schmidt-Rohlfing B, Mattfeldt T, Widmaier U, Gansauge F, Görich J, Beger HG. Cystic tumours of the pancreas: diagnostic accuracy, pathologic observations and surgical consequences. *Langenbecks Arch Surg* 1998; **383**: 56-61
48 **Song MH**, Lee SK, Kim MH, Lee HJ, Kim KP, Kim HJ, Lee SS, Seo DW, Min YI. EUS in the evaluation of pancreatic cystic lesions. *Gastrointest Endosc* 2003; **57**: 891-896
49 **Johnson CD**, Stephens DH, Charboneau JW, Carpenter HA, Welch TJ. Cystic pancreatic tumors: CT and sonographic assessment. *AJR Am J Roentgenol* 1988; **151**: 1133-1138
50 **Ariyama J**, Suyama M, Satoh K, Wakabayashi K. Endoscopic ultrasound and intraductal ultrasound in the diagnosis of small pancreatic tumors. *Abdom Imaging* 1998; **23**: 380-386
51 **Gress F**, Gottlieb K, Cummings O, Sherman S, Lehman G. Endoscopic ultrasound characteristics of mucinous cystic neoplasms of the pancreas. *Am J Gastroenterol* 2000; **95**: 961-965
52 **Torresan F**, Casadei R, Solmi L, Marrano D, Gandolfi L. The role of ultrasound in the differential diagnosis of serous and mucinous cystic tumours of the pancreas. *Eur J Gastroenterol Hepatol* 1997; **9**: 169-172
53 **Brugge WR**. The role of EUS in the diagnosis of cystic lesions of the pancreas. *Gastrointest Endosc* 2000; **52**: S18-S22
54 **Brugge WR**, Lewandrowski K, Lee-Lewandrowski E, Centeno BA, Szydlo T, Regan S, del Castillo CF, Warshaw AL. Diagnosis of pancreatic cystic neoplasms: a report of the cooperative pancreatic cyst study. *Gastroenterology* 2004; **126**: 1330-1336
55 **Frossard JL**, Amouyal P, Amouyal G, Palazzo L, Amaris J, Soldan M, Giostra E, Spahr L, Hadengue A, Fabre M. Performance of endosonography-guided fine needle aspiration and biopsy in the diagnosis of pancreatic cystic lesions. *Am J Gastroenterol* 2003; **98**: 1516-1524
56 **Sedlack R**, Affi A, Vazquez-Sequeiros E, Norton ID, Clain JE, Wiersema MJ. Utility of EUS in the evaluation of cystic pancreatic lesions. *Gastrointest Endosc* 2002; **56**: 543-547
57 **Ahmad NA**, Kochman ML, Lewis JD, Ginsberg GG. Can EUS alone differentiate between malignant and benign cystic lesions of the pancreas? *Am J Gastroenterol* 2001; **96**: 3295-3300
58 **Gerke H**, Jaffe TA, Mitchell RM, Byrne MF, Stiffler HL, Branch MS, Baillie J, Jowell PS. Endoscopic ultrasound and computer tomography are inaccurate methods of classifying cystic pancreatic lesions. *Dig Liver Dis* 2006; **38**: 39-44
59 **Compton CC**. Serous cystic tumors of the pancreas. *Semin Diagn Pathol* 2000; **17**: 43-55
60 **Warshaw AL**, Rutledge PL. Cystic tumors mistaken for pancreatic pseudocysts. *Ann Surg* 1987; **205**: 393-398
61 **Azar C**, Van de Stadt J, Rickaert F, Devière M, Baize M, Klöppel G, Gelin M, Cremer M. Intraductal papillary mucinous tumours of the pancreas. Clinical and therapeutic issues in 32 patients. *Gut* 1996; **39**: 457-464
62 **Hruban RH**, Takaori K, Klimstra DS, Adsay NV, Albores-Saavedra J, Biankin AV, Biankin SA, Compton C, Fukushima N, Furukawa T, Goggins M, Kato Y, Klöppel G, Longnecker DS, Lüttges J, Maitra A, Offerhaus GJ, Shimizu M, Yonezawa S. An illustrated consensus on the classification of pancreatic intraepithelial neoplasia and intraductal papillary mucinous neoplasms. *Am J Surg Pathol* 2004; **28**: 977-987
63 **Seicean A**, Tantau M, Badea R, Spârchez Z. The applicability of radial endoscopic ultrasonography in pancreatic diseases. *J Gastrointestin Liver Dis* 2007; **16**: 77-83
64 **Sakamoto H**, Kitano M, Komaki T, Imai H, Kamata K, Kimura M, Takeyama Y, Kudo M. Small invasive ductal

carcinoma of the pancreas distinct from branch duct intraductal papillary mucinous neoplasm. *World J Gastroenterol* 2009; **15**: 5489-5492
65 **Hara T**, Yamaguchi T, Ishihara T, Tsuyuguchi T, Kondo F, Kato K, Asano T, Saisho H. Diagnosis and patient management of intraductal papillary-mucinous tumor of the pancreas by using peroral pancreatoscopy and intraductal ultrasonography. *Gastroenterology* 2002; **122**: 34-43
66 **Koito K**, Namieno T, Nagakawa T, Shyonai T, Hirokawa N, Morita K. Solitary cystic tumor of the pancreas: EUS-pathologic correlation. *Gastrointest Endosc* 1997; **45**: 268-276
67 **Compagno J**, Oertel JE. Mucinous cystic neoplasms of the pancreas with overt and latent malignancy (cystadenocarcinoma and cystadenoma). A clinicopathologic study of 41 cases. *Am J Clin Pathol* 1978; **69**: 573-580
68 **Tanaka M**, Chari S, Adsay V, Fernandez-del Castillo C, Falconi M, Shimizu M, Yamaguchi K, Yamao K, Matsuno S. International consensus guidelines for management of intraductal papillary mucinous neoplasms and mucinous cystic neoplasms of the pancreas. *Pancreatology* 2006; **6**: 17-32
69 **Eloubeidi MA**, Gress FG, Savides TJ, Wiersema MJ, Kochman ML, Ahmad NA, Ginsberg GG, Erickson RA, Dewitt J, Van Dam J, Nickl NJ, Levy MJ, Clain JE, Chak A, Sivak MV Jr, Wong R, Isenberg G, Scheiman JM, Bounds B, Kimmey MB, Saunders MD, Chang KJ, Sharma A, Nguyen P, Lee JG, Edmundowicz SA, Early D, Azar R, Etemad B, Chen YK, Waxman I, Shami V, Catalano MF, Wilcox CM. Acute pancreatitis after EUS-guided FNA of solid pancreatic masses: a pooled analysis from EUS centers in the United States. *Gastrointest Endosc* 2004; **60**: 385-389
70 **Sakamoto H**, Kitano M, Komaki T, Noda K, Chikugo T, Dote K, Takeyama Y, Das K, Yamao K, Kudo M. Prospective comparative study of the EUS guided 25-gauge FNA needle with the 19-gauge Trucut needle and 22-gauge FNA needle in patients with solid pancreatic masses. *J Gastroenterol Hepatol* 2009; **24**: 384-390
71 **Sakamoto H**, Kitano M, Dote K, Tchikugo T, Takeyama Y, Kudo M. In situ carcinoma of pancreas diagnosed by EUS-FNA. *Endoscopy* 2008; **40** Suppl 2: E15-E16
72 **Harewood GC**, Wiersema MJ. Endosonography-guided fine needle aspiration biopsy in the evaluation of pancreatic masses. *Am J Gastroenterol* 2002; **97**: 1386-1391
73 **Raut CP**, Grau AM, Staerkel GA, Kaw M, Tamm EP, Wolff RA, Vauthey JN, Lee JE, Pisters PW, Evans DB. Diagnostic accuracy of endoscopic ultrasound-guided fine-needle aspiration in patients with presumed pancreatic cancer. *J Gastrointest Surg* 2003; **7**: 118-126; discussion 127-128
74 **Agarwal B**, Abu-Hamda E, Molke KL, Correa AM, Ho L. Endoscopic ultrasound-guided fine needle aspiration and multidetector spiral CT in the diagnosis of pancreatic cancer. *Am J Gastroenterol* 2004; **99**: 844-850
75 **Voss M**, Hammel P, Molas G, Palazzo L, Dancour A, O'Toole D, Terris B, Degott C, Bernades P, Ruszniewski P. Value of endoscopic ultrasound guided fine needle aspiration biopsy in the diagnosis of solid pancreatic masses. *Gut* 2000; **46**: 244-249
76 **Ardengh JC**, de Paulo GA, Ferrari AP. EUS-guided FNA in the diagnosis of pancreatic neuroendocrine tumors before surgery. *Gastrointest Endosc* 2004; **60**: 378-384
77 **Ardengh JC**, Lopes CV, Campos AD, Pereira de Lima LF, Venco F, Módena JL. Endoscopic ultrasound and fine needle aspiration in chronic pancreatitis: differential diagnosis between pseudotumoral masses and pancreatic cancer. *JOP* 2007; **8**: 413-421
78 **Sedlack R**, Affi A, Vazquez-Sequeiros E, Norton ID, Clain JE, Wiersema MJ. Utility of EUS in the evaluation of cystic pancreatic lesions. *Gastrointest Endosc* 2002; **56**: 543-547
79 **Sperti C**, Pasquali C, Guolo P, Polverosi R, Liessi G, Pedrazzoli S. Serum tumor markers and cyst fluid analysis are useful for the diagnosis of pancreatic cystic tumors. *Cancer* 1996; **78**: 237-243
80 **Carlson SK**, Johnson CD, Brandt KR, Batts KP, Salomao DR. Pancreatic cystic neoplasms: the role and sensitivity of needle aspiration and biopsy. *Abdom Imaging* 1998; **23**: 387-393
81 **Nguyen GK**, Suen KC, Villanueva RR. Needle aspiration cytology of pancreatic cystic lesions. *Diagn Cytopathol* 1997; **17**: 177-182
82 **Sperti C**, Pasquali C, Guolo P, Polverosi R, Liessi G, Pedrazzoli S. Serum tumor markers and cyst fluid analysis are useful for the diagnosis of pancreatic cystic tumors. *Cancer* 1996; **78**: 237-243
83 **Hammel P**. Role of tumor markers in the diagnosis of cystic and intraductal neoplasms. *Gastrointest Endosc Clin N Am* 2002; **12**: 791-801
84 **Brugge WR**, Lewandrowski K, Lee-Lewandrowski E, Centeno BA, Szydlo T, Regan S, del Castillo CF, Warshaw AL. Diagnosis of pancreatic cystic neoplasms: a report of the cooperative pancreatic cyst study. *Gastroenterology* 2004; **126**: 1330-1336
85 **van der Waaij LA**, van Dullemen HM, Porte RJ. Cyst fluid analysis in the differential diagnosis of pancreatic cystic lesions: a pooled analysis. *Gastrointest Endosc* 2005; **62**: 383-389
86 **Frossard JL**, Amouyal P, Amouyal G, Palazzo L, Amaris J, Soldan M, Giostra E, Spahr L, Hadengue A, Fabre M. Performance of endosonography-guided fine needle aspiration and biopsy in the diagnosis of pancreatic cystic lesions. *Am J Gastroenterol* 2003; **98**: 1516-1524
87 **Sand JA**, Hyoty MK, Mattila J, Dagorn JC, Nordback IH. Clinical assessment compared with cyst fluid analysis in the differential diagnosis of cystic lesions in the pancreas. *Surgery* 1996; **119**: 275-280
88 **Varadarajulu S**, Eloubeidi MA. The role of endoscopic ultrasonography in the evaluation of pancreatico-biliary cancer. *Gastrointest Endosc Clin N Am* 2005; **15**: 497-511, viii-ix
89 **Fujita N**, Noda Y, Kobayashi G, Kimura K, Ito K. Endoscopic approach to early diagnosis of pancreatic cancer. *Pancreas* 2004; **28**: 279-281
90 **Minami Y**, Kudo M. Contrast-enhanced harmonic ultrasound imaging in ablation therapy for primary hepatocellular carcinoma. *World J Radiol* 2009; **1**: 86-91
91 **Xu HX**. Contrast-enhanced ultrasound: The evolving applications. *World J Radiol* 2009; **1**: 15-24
92 **Minami Y**, Kudo M, Chung H, Kawasaki T, Yagyu Y, Shimono T, Shiozaki H. Contrast harmonic sonography-guided radiofrequency ablation therapy versus B-mode sonography in hepatocellular carcinoma: prospective randomized controlled trial. *AJR Am J Roentgenol* 2007; **188**: 489-494
93 **Minami Y**, Kudo M, Kawasaki T, Chung H, Ogawa C, Shiozaki H. Percutaneous radiofrequency ablation guided by contrast-enhanced harmonic sonography with artificial pleural effusion for hepatocellular carcinoma in the hepatic dome. *AJR Am J Roentgenol* 2004; **182**: 1224-1226
94 **Inoue T**, Kitano M, Kudo M, Sakamoto H, Kawasaki T, Yasuda C, Maekawa K. Diagnosis of gallbladder diseases by contrast-enhanced phase-inversion harmonic ultrasonography. *Ultrasound Med Biol* 2007; **33**: 353-361
95 **Kitano M**, Kudo M, Maekawa K, Suetomi Y, Sakamoto H, Fukuta N, Nakaoka R, Kawasaki T. Dynamic imaging of pancreatic diseases by contrast enhanced coded phase inversion harmonic ultrasonography. *Gut* 2004; **53**: 854-859
96 **Becker D**, Strobel D, Bernatik T, Hahn EG. Echo-enhanced color- and power-Doppler EUS for the discrimination between focal pancreatitis and pancreatic carcinoma. *Gastrointest Endosc* 2001; **53**: 784-789
97 **Ding H**, Kudo M, Onda H, Suetomi Y, Minami Y, Chung H, Kawasaki T, Maekawa K. Evaluation of posttreatment response of hepatocellular carcinoma with contrast-enhanced coded phase-inversion harmonic US: comparison with dynamic CT. *Radiology* 2001; **221**: 721-730
98 **Rickes S**, Mönkemüller K, Malfertheiner P. Echo-enhanced

ultrasound with pulse inversion imaging: A new imaging modality for the differentiation of cystic pancreatic tumours. *World J Gastroenterol* 2006; **12**: 2205-2208

99 **Wen YL**, Kudo M, Zheng RQ, Minami Y, Chung H, Suetomi Y, Onda H, Kitano M, Kawasaki T, Maekawa K. Radiofrequency ablation of hepatocellular carcinoma: therapeutic response using contrast-enhanced coded phase-inversion harmonic sonography. *AJR Am J Roentgenol* 2003; **181**: 57-63

100 **Hocke M**, Schulze E, Gottschalk P, Topalidis T, Dietrich CF. Contrast-enhanced endoscopic ultrasound in discrimination between focal pancreatitis and pancreatic cancer. *World J Gastroenterol* 2006; **12**: 246-250

101 **Kitano M**, Sakamoto H, Matsui U, Ito Y, Maekawa K, von Schrenck T, Kudo M. A novel perfusion imaging technique of the pancreas: contrast-enhanced harmonic EUS (with video). *Gastrointest Endosc* 2008; **67**: 141-150

102 **Gorce JM**, Arditi M, Schneider M. Influence of bubble size distribution on the echogenicity of ultrasound contrast agents: a study of SonoVue. *Invest Radiol* 2000; **35**: 661-671

103 **Rickes S**, Uhle C, Kahl S, Kolfenbach S, Monkemuller K, Effenberger O, Malfertheiner P. Echo enhanced ultrasound: a new valid initial imaging approach for severe acute pancreatitis. *Gut* 2006; **55**: 74-78

104 **Furukawa T**, Oohashi K, Yamao K, Naitoh Y, Hirooka Y, Taki T, Itoh A, Hayakawa S, Watanabe Y, Goto H, Hayakawa T. Intraductal ultrasonography of the pancreas: development and clinical potential. *Endoscopy* 1997; **29**: 561-569

105 **Furukawa T**, Tsukamoto Y, Naitoh Y, Hirooka Y, Hayakawa T. Differential diagnosis between benign and malignant localized stenosis of the main pancreatic duct by intraductal ultrasound of the pancreas. *Am J Gastroenterol* 1994; **89**: 2038-2041

106 **Menzel J**, Poremba C, Dietl KH, Domschke W. Preoperative diagnosis of bile duct strictures--comparison of intraductal ultrasonography with conventional endosonography. *Scand J Gastroenterol* 2000; **35**: 77-82

107 **Hara T**, Yamaguchi T, Ishihara T, Tsuyuguchi T, Kondo F, Kato K, Asano T, Saisho H. Diagnosis and patient management of intraductal papillary-mucinous tumor of the pancreas by using peroral pancreatoscopy and intraductal ultrasonography. *Gastroenterology* 2002; **122**: 34-43

108 **Giovannini M**. Contrast-enhanced endoscopic ultrasound and elastosonoendoscopy. *Best Pract Res Clin Gastroenterol* 2009; **23**: 767-779

109 **Saftoiu A**, Gheonea DI. Tridimensional (3D) endoscopic ultrasound - a pictorial review. *J Gastrointestin Liver Dis* 2009; **18**: 501-505

S- Editor Cheng JX **L- Editor** Webster JR **E- Editor** Zheng XM

World Journal of Radiology

Online Submissions: http://www.wjgnet.com/1949-8470office
wjr@wjgnet.com
doi:10.4329/wjr.v2.i4.135

World J Radiol 2010 April 28; 2(4): 135-142
ISSN 1949-8470 (online)

REVIEW

Proton therapy dosimetry using positron emission tomography

Matthew T Studenski, Ying Xiao

Matthew T Studenski, Ying Xiao, Bodine Cancer Center, Department of Radiation Oncology, Thomas Jefferson University Hospital, 111 S. 11th St., Room G-321 Gibbon Building, Philadelphia, PA 19107, United States
Author contributions: Studenski MT wrote the paper; Xiao Y reviewed and edited the paper.
Correspondence to: Matthew T Studenski, PhD, Bodine Cancer Center, Department of Radiation Oncology, Thomas Jefferson University Hospital, 111 S. 11th St., Room G-321 Gibbon Building, Philadelphia, PA 19107,
United States. matthew.studenski@Jeffersonhospital.org
Telephone: +1-215-9550300 Fax: +1-215-9550412
Received: March 11, 2010 Revised: April 1, 2010
Accepted: April 12, 2010
Published online: April 28, 2010

Abstract

Protons deposit most of their kinetic energy at the end of their path with no energy deposition beyond the range, making proton therapy a valuable option for treating tumors while sparing surrounding tissues. It is imperative to know the location of the dose deposition to ensure the tumor, and not healthy tissue, is being irradiated. To be able to extract this information in a clinical situation, an accurate dosimetry measurement system is required. There are currently two *in vivo* methods that are being used for proton therapy dosimetry: (1) online or in-beam monitoring and (2) offline monitoring, both using positron emission tomography (PET) systems. The theory behind using PET is that protons experience inelastic collisions with atoms in tissues resulting in nuclear reactions creating positron emitters. By acquiring a PET image following treatment, the location of the positron emitters in the patient, and therefore the path of the proton beam, can be determined. Coupling the information from the PET image with the patient's anatomy, it is possible to monitor the location of the tumor and the location of the dose deposition. This review summarizes current research investigating both of these methods with promising results and reviews the limitations along with the advantages of each method.

Key words: Positron emission tomography; Proton therapy; Dosimetry

Peer reviewers: Tove J Grönroos, PhD, Adjunct Professor, Turku PET Centre, Preclinical Imaging/Medicity Research Laboratory, Tykistokatu 6A, FI-20520 Turku, Finland; Sandip Basu, MBBS (Hons), DRM, DNB, MNAMS, Head, Nuclear Medicine Academic Programme, Radiation Medicine Centre, Bhabha Atomic Research Centre, Tata Memorial Hospital Annexe, Parel, Bombay 400012, India; Filippo Cademartiri, MD, PhD, Departmento of Radiology - c/o Piastra Tecnica - Piano 0, Azienda Ospedaliero-Universitaria di Parma, Via Gramsci, 14 - 43100 Parma, Italy

Studenski MT, Xiao Y. Proton therapy dosimetry using positron emission tomography. *World J Radiol* 2010; 2(4): 135-142 Available from: URL: http://www.wjgnet.com/1949-8470/full/v2/i4/135.htm DOI: http://dx.doi.org/10.4329/wjr.v2.i4.135

INTRODUCTION

Radiation can be delivered to kill tumors in a variety of ways. Treatments range from brachytherapy (implanting a radioactive seed in the tumor), to radioactively tagged molecules that are injected into the patient and are uptaken into the tumor, to external X-ray and electron beam treatments using linear accelerators or radioactive isotopes, to heavy ions produced in cyclotrons or synchrotrons. All of these therapies are used clinically but proton therapy is becoming more and more popular due to the unique dose deposition of heavy charged particles. Protons deposit almost all of their energy at the end of their path, called the Bragg peak, and therefore it is imperative that this Bragg peak is located in the tumor and not in healthy tissue.

As the power of proton therapy to treat cancer is recognized, new facilities are being constructed and commissioned worldwide. However, there are currently many unanswered questions regarding proton therapy. One of

the most important unknowns is the uncertainty in the location of the dose deposition. Knowing this location exactly is difficult due to internal motion of the patient's organs and the changing anatomy of the tumor over a course of radiation therapy. Furthermore, the range of the proton is uncertain due to tissue inhomogeneities and complications in modeling proton transport. It is essential to have a dosimetry system that can relate the location of the proton dose deposition to the patient's anatomy at the time of treatment for verification as well as for adaptation of the treatment plan as needed.

Investigation into devices like thermoluminescent dosimeters[1-4] to measure the dose from proton therapy shows potential but the emerging trend for *in vivo* proton therapy dosimetry is positron emission tomography (PET)[5-11]. The theory is that, as the protons enter the patient, they undergo inelastic collisions with atoms in tissues, which result in nuclear reactions producing positron emitters[12]. The PET system can detect the annihilation photons produced in the patient and therefore the location of the proton beam can be established and then related to the patient's anatomy.

PROTON THERAPY

History

Proton therapy was first suggested by Harvard physicist Robert Wilson in 1946[13]. Wilson went on to support his idea by showing that proton therapy can place the maximum radiation dose in the tumor without harming surrounding tissues. He also showed that for larger tumors, the normally narrow Bragg peak can be spread out using a modulator wheel. Following this publication, research on proton therapy began. In 1954, the first proton therapy treatment was performed on a pituitary tumor and, by 1958, proton therapy was widely accepted as a neurosurgery tool[14].

Theory

The physics of proton energy deposition is the driving factor for their use in radiation therapy as opposed to photons. The depth dose curve for photons follows a buildup region, a peak at a depth where the dose is at a maximum, and a long tail as the depth increases as seen in Figure 1. The shape of this curve is result of the exponential attenuation of photons in a medium[15]. Photons are indirectly ionizing radiation, that is, they must transfer energy to other charged particles, like electrons, which then deposit dose. Since one goal of radiation therapy is to spare healthy tissue, the exponential tail is undesirable because it will deposit dose in healthy tissues after passing through the tumor. Furthermore, the depth of the maximum dose is relatively fixed near the surface of the patient so treating deep tumors is inefficient since the maximum dose cannot be located on the tumor.

Protons are directly ionizing charged particles. Charged particles deposit energy through four interactions; (1) inelastic collisions with atomic electrons; (2) inelastic collisions with the nucleus; (3) elastic collisions with atomic electrons; and (4) elastic collisions with the nucleus[15]. Protons are considered heavy charged particles (opposed to electrons or positrons, which are light). The path of protons tends to be straight and the energy deposited (E) along the path ds can be calculated using Eq. 1[15].

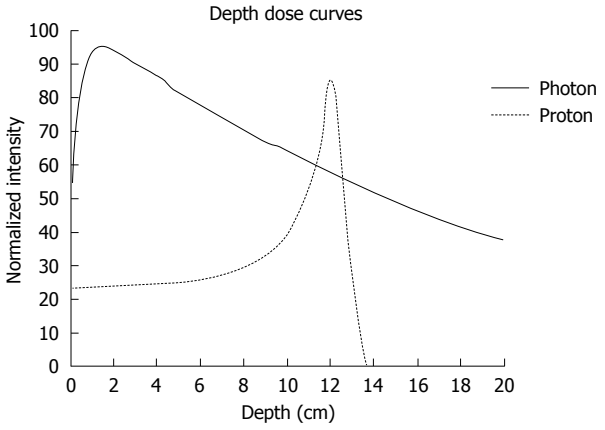

Figure 1 Depth dose curves for photons and protons. Notice the exponential tail seen in the photon curve that results in dose deposition through the entire patient. The proton curve shows that there is no dose deposition after the Bragg peak.

Eq. 1:

$$\frac{dE}{ds} = \frac{4\pi e^4 z^2}{m_0 V^2} NZ\left[\ln\frac{2m_0V^2}{I} - \ln\left(1-\beta^2\right) - \beta^2\right]$$

In this equation, the proton has charge ze, velocity $V = \beta c$, in a medium of N atoms/cm^3 and atomic number Z, and ionizing potential I.

Eq. 1 shows that the energy of the proton is constantly decreasing as it traverses through a medium. As the energy decreases, the amount of ionization per unit length increases[16]. The result of this is that most of the proton's energy is deposited at the end of the path in a region called the Bragg peak. The difference between proton dose deposition and that of photons can been seen in the depth dose profiles in Figure 1. The shape of the Bragg peak is determined by the average ionization per unit length $I(r)$ as defined in Eq. 2[15].

Eq. 2:

$$I(r) = \int_r^\infty \frac{i(x-r)}{\alpha\sqrt{\pi}} e^{-[(x-R)/\alpha]^2} dx$$

In Eq. 2, r is the distance from the source, x is the range of an individual particle, $i(x-r)$ is the specific ionization along the path of an individual particle at a distance $(x-r)$ from the end of its path, and a is the range straggling parameter.

As seen in Figure 1, the Bragg peak is the driving force behind using protons for radiation therapy because beyond the range of the proton, there is no more ionization and therefore no more dose deposition. In addition, the depth of the Bragg peak is energy dependent and therefore the location of the dose deposition can be controlled to be directly on the tumor. The Bragg peak can be spread out through modulation to treat larger

tumors. The overall result of this is a higher dose to the tumor with a reduced dose to the surrounding healthy tissue.

Problems

There are several issues with proton therapy that are currently under investigation. One of these is the lateral penumbra that results from the spread of the beam from proton scatterings in the modulator wheel, the aperture, the bolus, and in the patient. This causes protons to lose energy and have trajectories that are different than expected, widening the beam by as much as a few millimeters[17,18].

A second issue is that the treatment planning is done using a computed tomography (CT) scan to determine stopping powers in the different tissues for the protons. The CT images have pixels that are in Hounsfield units, which can then be related to electron density in tissue. Because of the errors in converting between Hounsfield units and proton stopping power, the expected range of the protons for treatment plans based on Hounsfield units can have errors up to several mm in bone and soft tissue[19-21].

Other uncertainties in proton therapy result from the treatment planning. There are three methods of treatment planning: ray-tracing, pencil beam approximation[22], and Monte Carlo simulations. The fastest is simple ray-tracing but this is very susceptible to errors from tissue inhomogeneities and at tissue interfaces. The pencil beam approximation is more accurate but this method only convolves functions that represent the incident beam and the scattering conditions so there is still uncertainty in the result. The most accurate is a Monte Carlo simulation, but this is extremely time consuming. However, physical processes like nuclear fragmentation and energy loss straggling can be ignored to reduce computation time. With the rapid advancement of computing technology, the speed may become less of an issue.

One of the most important issues is that of accurate delivery of dose to the patient[23]. This depends both on the delivery of the beam and monitoring the changes in patient anatomy from motion or deformations of targets and structures between treatments. If one can accurately monitor the dose delivered to the patient, the dose to the tumor and surrounding tissues can be measured and modified, if necessary. One of the most promising methods of dosimetry for proton therapy is to use PET imaging to track the positron emitters created from inelastic nuclear collisions of protons with the elements in tissues.

PET FOR PROTON THERAPY DOSIMETRY

As stated above, the rational behind using PET for dosimetry is that as the protons enter the patient and interact with the elements in tissue, there are inelastic collisions that produce positron emitters. The positron emitters are only produced in very small quantities and are short lived, but the detected signal is strong enough to be used as a method for dosimetry. Table 1 shows the main isotopes produced by inelastic collisions of protons in tissue.

Table 1 Relevant positron emitter reactions in tissue from proton therapy

Reaction	Threshold energy (MeV)	Half life (min)	Positron energy (MeV)
$^{16}O(p, pn)^{15}O$	16.79	2.037	1.72
$^{16}O(p, \alpha)^{13}N$	5.66	9.965	1.19
$^{14}N(p, pn)^{13}N$	11.44	9.965	1.19
$^{12}C(p, pn)^{11}C$	20.61	20.390	0.96
$^{14}N(p, \alpha)^{11}C$	3.22	20.390	0.96
$^{16}O(p, \alpha pn)^{11}C$	59.64	20.390	0.96

The image obtained from a PET scan after proton therapy is essentially the negative of the dose deposited[8,10]. Because of the energy dependence of the reaction cross sections, the inelastic scattering nuclear reactions tend to occur at higher proton energies than at the proton energies associated with the Bragg peak. Because of this, at the Bragg peak, the concentration of the positron emitters rapidly decreases because energy deposition happens through other interactions, not inelastic collisions. Therefore, the PET image shows activity up to the Bragg peak and then falls off, which is extremely important because the location of the Bragg peak can then be determined.

Due to scatterings in the beam delivery system, patient motion, and changes in the anatomy of the patient throughout treatment, an ideal treatment delivery can be difficult to achieve. The activity distribution of the positron emitters seen in the PET images provides information on where the dose was actually delivered for that particular treatment. By tracking the delivered dose from fraction to fraction, the treatment plan can be modified as needed to ensure the dose is delivered to the tumor.

There are two ways to acquire a PET image from proton therapy for dosimetry. The first of these is what is called in-beam or online PET monitoring. This method consists of a small field-of-view dual head PET system that is physically attached to the proton gantry as seen in Figure 2[24]. The advantage of this approach is that the acquisitions are performed during or very soon after the treatment so there is minimal decay from the short lived positron emitters. Also, the patient remains in the treatment position so there is no anatomical shifting.

The second approach is called offline monitoring and the patient is moved following treatment to a dedicated PET/CT scanner. This transfer can take up to 30 min during which many of the positron emitters have decayed or been transported away from their original location by the circulatory or lymphatic system in a process called biological washout. On the other hand, the image acquired on the dedicated PET/CT scanner is easily fused to obtain anatomical information and the sensitivity and spatial resolution is improved. Both approaches are cur-

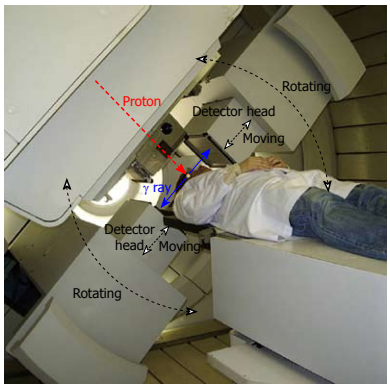

Figure 2 Setup of the on-line positron emission tomography (PET) system mounted on the rotating proton gantry. The proton beam direction is shown by the red line and the direction of the detected annihilation photons is shown in blue. (Reprinted from[24] with permission from Elsevier Limited).

rently under investigation and show promising results in proton therapy dosimetry.

Online monitoring

Online monitoring of positron emitters for radiation therapy was introduced in the late 1990s for carbon ion therapy[25,26]. More recently, two groups have applied this method to proton therapy. The first group, led by Parodi K, focused mainly on the feasibility of this approach for proton therapy. The investigators compared the activity distributions of positron emitters from carbon therapy and proton therapy[27,28]. In carbon therapy, because of the interaction of the heavier carbon ions, spallation products form a peak of activity very close to the actual Bragg peak. With protons, the activity distribution is constant as the beam enters the patient and falls off at the Bragg peak (due to the dependence of the reaction cross section on energy). Although it was not as easy as using the activity peak as with carbon therapy, it was found that there was a correlation between the 50% level of the fall-off region and the location of the Bragg peak. There was also good agreement with the lateral spread of the beam. The greatest advantage of the on-line system was that the acquisition was performed immediately following treatment reducing both the decay of the short lived isotopes and also the effect of biological washout.

The second group, led by Nishio T, also performed preliminary studies with their system and found the results to be satisfactory[29]. Along with the reduced decay and biological washout, it was found to be much easier to perform daily PET imaging with the online system. With this in mind, a workflow for quality assurance was developed where a daily PET image was acquired and compared to the initial PET image (Figure 3[24]). It was found that as treatment progressed, the tumor would shrink and the patient's anatomy would change. This change resulted in a deformation of the activity distribution from the initial plan. When this deviation in the daily PET image was found, the patient would be replanned to account for the change in the anatomy. This workflow was put into clinical practice and the results were analyzed for 48 patients with tumors in the head and neck, liver, lungs, prostate, and brain[24]. The daily monitoring showed that reduction in the head and neck tumors changed the dose distribution and the plans were adjusted accordingly. It was also found that biological washout of the positron emitters in liver cells was slower in necrotic cells than in non-necrotic cells. Overall, this method of daily, online monitoring of the dose distribution from proton therapy was confirmed as feasible in a clinical environment.

Although this method shows promise for proton therapy dosimetry, disadvantages of using the on-line system include reduced sensitivity of the detectors, a small field of view, and geometrical problems from the orientation of the beam and the detectors interferes with 3D image acquisition[26,30,31]. The reduced sensitivity and small field of view are in relationship to a dedicated PET system since in a dedicated system, there are essentially multiple opposed detector heads forming a ring around the patient, increasing both sensitivity and field of view size. Furthermore, anatomical images are not obtained daily with the online system. Nishio mentions that the addition of daily cone-beam CT would alleviate this problem.

Offline monitoring

As with the on-line systems, initial research using an offline PET/CT scanner following proton therapy showed promise for clinical investigation[17,18,32,33]. The problem faced with this method is the time required to move the patient from the treatment room to the PET/CT scanner resulting in time for decay causing loss of signal, biological washout, and anatomical motion, depending on the treatment site. The loss in signal from decay is partially offset by the high sensitivity and spatial resolution of new PET/CT systems and that the field-of-view is much larger. Another advantage of the PET/CT scanner is the ease of fusing anatomical information to the activity image. Performing a full CT scan before the PET scan allows for accurate attenuation corrections and a co-registered image to be used with the PET scan.

Three clinical studies have recently been completed using the offline approach for dosimetry[34-36]. The group led by Nishio T studied about 20 patients undergoing proton therapy to the brain, head and neck, liver, lungs, and sacrum. One focus of this study was the effect of the biological washout of the positron emitters during the time it took to transport the patient to the PET/CT scanner. This motivation was spurred by the group's research into the on-line PET method. Upon visual inspection of the activity images following treatment of the different sites, it was found that activity conformed well to the planned treatment area (treatment depth and lateral spread). The highest activity was found in adipose tissue and in bone. To quantify this observation, three points were taken for each site of interest, one in the

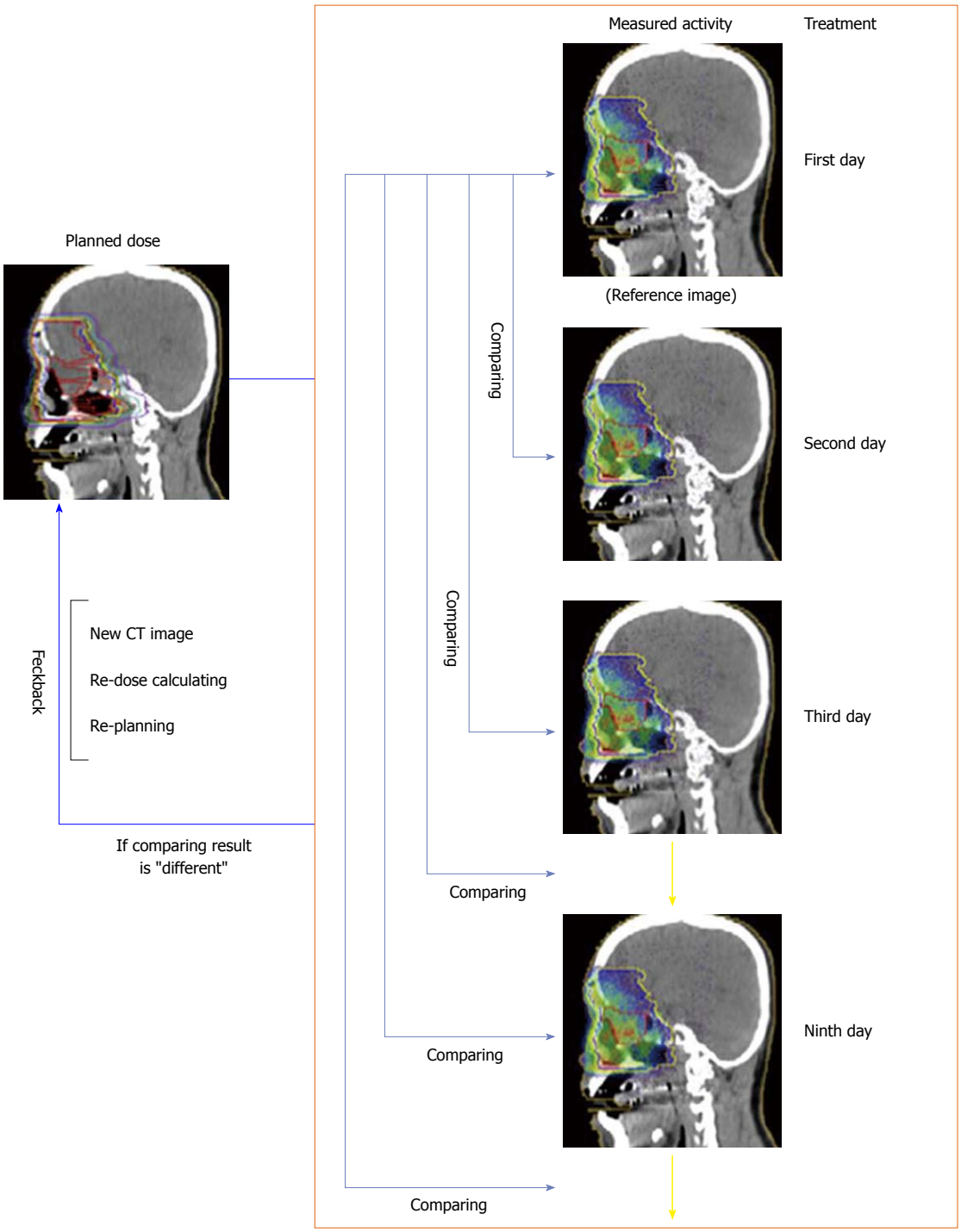

Figure 3 Flow diagram of the procedure for the clinical use of an on-line PET system (Reprinted from[24] with permission from Elsevier Limited).

soft tissue (or tumor), one in the adipose tissue, and one in the bone tissue. The measured activity was compared to both a calculated activity based on tissue composition, decay, and biological washout effects, and to a simulation of the activity that would be obtained with an on-line system immediately following treatment. Results showed good agreement between the measured and calculated activity in soft tissue, an increase of two to four in the calculated adipose tissue activity, and an increase of two times the activity in bone. The increase in activity was believed to be a result of inaccurate attenuation corrections for the adipose tissue near the surface and the increase in bone tissue was believed to be from inaccuracies in the Ca-40 fragmentation cross section. The simulation of using an on-line system showed losses in activity intensity from transportation to the offline system of up to 75%, depending on the type of tissue. Also, it was found that the effect of biological washout was lower than the previously estimated 50%-65%, although the overall effect was not quantified[37,38].

The study led by Parodi K took nine patients with different types of head and neck cancers and used a PET/

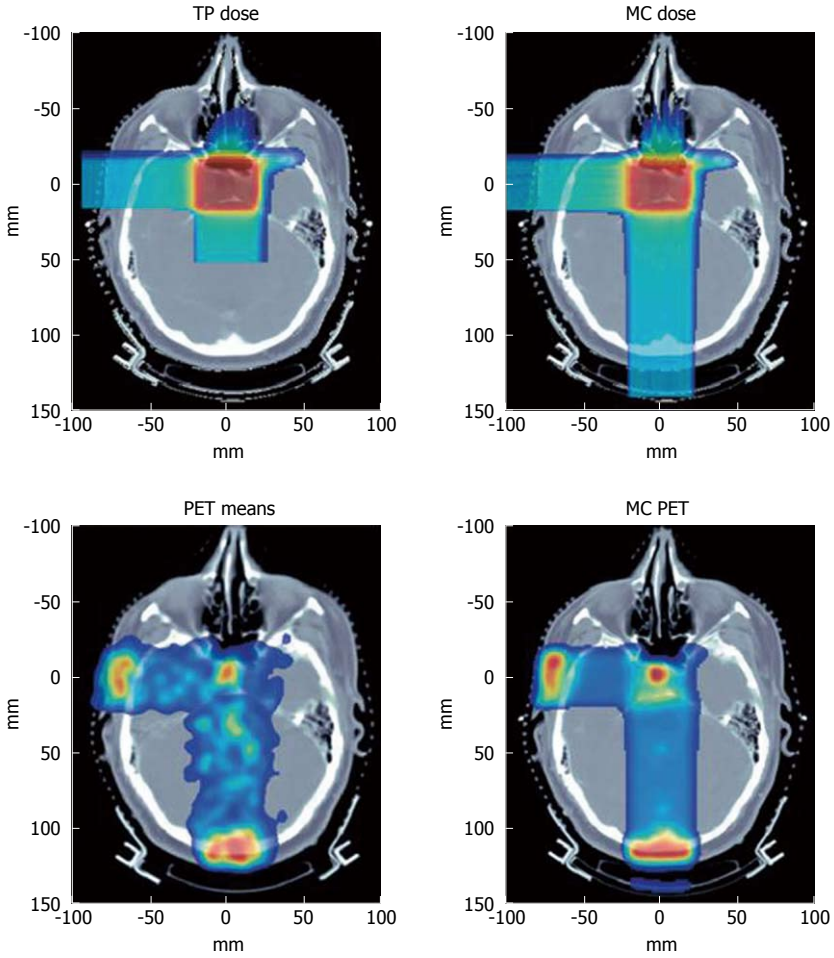

Figure 4 Top: Treatment plan (TP) and Monte Carlo (MC) dose for a patient with pituitary adenoma receiving two orthogonal fields. Bottom: Measured and Monte Carlo PET images. Delay times from the beginning of imaging were about 26 and 18 min from the end of the first and second field applications, respectively. Range of color wash is from blue (minimum) to red (maximum) (Reprinted from[34] with permission from Elsevier Limited).

CT system to verify the dose to the patient with the motivation that an on-line system can only be used for a visual inspection of dose deposition since the activity is not directly proportional to the dose. In this study, the measured activity from the offline PET scan was compared to the expected activity distribution calculated using the FLUKA Monte Carlo code accounting for biological decay and image formation[39]. The results from a patient with a pituitary adenoma can be seen in Figure 4[34]. With this method, range monitoring of proton depth was accurate to within 2 mm. As with the study by T. Nishio, the biological washout in different tissues was also examined. It was found that there was reduced biological decay in adipose tissue and bone and increased perfusion throughout the muscle and brain. Overall, this method was shown to be feasible for clinical *in vivo* dosimetry following proton therapy and it was suggested that new technology such as time-of-flight PET and new filtering methods to account for activity distributions over time could further improve this technique[40,41].

The final study led by Hsi W and Indelicato D acquired 50 PET/CT imaging studies on 10 different prostate cancer patients[36]. Instead of trying to quantify the dose delivered, this study defined the activity seen in the pelvic bone as the PET-defined beam path and compared this to the marker-defined beam path, which was calculated from seeds implanted in the prostate. The pelvic bone was chosen as the anatomical landmark to reduce the activity inhomogeneities seen in other tissues. The goal was to determine if the margins (4 mm axial, 6 mm superior and inferior perpendicular to the beam path, 7 mm proximal to the beam path, and 5 mm distal to the beam path) used for treatment were sufficient to account for prostate motion throughout treatment. The deviations between the PET-defined path and the marker-defined path were analyzed for these 10 patients. The images from one patient are seen in Figure 5[36]. Results of this study showed that with the proper immobilization device, less than 2° of angular rotation was seen for all patients. The motion of the prostate was also traced in the superior-inferior direction and in the anterior-posterior direction. It was found that for 30 of the 50 cases, motion in both of those directions was less than 6 mm, meaning that the planning margins were sufficient. For the other 20 cases, 13 of these were considered motion-after-treatment cases where large volumes of rectal gas caused prostate motion of more than 6 mm in any direction. The final seven cases were deemed position-error cases which showed no misalignment but the prostate moved more than 6 mm. These cases showed that there was either an error in positioning the patient or the prostate moved after positioning but before the proton beam was turned on.

This study demonstrated that the accepted clinical

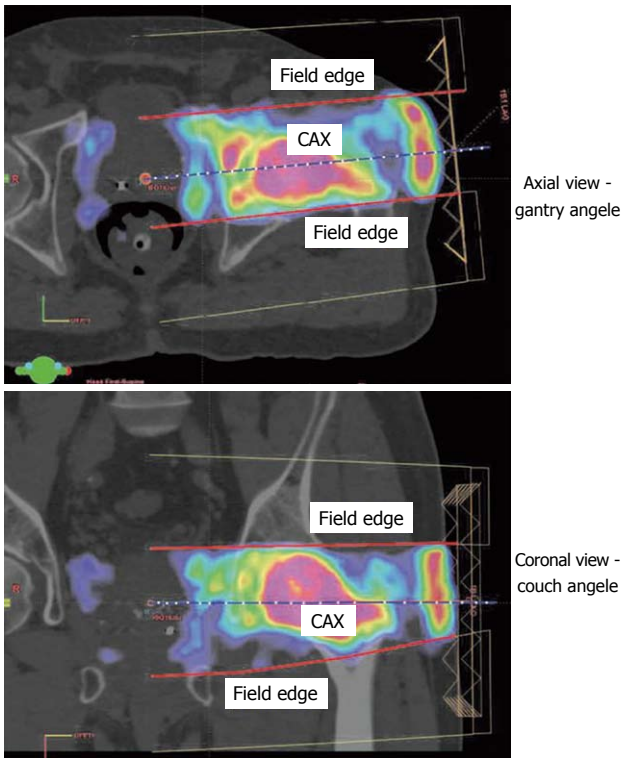

Figure 5 Registered PET images are shown in the axial and coronal views through the prostate. The PET images are fused with the planning computed tomography (CT). The CAX is the central beam axis. The field edge is only extended to the isocenter as provided by the TPS. The isocenter in the lateral direction was set to be the location of the marker-defined path. Good alignment between the field edge and the outer surface of the emitter distribution suggests that no prostate motion occurred after proton beam delivery (Reprinted from[36] with permission from Medical Physics).

margins for treating prostate cancer are sufficient for 86% of the patients. Using this method, the patients with insufficient margins would be noticed during treatment and the margins could be adjusted to account for the extra prostate motion. Again, as with the other studies, offline PET/CT was shown to be a feasible option for proton therapy dosimetry.

CONCLUSION

What method is better, online or offline PET imaging for proton therapy dosimetry? Does the ability to obtain daily activity images in the treatment position outweigh the lack of anatomical data and the smaller field-of-view or is it better to have a good fusion of anatomy and activity with a reduced signal and the possibility of anatomical motion as the patient is transported to the PET/CT scanner? As research progresses into each of these methods, one might develop imaging devices that combine the advantages of both methods. Overall, PET imaging is a robust method for determining the dose to the patient from proton therapy in a noninvasive manner.

REFERENCES

1 **Zullo JR**, Kudchadker RJ, Zhu XR, Sahoo N, Gillin MT. LiF TLD-100 as a dosimeter in high energy proton beam therapy--can it yield accurate results? *Med Dosim* 2010; **35**: 63-66
2 **Hoffman W**, Bienen J, Filges D, Schmitz T. TLD-300 dosimetry in a 175 MeV proton beam. *Rad Prot Dosim* 1999; **85**: 341-343
3 **Hoffman W**. TL dosimetry in high LET radiotherapeutic fields. *Rad Prot Dosim* 1996; **66**: 243-248
4 **Chu TC**, Lin SY, Hsu CC, Li JP. The response of a thermoluminescent dosimeter to low energy protons in the range 30-100 keV. *Appl Radiat Isot* 2001; **55**: 679-684
5 **Oelfke U**, Lam GK, Atkins MS. Proton dose monitoring with PET: quantitative studies in Lucite. *Phys Med Biol* 1996; **41**: 177-196
6 **Litzenberg DW**, Roberts DA, Lee MY, Pham K, Vander Molen AM, Ronningen R, Becchetti FD. On-line monitoring of radiotherapy beams: experimental results with proton beams. *Med Phys* 1999; **26**: 992-1006
7 **Paans AJM**, Schippers JM. Proton therapy in combination with PET as monitor: a feasibility study. *IEEE Trans Nucl Sci* 1993; **40**: 1041-1044
8 **Parodi K**, Enghardt W. Potential application of PET in quality assurance of proton therapy. *Phys Med Biol* 2000; **45**: N151-N156
9 **Vynckier S**, Derreumaux S, Richard F, Bol A, Michel C, Wambersie A. Is it possible to verify directly a proton-treatment plan using positron emission tomography? *Radiother Oncol* 1993; **26**: 275-277
10 **Beebe-Wang JJ**, Dilmanian FA, Peggs SG, Schlyer DJ, Vaska P. Feasibility of Positron Emission Tomography of Dose Distribution in Proton Beam Cancer Therapy. Proceedings of EPAC. Paris, France, 2002
11 **Hishikawa Y**, Kagawa K, Murakami M, Sakai H, Akagi T, Abe M. Usefulness of positron-emission tomographic images after proton therapy. *Int J Radiat Oncol Biol Phys* 2002; **53**: 1388-1391
12 **Tobias CA**, Benton EV, Capp MP, Chatterjee A, Cruty MR, Henke RP. Particle radiography and autoactivation. *Int J Radiat Oncol Biol Phys* 1977; **3**: 35-44
13 **Wilson RR**. Radiological use of fast protons. *Radiology* 1946; **47**: 487-491
14 History of Proton Beam Therapy. Synthesis 2006; Vol. 9, No. 2. Accessed on February 15, 2010. Available from: URL: http://www.ucdmc.ucdavis.edu/synthesis/issues/fall_winter_06-07/features/history.html
15 **Evans R**. The atomic nucleus. Malabar, FL: Krieger Publishing Company, 1955
16 **Jentschke W**. Messungen an harten H-Strahlung. *Physikal Z* 1940; **41**: 524
17 **Nishio T**, Sato T, Kitamura H, Murakami K, Ogino T. Distributions of beta+ decayed nuclei generated in the CH2 and H2O targets by the target nuclear fragment reaction using therapeutic MONO and SOBP proton beam. *Med Phys* 2005; **32**: 1070-1082
18 **Parodi K**, Ferrari A, Sommerer F, Paganetti H. Clinical CT-based calculations of dose and positron emitter distributions in proton therapy using the FLUKA Monte Carlo code. *Phys Med Biol* 2007; **52**: 3369-3387
19 **Schaffner B**, Pedroni E. The precision of proton range calculations in proton radiotherapy treatment planning: experimental verification of the relation between CT-HU and proton stopping power. *Phys Med Biol* 1998; **43**: 1579-1592
20 **Schneider W**, Bortfeld T, Schlegel W. Correlation between CT numbers and tissue parameters needed for Monte Carlo simulations of clinical dose distributions. *Phys Med Biol* 2000; **45**: 459-478
21 **Nishio T**, Ogino T, Sakudo M, Tanizaki N, Yamada M, Nishida G, Nishimura G, Ikeda H. Present proton treatment planning system at National Cancer Center Hospital East. *Jpn J Med Phys Proc* 2000; **20** Suppl 4: 174-177
22 **Hong L**, Goitein M, Bucciolini M, Comiskey R, Gottschalk B, Rosenthal S, Serago C, Urie M. A pencil beam algorithm for

proton dose calculations. *Phys Med Biol* 1996; **41**: 1305-1330
23 **Lin L**, Vargas C, Hsi W, Indelicato D, Slopsema R, Li Z, Yeung D, Horne D, Palta J. Dosimetric uncertainty in prostate cancer proton radiotherapy. *Med Phys* 2008; **35**: 4800-4807
24 **Nishio T**, Miyatake A, Ogino T, Nakagawa K, Saijo N, Esumi H. The development and clinical use of a beam ON-LINE PET system mounted on a rotating gantry port in proton therapy. *Int J Radiat Oncol Biol Phys* 2010; **76**: 277-286
25 **Pawelke J**, Byars L, Enghardt W, Fromm WD, Geissel H, Hasch BG, Lauckner K, Manfrass P, Schardt D, Sobiella M. The investigation of different cameras for in-beam PET imaging. *Phys Med Biol* 1996; **41**: 279-296
26 **Pawelke J**, Enghardt W, Haberer T, Hasch BG, Hinz R, Kramer M, Lauckner K, Sobiella M. In-beam PET imaging for the control of heavy-ion tumour therapy. *IEEE Trans Nucl Sci* 1997; **44**: 1492-1498
27 **Parodi K**, Enghardt W, Haberer T. In-beam PET measurements of beta+ radioactivity induced by proton beams. *Phys Med Biol* 2002; **47**: 21-36
28 **Parodi K**, Ponisch F, Enghardt W. Experimental study on the feasibility of in-beam PET for accurate monitoring of proton therapy. *IEEE Trans Nucl Sci* 2005; **52**: 778-786
29 **Nishio T**, Ogino T, Nomura K, Uchida H. Dose-volume delivery guided proton therapy using beam on-line PET system. *Med Phys* 2006; **33**: 4190-4197
30 **Enghardt W**, Parodi K, Crespo P, Fiedler F, Pawelke J, Pönisch F. Dose quantification from in-beam positron emission tomography. *Radiother Oncol* 2004; **73** Suppl 2: S96-S98
31 **Parodi K**, Crespo P, Eickhoff H, Haberer T, Pawelke J, Schardt D, Enghardt W. Random coincidences during in-beam PET measurements at microbunched therapeutic ion beams. *Nucl Instr Meth* 2005; **545**: 446-458
32 **Parodi K**, Paganetti H, Cascio E, Flanz JB, Bonab AA, Alpert NM, Lohmann K, Bortfeld T. PET/CT imaging for treatment verification after proton therapy: a study with plastic phantoms and metallic implants. *Med Phys* 2007; **34**: 419-435
33 **Lin L**, Hsi W, Indelicato D, Vargas C, Flampouri S, Slopesema R, Keole SR, Li Z, Yeung D, Palta JR. In vivo verification of dose delivery to prostate cancer by utilizing PET/CT images taken after proton therapy. *Int J Radiat Oncol Biol Phys* 2008; **72** Suppl 1: S144
34 **Parodi K**, Paganetti H, Shih HA, Michaud S, Loeffler JS, DeLaney TF, Liebsch NJ, Munzenrider JE, Fischman AJ, Knopf A, Bortfeld T. Patient study of in vivo verification of beam delivery and range, using positron emission tomography and computed tomography imaging after proton therapy. *Int J Radiat Oncol Biol Phys* 2007; **68**: 920-934
35 **Nishio T**, Miyatake A, Inoue K, Gomi-Miyagishi T, Kohno R, Kameoka S, Nakagawa K, Ogino T. Experimental verification of proton beam monitoring in a human body by use of activity image of positron-emitting nuclei generated by nuclear fragmentation reaction. *Radiol Phys Technol* 2008; **1**: 44-54
36 **Hsi WC**, Indelicato DJ, Vargas C, Duvvuri S, Li Z, Palta J. In vivo verification of proton beam path by using post-treatment PET/CT imaging. *Med Phys* 2009; **36**: 4136-4146
37 **Tomitani T**, Pawelke J, Kanazawa M, Yoshikawa K, Yoshida K, Sato M, Takami A, Koga M, Futami Y, Kitagawa A, Urakabe E, Suda M, Mizuno H, Kanai T, Matsuura H, Shinoda I, Takizawa S. Washout studies of 11C in rabbit thigh muscle implanted by secondary beams of HIMAC. *Phys Med Biol* 2003; **48**: 875-889
38 **Mizuno H**, Tomitani T, Kanazawa M, Kitagawa A, Pawelke J, Iseki Y, Urakabe E, Suda M, Kawano A, Iritani R, Matsushita S, Inaniwa T, Nishio T, Furukawa S, Ando K, Nakamura YK, Kanai T, Ishii K. Washout measurement of radioisotope implanted by radioactive beams in the rabbit. *Phys Med Biol* 2003; **48**: 2269-2281
39 **Ferrari A**, Sala PR, Fassò A, Ranft J. FLUKA: a multi-particle transport code. CERN yellow report, INFN/TC_05/11, SLAC-R-773. Geneva, 2005
40 **Conti M**, Bendriem B, Casey M, Chen M, Kehren F, Michel C, Panin V. First experimental results of time-of-flight reconstruction on an LSO PET scanner. *Phys Med Biol* 2005; **50**: 4507-4526
41 **Parodi K**, Bortfeld T. A filtering approach based on Gaussian-powerlaw convolutions for local PET verification of proton radiotherapy. Phys Med Biol 2006; 51: 1991-2009

S- Editor Cheng JX **L- Editor** Negro F **E- Editor** Zheng XM

World Journal of Radiology

Online Submissions: http://www.wjgnet.com/1949-8470office
wjr@wjgnet.com
doi:10.4329/wjr.v2.i4.143

World J Radiol 2010 April 28; 2(4): 143-147
ISSN 1949-8470 (online)

CASE REPORT

Caseous mitral annular calcifications: Multimodality imaging characteristics

Jabi Shriki, Christine Rongey, Bobby Ghosh, Samuel Daneshvar, Patrick M Colletti, Ali Farvid, Alison Wilcox

Jabi Shriki, Partick M Colletti, Alison Wilcox, Department of Radiology, University of Southern California, Keck School of Medicine, Los Angeles, California, CA 90012, United States
Christine Rongey, Bobby Ghosh, University of Southern California, Keck School of Medicine, Los Angeles, CA 90012, United States
Samuel Daneshvar, Ali Farvid, Division of Cardiovascular Medicine, Department of Internal Medicine, University of Southern California, Keck School of Medicine, Los Angeles, CA 90012, United States
Author contributions: Shriki J served as the primary author and wrote and finalized the manuscript; Rongey C and Ghosh B researched and wrote the clinical histories of the patients presented; Daneshvar S obtained echocardiographic images and contributed to the sections of the manuscript discussing the echocardiographic appearance of caseous mitral annular calcifications; Colletti PM contributed to the discussion regarding the cardiac MR findings in the patients who were discussed; Farvid A assisted in the discussion of the clinical significance of mitral annular calcifications, and obtained IRB approval for this review; Wilcox A assisted in editing and finalizing the manuscript.
Correspondence to: Jabi Shriki, MD, Assistant Professor, Department of Radiology, University of Southern California, Keck School of Medicine, 1200 N. State Street, D&T Rm 3D321, Los Angeles, CA 90033, United States. jshriki@gmail.com
Telephone: +1-323-2267257 Fax: +1-323-4428550
Received: February 24, 2010 Revised: March 24, 2010
Accepted: April 1, 2010
Published online: April 28, 2010

Abstract

The authors report herein a series of 3 patients with caseous mitral annular calcifications (MAC). One of the patients presented with mass-like, caseous MAC as an incidental finding on a staging computed tomography (CT) for metastatic colorectal carcinoma. Another patient presented with a nodule on a chest radiograph, which was later found on CT to be due to caseous MAC. In the third patient, caseous MAC was initially detected on echocardiography, and was further evaluated with CT and cardiac magnetic resonance imaging. In all three patients, the appearances posed a diagnostic dilemma. The appearance of caseous MAC is dissimilar to non-caseous MAC and is usually seen as an ovoid, mass-like structure, with homogeneous hyperattenuation, representing a liquefied form of calcium and proteinaceous fluid. This homogeneous center is surrounded by peripheral, shell-like calcifications. Caseous MAC is likely an under-recognized entity and may present a diagnostic dilemma at CT, magnetic resonance imaging, or echocardiography.

Key words: Computed tomography echocardiography; Magnetic resonance imaging; Mitral annular calcifications; Plain radiography; Echocardiography; Computed tomography; Cardiac magnetic resonance imaging

Peer reviewers: Kai U Juergens, MD, Associate Professor of Radiology, MR- and PET/CT-Centre Bremen, Head of MRI Department, Sankt-Jürgen-Strasse 1, 28177 Bremen, Germany; Piet Vanhoenacker, MD, PhD, Department of Radiology, OLV Ziekenhuis Aalst, Moorselbaan 164, 9300 Aalst, Belgium

Shriki J, Rongey C, Ghosh B, Daneshvar S, Colletti PM, Farvid A, Wilcox A. Caseous mitral annular calcifications: Multimodality imaging characteristics. *World J Radiol* 2010; 2(4): 143-147 Available from: URL: http://www.wjgnet.com/1949-8470/full/v2/i4/143.htm DOI: http://dx.doi.org/10.4329/wjr.v2.i4.143

INTRODUCTION

Mitral annular calcification (MAC) is a commonly encountered phenomenon, and is one of the most common findings in the heart in autopsy series[1]. A variant of this entity is caseous MAC, in which an ovoid, focal mass is found with internal, caseous fluid-like calcifications and debris[2]. Caseous MAC contains a mixture of calcium, salts, fatty acids, and cholesterol and results

in a soft mass in the mitral annulus[3]. Although caseous MAC can be definitively diagnosed by its imaging features and by its classic location, it may present a diagnostic dilemma. Several reports have described the misdiagnosis of caseous MAC as a cardiac neoplasm or as an abscess, resulting in unnecessary surgery[4-6].

Herein, we report 3 patients in whom a diagnosis of caseous MAC was ultimately made. These cases and the associated images demonstrate the characteristic appearance of caseous MAC, and the features of this entity that differentiate it from other cardiac masses which it may mimic.

CASE REPORT

Case 1

A 63-year-old male with a T3N2M0 sigmoid cancer underwent surgical resection and subsequent post-operative chemotherapy. The patient had a series of non-cardiac, non-gated contrast-enhanced computed tomography (CT) scans of his chest, abdomen, and pelvis performed for staging of his sigmoid cancer. During the patient's third restaging CT scan, an ovoid structure was detected at the aorto-atrial septum (Figure 1). Review of the two prior restaging CT studies in this patient also showed this finding to be present, upon retrospective evaluation. The mass had central, homogeneous hyperattenuation, liquefied calcium, with a shell-like, peripheral, calcified rim. This mass was noted to be present and stable on two subsequent CT scans. A presumptive diagnosis of caseous MAC was made. Because of the characteristic appearance of the mass, further diagnostic studies were not pursued.

Case 2

This patient was an 84-year-old Hispanic female admitted to the hospital for nausea and vomiting, with a history of Type II diabetes mellitus, dyslipidemia, hypertension, peripheral vascular disease, dementia, asthma, and hypothyroidism. She also had a long-standing history of dyspnea on exertion. On cardiac exam, the patient had an S4 gallop and a grade 4/6 systolic murmur at the left sternal border. The admission chest radiograph showed a 2.5 cm nodule overlying the cardiac silhouette, which was initially incorrectly interpreted as being within the lung (Figure 2). Echocardiogram (Figure 3) showed mild enlargement of the left atrium, and mild concentric hypertrophy of the left ventricle with normal function. The mitral valve annulus on echocardiogram showed an ovoid mass which was peripherally echogenic and centrally less so. The echocardiogram also demonstrated mild mitral regurgitation. To further clarify the nature of the potential lung nodule, the patient had a chest CT scan with contrast (Figure 4). From review of the CT scan and correlation with prior chest radiographs, it was concluded that caseous MAC were present and the likely reason for the radiographically apparent nodule.

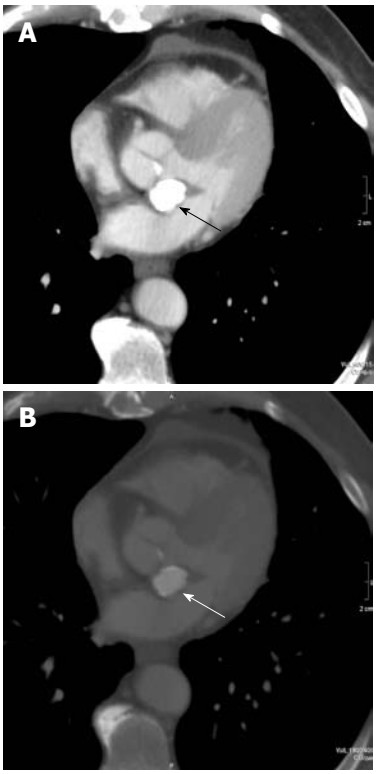

Figure 1 Transverse, non-gated, post-contrast CT images at a level through the heart with mediastinal (A) and bone (B) windows and level settings shown (kVp = 120, mAs = 214, DFOV = 314 mm). Caseous mitral annular calcifications are noted in the aorto-atrial septum (arrows). On the mediastinal window and level settings, the mass shows homogeneous hyperattenuation which cannot be differentiated from other calcific structures. When the window and level settings are adjusted, there is a rim of peripheral calcification with central, homogeneous hyperattenuation. This mass was stable in comparison to CT scans before and after this study (not shown).

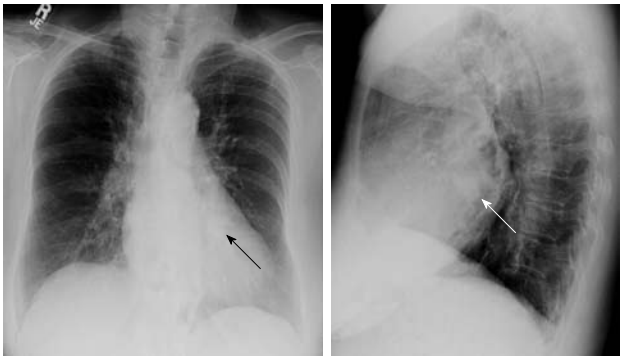

Figure 2 P-A (left) and lateral (right) views of the chest demonstrate an ovoid nodule overlying the cardiac silhouette on both views (arrows). This was misinterpreted as a possible pulmonary nodule. On plain radiography, its nature is difficult to delineate.

Case 3

An 82-year-old male presented with mild, progressive dyspnea on exertion. A chest radiograph performed at an outside institution was unavailable, but was unremarkable by report. An echocardiogram, also performed at an outside institution, by report demonstrated a hypoechoic mass along the posterior annulus with some echogenic

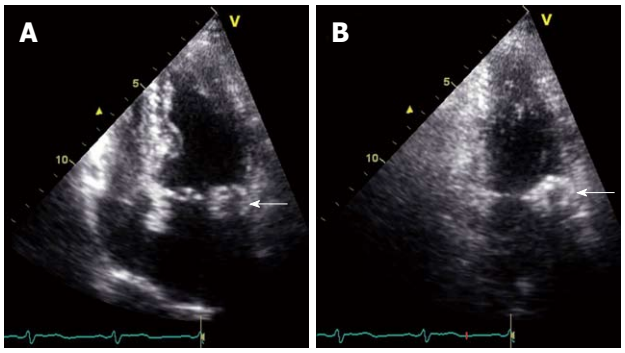

Figure 3 Slightly oblique four-chamber (A) and two-chamber (B) still frame images are obtained from an echocardiogram. These views demonstrate a mass along the mitral annulus (white arrows). The caseous mitral annular calcifications are seen as an ovoid mass. A difference between the relatively echolucent center and the more echogenic periphery of this structure is perceptible. This is consistent with the centrally liquefied calcium and the peripheral more dense calcium observed on other modalities.

components, which was felt to represent a possible myxoma with calcifications. Cardiac magnetic resonance imaging (CMR) was performed. Cine balanced steady state free precession sequences demonstrated focal prominence of the posterolateral wall of the left ventricle. Further sequences demonstrated an ovoid mass with low signal on T2, but bright signal on T1 (Figure 5). Closer inspection revealed a subtle rim of dark signal on SSFP sequences, likely representing shell-like, peripheral calcifications. Caseous MAC were included among differential considerations. A CT scan of the chest was subsequently performed without contrast and demonstrated the typical appearance of caseous MAC (Figure 5).

DISCUSSION

Calcification of the mitral annulus is usually considered an idiopathic, degenerative condition of the mitral annulus, occurring most commonly in older, female patients[7]. This condition is characterized by the development of coarse calcifications along the mitral annulus, and is seldom associated with other signs of mitral valve disease[8]. Rarely, MAC have also been described in patients with Marfan's Syndrome[9], and in Barlow's Disease, a disease of MAC and severe mitral valve prolapse[10].

Several studies have demonstrated that although commonly seen in asymptomatic patients, MAC may be a risk factor for more significant cardiovascular pathology. For example, MAC have been associated with conduction abnormalities[8], including atrial fibrillation[11], and with other cardiovascular diseases including coronary artery disease[12], and stroke risk[13]. In one study, the presence of MAC was associated with a two-fold increase in the risk of stroke, even in the absence of other risk factors[14]. This risk and other risks associated with MAC remain somewhat controversial, however[15].

MAC should be differentiated from calcifications within the mitral valve itself, which are usually related to significant mitral valve pathology and dysfunction, and

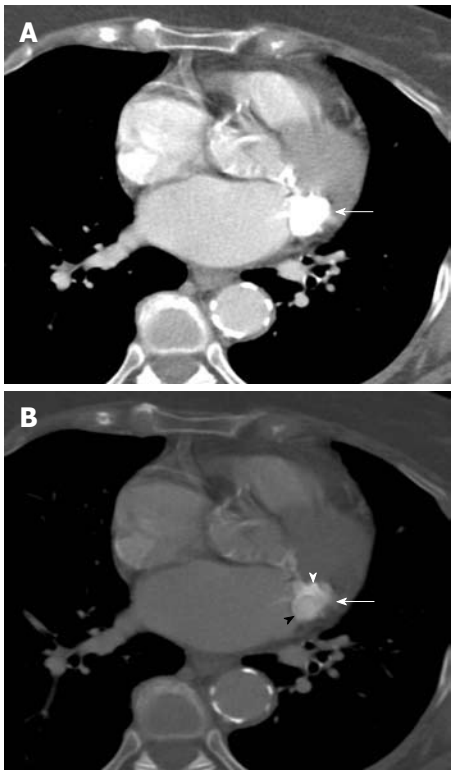

Figure 4 Transverse, non-gated, post-contrast CT images at a level through the heart are shown with mediastinal (A) and bone (B) windows and level settings (kVp = 120, mAs = 220, DFOV = 310 mm). An ovoid mass of caseous mitral annular calcifications is seen high along the posterior portion of the mitral annular leaflet (white arrows). Although there is motion artifact, there is differing attenuation between the calcific rim of this structure (white arrowhead) and the central homogeneous liquefied calcium, which is slightly less hyperattenuating (black arrowhead). This difference is seen on the bone window image (B), but is not demonstrable on the mediastinal window/level settings (A). Based on correlation with the scout view (not shown), this was felt to be the cause of the nodule seen on plain radiography (Figure 3).

are commonly seen in rheumatic heart disease. Valvular calcifications only extend to the annulus in end-stage or in severe rheumatic disease[16]. Unlike valvular calcifications, annular calcifications are more common and are more seldom associated with significant mitral valvular dysfunction, although when severe, MAC may in some cases be associated with mitral regurgitation[2,17,18]. To our knowledge, no studies have been conducted thus far to ascertain the clinical significance of caseous MAC specifically or differentiate the implications of caseous from non-caseous MAC.

Although MAC are encountered commonly, especially in the imaging of older patients, the liquefaction of MAC is an uncommon entity, and has been reported to occur in only approximately 0.6% of patients with MAC[2]. Caseous MAC are also rarely reported in the literature. The largest series to date of patients with caseous MAC includes 18 patients[19]. However, a large autopsy series reported an incidence of 2.7% of caseous MAC, suggesting that this entity may be under-recognized[1].

The distinction between MAC and caseous MAC can be made by the different imaging features of these entities. When these calcifications liquefy and become case-

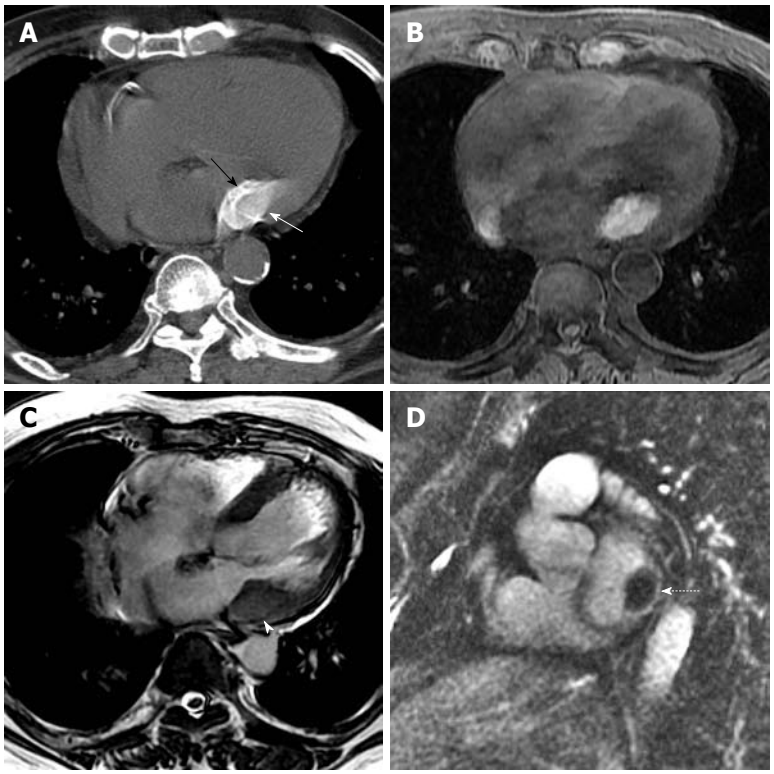

Figure 5 A non-contrast CT image (kVp = 120, mAs = 214, DFOV = 322 mm) (A) performed after the cardiac MRI demonstrates again, a homogeneously hyperattenuating structure in the posterolateral mitral annulus (white arrow) with a shell of calcification (black arrow). This corresponded with a T1 hyperintense structure in the region of the mitral annulus (B) (TR = 5.28, TE = 2.55, FA = 12). On a screen capture from a cine balanced steady state free precession sequence, the mass shows low T2 signal (C) (TR = 3.19, TE = 1.15, FA = 40), although the shell of calcification around the mass is slightly lower in T2 intensity than the central portion of the mass (white arrowhead). A short axis, delayed enhancement, inversion recovery image (D) (TR = 4.39, TE = 1.26, FA = 13) shows central low signal intensity as well, although there is some peripheral delayed enhancement around the mass (dashed arrow).

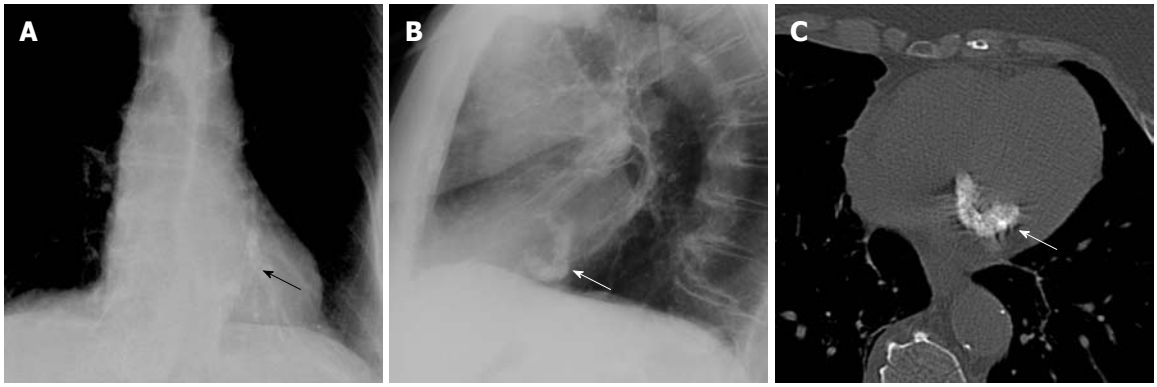

Figure 6 In a different patient, not described herein, the more characteristic appearance of mitral annular calcifications is demonstrated (arrows). These are seen on the P-A view (A), with window and level settings adjusted to better visualize the mitral annular calcifications. The typical C-shape of the mitral annular calcifications is also demonstrated on the lateral view (B) and on a non-contrast CT image through the level of the heart (C) (kVp = 120, mAs = 212, DFOV = 310 mm). Note the difference between the chunky, coarse, C-shaped calcifications seen in this patient and the ovoid, mass-like calcifications with liquefied calcium that we describe.

ous, they have a more ovoid, mass-like appearance than non-caseous MAC. Whereas MAC seldom mimic a mass, caseous MAC are more focal, may be tumefactive, and should be included in differential diagnostic considerations of an intracardiac mass[20]. This entity is however, easily differentiated from other cardiac masses by the baseline, precontrast hyperattenuation on CT, without enhancement. As we report, the MRI characteristics are consistent with that of proteinaceous fluid. Identification of the shell of calcium, and classic localization in the mitral annulus are other classic features of this process. MAC typically have a coarse nature and form a C-shape around the mitral valve (Figure 6). These are most prominent along the posterolateral aspect of the mitral annulus. In contradistinction, caseous MAC have a more homogeneous attenuation, and are slightly less hyperattenuating than the non-liquefied state of calcium. This subtle difference in attenuation is usually masked on typical window and level settings employed for mediastinal settings. The caseous nature of MAC is however, better recognized on "bone windows". This is elucidated in the first two patients presented. There is usually a shell of peripheral calcifications around the central homogeneous hyperattenuation, which was visible in all three of the cases presented in this study. Grossly, the caseous material found in this entity is described as toothpaste-like material[21].

On MRI, calcium is generally low in signal on all sequences. However, the calcium salts and proteinaceous fluid in caseous MAC can generate high signal on T1

non-contrast sequences, which was seen on the CMR of the third patient we presented (Figure 5). Precontrast T1 weighted sequences are helpful in demonstrating the distinction between MAC which have low signal on T1, and caseous MAC which demonstrate high signal on T1. Liquefied calcium is low in T2 signal intensity. The T2 gated sequences in our patient showed decreased signal. Low signal was also seen on the cine SSFP sequences. In our patient, the calcified shell seen also demonstrated lower signal intensity than the rest of the mass of caseous MAC on cine SSFP. Delayed contrast enhancement has been reported along the periphery of caseous MAC[22]. This feature was noted in the third case presentation discussed above (Figure 5D).

The authors postulate that caseous MAC might be more common than usually recognized. This is supported by the presentations of the patients we have described. In the case of the first patient, the abnormality was present on two previous CT scans of the chest. In the second patient, the presence of caseous MAC initially was a diagnostic dilemma, but was recognized when the study was compared with a prior chest radiograph. These cases show that caseous MAC are not a commonly recognized entity.

Caseous MAC may mimic cardiac masses, but have a characteristic appearance which allows differentiation from more commonly encountered, non-caseous MAC. Although the presence of caseous MAC may pose a diagnostic dilemma, familiarity with the entity enables accurate diagnosis.

REFERENCES

1 **Pomerance A**. Pathological and clinical study of calcification of the mitral valve ring. *J Clin Pathol* 1970; **23**: 354-361
2 **Novaro GM**, Griffin BP, Hammer DF. Caseous calcification of the mitral annulus: an underappreciated variant. *Heart* 2004; **90**: 388
3 **Kronzon I**, Winer HE, Cohen ML. Sterile, caseous mitral anular abscess. *J Am Coll Cardiol* 1983; **2**: 186-190
4 **Borowski A**, Korb H, Voth E, de Vivie ER. Asymptomatic myocardial abscess. *Thorac Cardiovasc Surg* 1988; **36**: 338-340
5 **Gilbert HM**, Grodman R, Chung MH, Hartman G, Krieger KH, Hartman BJ. Sterile, caseous mitral valve "abscess" mimicking infective endocarditis. *Clin Infect Dis* 1997; **24**: 1015-1016
6 **Kautzner J**, Vondrácek V, Jirásek A, Bélohlávek M. Tumor-like mitral annular calcification with central liquefaction. *Echocardiography* 2007; **10**: 459-463
7 **Movahed MR**, Saito Y, Ahmadi-Kashani M, Ebrahimi R. Mitral annulus calcification is associated with valvular and cardiac structural abnormalities. *Cardiovasc Ultrasound* 2007; **5**: 14
8 **Fulkerson PK**, Beaver BM, Auseon JC, Graber HL. Calcification of the mitral annulus: etiology, clinical associations, complications and therapy. *Am J Med* 1979; **66**: 967-977
9 **Goodman HB**, Dorney ER. Marfan's syndrome with massive calcification of the mitral annulus at age twenty-six. *Am J Cardiol* 1969; **24:** 426-431
10 **Carpentier AF**, Pellerin M, Fuzellier JF, Relland JY. Extensive calcification of the mitral valve anulus: pathology and surgical management. *J Thorac Cardiovasc Surg* 1996; **111**: 718-729; discussion 729-730
11 **Fox CS**, Parise H, Vasan RS, Levy D, O'Donnell CJ, D'Agostino RB, Plehn JF, Benjamin EJ. Mitral annular calcification is a predictor for incident atrial fibrillation. *Atherosclerosis* 2004; **173**: 291-294
12 **Fox CS**, Vasan RS, Parise H, Levy D, O'Donnell CJ, D'Agostino RB, Benjamin EJ. Mitral annular calcification predicts cardiovascular morbidity and mortality: the Framingham Heart Study. *Circulation* 2003; **107**: 1492-1496
13 **Furlan AJ**, Craciun AR, Salcedo EE, Mellino M. Risk of stroke in patients with mitral annulus calcification. *Stroke* 1984; **15**: 801-803
14 **Benjamin EJ**, Plehn JF, D'Agostino RB, Belanger AJ, Comai K, Fuller DL, Wolf PA, Levy D. Mitral annular calcification and the risk of stroke in an elderly cohort. *N Engl J Med* 1992; **327**: 374-9
15 **Boon A**, Lodder J, Cheriex E, Kessels F. Mitral annulus calcification is not an independent risk factor for stroke: a cohort study of 657 patients. *J Neurol* 1997; **244**: 535-541
16 **Roberts WC**, Perloff JK. Mitral valvular disease. A clinicopathologic survey of the conditions causing the mitral valve to function abnormally. *Ann Intern Med* 1972; **77**: 939-975
17 **Carabello BA**. Mitral valve regurgitation. *Curr Probl Cardiol* 1998; **23**: 202-241
18 **Mann JM**. Mitral valve diesease. London: Butterworths, 1996: 16-27
19 **Harpaz D**, Auerbach I, Ver ed Z, Motro M, Tobar A, Rosenblatt S. Caseous calcification of the mitral annulus: a neglected, unrecognized diagnosis. *J Am Soc Echocardiogr* 2001; **14**: 825-831
20 **Teja K**, Gibson RS, Nolan SP. Atrial extension of mitral annular calcification mimicking intracardiac tumor. *Clin Cardiol* 1987; **10**: 546-548
21 **Alkadhi H**, Leschka S, Prêtre R, Perren A, Marincek B, Wildermuth S. Caseous calcification of the mitral annulus. *J Thorac Cardiovasc Surg* 2005; **129**: 1438-1440
22 **Di Bella G**, Masci PG, Ganame J, Dymarkowski S, Bogaert J. Images in cardiovascular medicine. Liquefaction necrosis of mitral annulus calcification: detection and characterization with cardiac magnetic resonance imaging. *Circulation* 2008; **117**: e292-e294

S- Editor Cheng JX **L- Editor** Webster JR **E- Editor** Zheng XM

World Journal of Radiology

Online Submissions: http://www.wjgnet.com/1949-8470office
wjr@wjgnet.com
doi:10.4329/wjr.v2.i4.148

World J Radiol 2010 April 28; 2(4): 148-150
ISSN 1949-8470 (online)

CASE REPORT

Could helical tomotherapy do whole brain radiotherapy and radiosurgery?

Youlia M Kirova, Cyrus Chargari, Sofia Zefkili, François Campana

Youlia M Kirova, Cyrus Chargari, Sofia Zefkili, François Campana, Department of Radiation Oncology, Institut Curie, 75005 Paris, France
Author contributions: Kirova YM and Chargari C wrote and edited the paper, performed the dosimetry and treated the patient; Zefkili S performed the dosimetry and edited the paper; Campana F treated the patient and edited the paper.
Correspondence to: Youlia M Kirova, MD, Department of Radiation Oncology, Institut Curie, 26, rue d'Ulm, 75005 Paris, France. youlia.kirova@curie.net
Telephone: +33-1-44324637 Fax: +33-1-53102653
Received: February 6, 2010 Revised: March 23, 2010
Accepted: April 1, 2010
Published online: April 28, 2010

Peer reviewer: George Panayiotakis, Professor, Department of Medical Physics, School of Medicine University of Patras, 26500, Patras, Greece; Kundan Singh Chufal, MD, Consultant, Radiation Oncology, Batra Cancer Centre, Batra Hospital and Medical Research Centre, 1, Tughlakabad Institutional Area, New Delhi 110062, India

Kirova YM, Chargari C, Zefkili S, Campana F. Could helical tomotherapy do whole brain radiotherapy and radiosurgery? *World J Radiol* 2010; 2(4): 148-150 Available from: URL: http://www.wjgnet.com/1949-8470/full/v2/i4/148.htm DOI: http://dx.doi.org/10.4329/wjr.v2.i4.148

Abstract

Whole brain radiotherapy (WBRT) remains the standard management of breast cancer patients with brain metastases, allowing for symptomatic improvement and good local control in most patients. However, its results remain suboptimal in terms of both efficacy and toxicity. In highly selected breast cancer patients, stereotaxic radiotherapy demonstrates a very good local control with a low toxicity. With the purpose of improving the efficacy/toxicity ratio, we report the association of integrated boost with WBRT in a breast cancer patient with brain metastases. Two and a half years after completion of helical tomotherapy (HT), the patient experienced clinical and radiological complete remission of her brain disease. No delayed toxicity occurred and the patient kept her hair without need of radiosurgical procedure. The HT provided a high dosimetric homogeneity, delivering integrated radiation boosts, and avoiding critical structures involved in long-term neurological toxicity. Further assessment is required and recruitment of breast cancer patients into clinical trials is encouraged.

Key words: Brain metastases; Radiotherapy; Breast cancer; Tomotherapy

INTRODUCTION

Brain metastases are usually seen as a late complication of advanced breast cancer, for which most available treatment options are generally unsatisfactory. Whole brain radiotherapy (WBRT) provides effective but short-term palliation, improving survival by about 6 mo and quality of life with radiologic response in up to 60% of cases[1,2]. It was suggested that selected subgroups of patients may benefit from more aggressive local treatment of their intracranial disease with surgery or radiosurgery with or without WBRT [2,3]. Providing a potential alternative to conventional stereotactic frame systems for precision radiotherapy, helical tomotherapy (HT) combines intensity modulated fan-beam radiotherapy with megavoltage computed tomography imaging for patient positioning. Its availability has recently opened new fields of exploration for radiation therapy due to its ability to tailor very sharp dose distributions around the target volumes[4-9]. Here we report the use of HT with synchronous boost in a breast cancer patient with multiple brain metastases.

CASE REPORT

In October 2007, a 40-year-old female presented with multiple brain metastases from breast cancer measuring 17 mm in greatest dimension, discovered at systemic

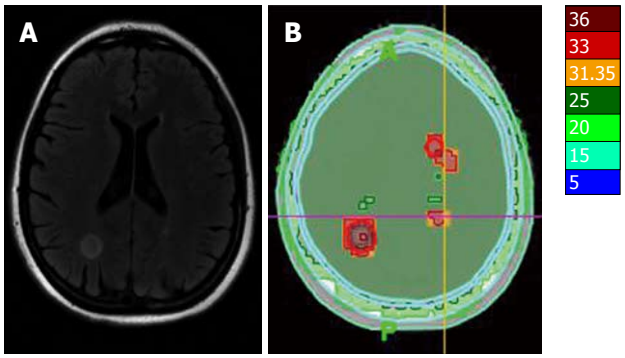

Figure 1 Magnetic resonance imaging appearances at diagnosis (A) and helical tomotherapy (HT) isodoses (Gy) (B).

magnetic resonance imaging (Figure 1A). She had a history of infiltrative ductal carcinoma with lymph nodes, bone, and lung metastases treated since 2005. She received only one systemic regimen used for brain metastases (vinorelbine) prior to radiotherapy. The patient refused to accept the long period hair lost.

The patient was deferred for HT, delivering 30 Gy using 6 MV photons, at 3 Gy *per* daily fraction, in the whole brain for 14 d, concurrently with vinorebine. The only acute toxicity observed was nausea. Integrated synchronous boost treatments were used, in order to deliver 36 Gy in the growth tumoral volumes (Figure 1B). The dose delivered to the scalp was less than 15 Gy. Six months after HT, the metastases were stable in size, with intra-tumoral necrosis and rounded with an edema that accurately drew the shape of isodoses (Figure 1B). The dose volume histograms are given in Figure 2.

Two and a half years after completion of HT, the patient experienced clinical and radiological complete remission of her brain disease. No delayed toxicity occurred and the patient kept her hair without need of radiosurgical procedure.

DISCUSSION

Since the progress of systemic regimens allowed for a prolonged survival time of some patients with metastatic breast cancer[2], it has become an ordinate challenge for radiation oncologists to make an attempt to reduce the radiation-induced toxicity of WBRT, including progressive neurocognitive disorders. Highly conformational HT allows for efficient target coverage and critical organs sparing, including the scalp. A recent assessment of HT for metastatic brain tumors has suggested comparable normal tissue sparing and target coverage compared with other precision radiotherapy techniques[5]. With HT, multiple targets can be easily treated at different dose levels in the course of rotational delivery[1]. This specificity allows for integrated synchronous boost treatments that may be efficiently used to increase the radiation dose delivered to the brain metastases, thus preserving the patient quality of life.

Our patient well tolerated the radiotherapy without any early toxicity. Two and a half years after the treatment, the patient was still alive at the time when we wrote this paper, without any sequels associated with radiotherapy treatment.

The association of chemotherapy permitted the continuing systemic treatment during the radiotherapy. We

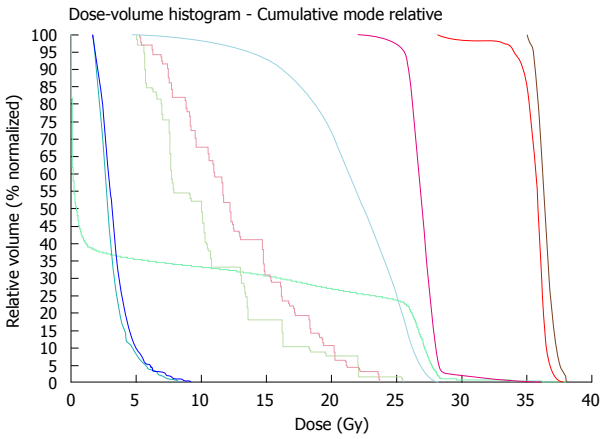

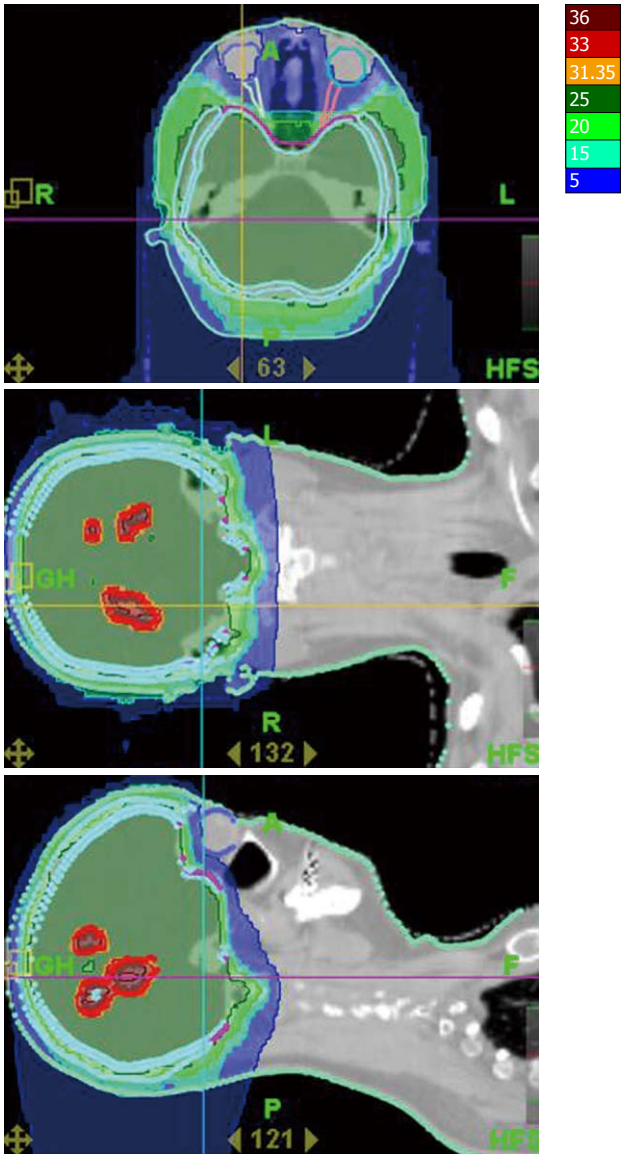

Figure 2 Dose-volume histograms and dose distribution.

have already published our experience with concurrent radiotherapy - Xeloda regimen[2], as well as vinorelbine-5FU-radiotherapy for breast cancer patients. These regimens were well tolerated without any alopecia and adapted to the patient's desires.

In conclusion, the doses of HT used in brain tissue are significantly lower than those of conventional WBRT. Moreover, HT may contribute to the prevention of definitive alopecia which is a universal complication of WBRT, and to patient anxiety over treatment. This is an acceptable treatment option in such patients.

REFERENCES

1 **Weil RJ**, Palmieri DC, Bronder JL, Stark AM, Steeg PS. Breast cancer metastasis to the central nervous system. *Am J Pathol* 2005; **167**: 913-920

2 **Chargari C**, Kirova YM, Diéras V, Castro Pena P, Campana F, Cottu PH, Pierga J, Fourquet A. Concurrent capecitabine and whole-brain radiotherapy for treatment of brain metastases in breast cancer patients. *J Neurooncol* 2009; **93**: 379-384

3 **Tsao MN**, Lloyd NS, Wong RK, Rakovitch E, Chow E, Laperriere N. Radiotherapeutic management of brain metastases: a systematic review and meta-analysis. *Cancer Treat Rev* 2005; **31**: 256-273

4 **Bauman G**, Yartsev S, Fisher B, Kron T, Laperriere N, Heydarian M, VanDyk J. Simultaneous infield boost with helical tomotherapy for patients with 1 to 3 brain metastases. *Am J Clin Oncol* 2007; **30**: 38-44

5 **Yartsev S**, Kron T, Cozzi L, Fogliata A, Bauman G. Tomotherapy planning of small brain tumours. *Radiother Oncol* 2005; **74**: 49-52

6 **Chargari C**, Kirova YM, Cottu P, Salmon RJ, Fourquet A. Progressive inflammatory breast cancer in patient receiving chemotherapy: the importance of radiotherapy as a part of locoregional treatment. *Radiother Oncol* 2009; **90**: 160-161

7 **Chargari C**, Campana F, Beuzeboc P, Zefkili S, Kirova YM. Preliminary experience of helical tomotherapy for locally advanced pancreatic cancer. *World J Gastroenterol* 2009; **15**: 4444-4445

8 **Chargari C**, Kirova YM, Zefkili S, Caussa L, Amessis M, Dendale R, Campana F, Fourquet A. Solitary plasmocytoma: improvement in critical organs sparing by means of helical tomotherapy. *Eur J Haematol* 2009; **83**: 66-71

9 **Chargari C**, Kirova YM, Zefkili S, Campana F. Improve the management of patients with skull bone metastases by means of helical tomotherapy. *Support Care Cancer* 2009; **17**: 613-615

S- Editor Cheng JX **L- Editor** Wang XL **E- Editor** Zheng XM

World Journal of Radiology

Online Submissions: http://www.wjgnet.com/1949-8470office
wjr@wjgnet.com
www.wjgnet.com

World J Radiol 2010 April 28; 2(4): I
ISSN 1949-8470 (online)

Acknowledgments to reviewers of *World Journal of Radiology*

Many reviewers have contributed their expertise and time to the peer review, a critical process to ensure the quality of *World Journal of Radiology*. The editors and authors of the articles submitted to the journal are grateful to the following reviewers for evaluating the articles (including those published in this issue and those rejected for this issue) during the last editing time period.

Sandip Basu, MBBS (Hons), DRM, DNB, MNAMS, Head, Nuclear Medicine Academic Programme, Radiation Medicine Centre, Bhabha Atomic Research Centre, Tata Memorial Hospital Annexe, Parel, Bombay 400012, India

Arne S Borthne, MD, PhD, Associate Professor, Diagnostic Imaging Center, Akershus University Hospital, Sykehusveien 27, Nordbyhagen, NO-1478 Lørenskog, Norway

Filippo Cademartiri, MD, PhD, Departmento of Radiology - c/o Piastra Tecnica - Piano 0, Azienda Ospedaliero-Universitaria di Parma, Via Gramsci, 14 - 43100 Parma, Italy

Kundan Singh Chufal, MD, Consultant, Radiation Oncology, Batra Cancer Centre, Batra Hospital and Medical Research Centre, 1, Tughlakabad Institutional Area, New Delhi 110062, India

Kenneth Coenegrachts, MD, PhD, Department of Radiology, AZ St.-Jan AV, Ruddershove 10, B-8000 Bruges, Belgium

Ragab Hani Donkol, Professor, Radiology Department, Aseer Central Hospital, 34 Abha, Saudi Arabia

Tove J Grönroos, PhD, Adjunct Professor, Turku PET Centre, Preclinical Imaging/Medicity Research Laboratory, Tykistokatu 6A, FI-20520 Turku, Finland

Joon Koo Han, MD, PhD, Professor, Department of Radiology, Seoul National University College of Medicine, 103, Daehangno, Jongno-gu, Seoul 110-744, South Korea

Kai U Juergens, MD, Associate Professor of Radiology, MR- and PET/CT-Centre Bremen, Head of MRI Department, Sankt-Jürgen-Strasse 1, 28177 Bremen, Germany

Adnan Kabaalioglu, MD, Professor, Akdeniz University Hospital, 07059, Antalya, Turkey

Wellington P Martins, PhD, Departamento de Ginecologia e, Obstetrícia da Faculdade de Medicina de Ribeirão Preto da Universidade de São Paulo, Avenida dos Bandeirantes 3900, 8º andar, Ribeirão Preto, São Paulo 14049-900, Brazil

Oliver Micke, MD, Department of Radiotherapy and Radiation Oncology, Franziskus Hospital, Kiskerstraße 26, D-33615 Bielefeld, Germany

George Panayiotakis, Professor, Department of Medical Physics, School of Medicine University of Patras, 26500, Patras, Greece

Piet Vanhoenacker, MD, PhD, Department of Radiology, OLV Ziekenhuis Aalst, Moorselbaan 164, 9300 Aalst, Belgium

Hong-Gyun Wu, MD, PhD, Associated Professor, Department of Radiation Oncology, Seoul National University College of Medicine, 103 Daehangno, Jongno-gu, Seoul 110-799, South Korea

World Journal of Radiology

Online Submissions: http://www.wjgnet.com/1949-8470office
wjr@wjgnet.com
www.wjgnet.com

World J Radiol 2010 April 28; 2(4): I
ISSN 1949-8470 (online)

Meetings

Events Calendar 2010

January 4-8
Beaver Creek, Colorado, United States
18th Annual Winter Diagnostic Imaging Update

January 7-9
Leuven, Belgium
4th Leuven Course on Ear Imaging

January 16-17
Hollywood, Florida, United States
The Symposium on Clinical Interventional Oncology

January 17-21
Hollywood, Florida, United States
The International Symposium on Endovascular Therapy

January 21-22
Cairo, Egypt
BGICC Breast Gyne International Cancer Conference

January 21-24
Phoenix, AZ, United States
13th Society for Cardiovascular Magnetic Resonance (SCMR) Annual Scientific Sessions

January 23-23
Atlanta, GA, United States
Emory Winship Cancer Institute: Breast Cancer 2010: Advances in Science, Emerging Data, and Novel Therapeutics

January 25-29
Maui, HI, United States
Musculoskeletal & Neuroradiology MR Imaging Update in Maui

January 27-February 2
Albuquerque, NM, United States
2010 SNM Conjoint Mid-Winter Meetings

January 29-30
Barcelona, Spain
7th European Congress: Perspectives in Gynecologic Oncology

February 7-12
Vail, CO, United States
15th Annual Vail 2010: Multislice CT in Clinical Practice

February 11-13
Las Vegas, NV, United States
5th Annual Symposium on PET/CT and Molecular Imaging

February 16-19
Park City, UT, United States
6th Interventional/ Neurointerventional Conference

February 18-19
London, United Kingdom
Diagnostic and Interventional Radiology

February 18-21
Las Vegas, NV, United States
American Society of Spine Radiology Annual Symposium

February 20-20
Jacksonville, Florida, United States
Mayo Clinic Molecular Markers and Management of Breast Cancer

February 20-21
Bethesda, Maryland, United States
25th Anniversary Washington Neuroradiology Review

February 21-26
Orlando, FL, United States
The Abdominal Radiology Course

February 21-27
Snowmass, CO, United States
16th Annual Snowmass 2010: Clinical Ultrasound

February 22-26
Bethesda, MD, United States
48th Annual Dr. Kenneth M. Earle Memorial Neuropathology Review

February 24-27
Lake Buena Vista, FL, United States
ACRO 2010 American College of Radiation Oncology Symposium: Clinical Radiation Oncology Challenges

February 25-27
Chandler, AZ, United States
Multidisciplinary Head and Neck Cancer Symposium

February 26-27
Brussels, Belgium
10èmes Mises au Point en Imagerie Ostéo-Articulaire

February 27-March 1
Cairo, Egypt
7th Gastroenterology Hepatology & Endoscopy Symposium

February 28-March 4
Scottsdale, AZ, United States
International Congress XXIII on Endovascular Interventions

February 28-March 5
Breckenridge, CO, United States
5th Annual Breckenridge 2010: Musculoskeletal MRI

March 3-6
Las Vegas, Nevada, United States
11th Annual Advances in Breast Imaging and Interventions

March 4-8
Vienna, Austria
European Congress of Radiology (ECR 2010) Annual Meeting

March 5-7
Mt Tremblant, QC, Canada
Neuroimaging and Head & Neck Radiology Update in Mt Tremblant

March 7-11
San Diego, CA, United States
SCBT-MR Masters in Body Imaging: "What's New, What's Hot, What You May Not Have Known"

March 10-13
San Antonio, Texas, United States
Clinical Osteoporosis 2010: An ISCD-NOF Symposium

March 11-13
Barcelona, Spain
EORTC Group Meeting: EORTC Radiation Oncology Group

March 11-13
Hannover, Germany
40. Kongress der Deutschen Gesellschaft für Endoskopie und Bildgebende Verfahren e.V.

March 13-18
Tampa, FL, United states
Society of interventional radiology 35th Annual Scientific Meeting

March 14-17
Park City, UT, United States
14th Annual Park City 2010: MRI in Clinical Practice

March 22-26
Beaver Creek, CO, United States
NYU Radiology Spring Skiing Symposium in Beaver Creek

March 22-26
Maui, HI, United States
18th Annual Spring Diagnostic Imaging Update

March 24-27
San Diego, California, United States
2010 American institute of ultrasound in Medicine Annual Convention Preliminary Program

March 24-27
Barcelona, Spain
7th European Breast Cancer Conference

April 8-12
Shanghai, China
The 26th International Congress of Radiology

September 8-12
Guangzhou, China
Chinese Society of Interventional Radiology, 2010 CSIR

November 28-December 03
Chicago, United States
Radiological Society of North America: 2010 Annual Meeting

World Journal of Radiology

Online Submissions: http://www.wjgnet.com/1949-8470office
wjr@wjgnet.com
www.wjgnet.com

World J Radiol 2010 April 28; 2(4): I-V
ISSN 1949-8470 (online)

Instructions to authors

GENERAL INFORMATION

World Journal of Radiology (*World J Radiol*, *WJR*, online ISSN 1949-8470, DOI: 10.4329), is a monthly, open-access (OA), peer-reviewed journal supported by an editorial board of 307 experts in Radiology from 39 countries.

The biggest advantage of the OA model is that it provides free, full-text articles in PDF and other formats for experts and the public without registration, which eliminates the obstacle that traditional journals possess and usually delays the speed of the propagation and communication of scientific research results. The open access model has been proven to be a true approach that may achieve the ultimate goal of the journals, i.e. the maximization of the value to the readers, authors and society.

The role of academic journals is to exhibit the scientific levels of a country, a university, a center, a department, and even a scientist, and build an important bridge for communication between scientists and the public. As we all know, the significance of the publication of scientific articles lies not only in disseminating and communicating innovative scientific achievements and academic views, as well as promoting the application of scientific achievements, but also in formally recognizing the "priority" and "copyright" of innovative achievements published, as well as evaluating research performance and academic levels. So, to realize these desired attributes of *WJR* and create a well-recognized journal, the following four types of personal benefits should be maximized. The maximization of personal benefits refers to the pursuit of the maximum personal benefits in a well-considered optimal manner without violation of the laws, ethical rules and the benefits of others. (1) Maximization of the benefits of editorial board members: The primary task of editorial board members is to give a peer review of an unpublished scientific article *via* online office system to evaluate its innovativeness, scientific and practical values and determine whether it should be published or not. During peer review, editorial board members can also obtain cutting-edge information in that field at first hand. As leaders in their field, they have priority to be invited to write articles and publish commentary articles. We will put peer reviewers' names and affiliations along with the article they reviewed in the journal to acknowledge their contribution; (2) Maximization of the benefits of authors: Since *WJR* is an open-access journal, readers around the world can immediately download and read, free of charge, high-quality, peer-reviewed articles from *WJR* official website, thereby realizing the goals and significance of the communication between authors and peers as well as public reading; (3) Maximization of the benefits of readers: Readers can read or use, free of charge, high-quality peer-reviewed articles without any limits, and cite the arguments, viewpoints, concepts, theories, methods, results, conclusion or facts and data of pertinent literature so as to validate the innovativeness, scientific and practical values of their own research achievements, thus ensuring that their articles have novel arguments or viewpoints, solid evidence and correct conclusion; and (4) Maximization of the benefits of employees: It is an iron law that a first-class journal is unable to exist without first-class editors, and only first-class editors can create a first-class academic journal. We insist on strengthening our team cultivation and construction so that every employee, in an open, fair and transparent environment, could contribute their wisdom to edit and publish high-quality articles, thereby realizing the maximization of the personal benefits of editorial board members, authors and readers, and yielding the greatest social and economic benefits.

The major task of *WJR* is to rapidly report the most recent improvement in the research of medical imaging and radiation therapy by the radiologists. *WJR* accepts papers on the following aspects related to radiology: Abdominal radiology, women health radiology, cardiovascular radiology, chest radiology, genitourinary radiology, neuroradiology, head and neck radiology, interventional radiology, musculoskeletal radiology, molecular imaging, pediatric radiology, experimental radiology, radiological technology, nuclear medicine, PACS and radiology informatics, and ultrasound. We also encourage papers that cover all other areas of radiology as well as basic research.

The columns in the issues of *WJR* will include: (1) Editorial: To introduce and comment on major advances and developments in the field; (2) Frontier: To review representative achievements, comment on the state of current research, and propose directions for future research; (3) Topic Highlight: This column consists of three formats, including (A) 10 invited review articles on a hot topic, (B) a commentary on common issues of this hot topic, and (C) a commentary on the 10 individual articles; (4) Observation: To update the development of old and new questions, highlight unsolved problems, and provide strategies on how to solve the questions; (5) Guidelines for Basic Research: To provide guidelines for basic research; (6) Guidelines for Clinical Practice: To provide guidelines for clinical diagnosis and treatment; (7) Review: To review systemically progress and unresolved problems in the field, comment on the state of current research, and make suggestions for future work; (8) Original Articles: To report innovative and original findings in radiology; (9) Brief Articles: To briefly report the novel and innovative findings in radiology; (10) Case Report: To report a rare or typical case; (11) Letters to the Editor: To discuss and make reply to the contributions published in *WJR*, or to introduce and comment on a controversial issue of general interest; (12) Book Reviews: To introduce and comment on quality monographs of radiology; and (13) Guidelines: To introduce consensuses and guidelines reached by international and national academic authorities worldwide on the research in radiology.

CSSN
ISSN 1949-8470 (online)

Published by
Beijing Baishideng BioMed Scientific Co., Ltd.

SUBMISSION OF MANUSCRIPTS

Manuscripts should be typed in 1.5 line spacing and 12 pt. Book Antiqua with ample margins. Number all pages consecutively, and start each of the following sections on a new page: Title Page, Abstract, Introduction, Materials and Methods, Results, Discussion, Acknowledgements, References, Tables, Figures, and Figure Legends. Neither the editors nor the publisher are responsible for the opinions expressed by contributors. Manuscripts formally accepted for publication become the permanent property of Beijing Baishideng BioMed Scientifc Co., Ltd., and may not be reproduced by any means, in whole or in part, without the written permission of both the authors and the publisher. We reserve the right to copy-edit and put onto our website accepted manuscripts. Authors should follow the relevant guidelines for the care and use of laboratory animals of their institution or national animal welfare committee. For the sake of transparency in regard to the performance and reporting of clinical trials, we endorse the policy of the International Committee of Medical Journal Editors to refuse to publish papers on clinical trial results if the trial was not recorded in a publicly-accessible registry at its outset. The only register now available, to our knowledge, is http://www. clinicaltrials.gov sponsored by the United States National Library of Medicine and we encourage all potential contributors to register with it. However, in the case that other registers become available you will be duly notified. A letter of recommendation from each author's organization should be provided with the contributed article to ensure the privacy and secrecy of research is protected.

Authors should retain one copy of the text, tables, photographs and illustrations because rejected manuscripts will not be returned to the author(s) and the editors will not be responsible for loss or damage to photographs and illustrations sustained during mailing.

Online submissions

Manuscripts should be submitted through the Online Submission System at: http://www.wjgnet.com/1949-8470office. Authors are highly recommended to consult the ONLINE INSTRUCTIONS TO AUTHORS (http://www.wjgnet.com/1949-8470/g_info_20100316162358.htm) before attempting to submit online. For assistance, authors encountering problems with the Online Submission System may send an email describing the problem to wjr@wjgnet.com, or by telephone: +86-10-59080036. If you submit your manuscript online, do not make a postal contribution. Repeated online submission for the same manuscript is strictly prohibited.

MANUSCRIPT PREPARATION

All contributions should be written in English. All articles must be submitted using word-processing software. All submissions must be typed in 1.5 line spacing and 12 pt. Book Antiqua with ample margins. Style should conform to our house format. Required information for each of the manuscript sections is as follows:

Title page

Title: Title should be less than 12 words.

Running title: A short running title of less than 6 words should be provided.

Authorship: Authorship credit should be in accordance with the standard proposed by International Committee of Medical Journal Editors, based on (1) substantial contributions to conception and design, acquisition of data, or analysis and interpretation of data; (2) drafting the article or revising it critically for important intellectual content; and (3) final approval of the version to be published. Authors should meet conditions 1, 2, and 3.

Institution: Author names should be given first, then the complete name of institution, city, province and postcode. For example, Xu-Chen Zhang, Li-Xin Mei, Department of Pathology, Chengde Medical College, Chengde 067000, Hebei Province, China. One author may be represented from two institutions, for example, George Sgourakis, Department of General, Visceral, and Transplantation Surgery, Essen 45122, Germany; George Sgourakis, 2nd Surgical Department, Korgialenio-Benakio Red Cross Hospital, Athens 15451, Greece

Author contributions: The format of this section should be: Author contributions: Wang CL and Liang L contributed equally to this work; Wang CL, Liang L, Fu JF, Zou CC, Hong F and Wu XM designed the research; Wang CL, Zou CC, Hong F and Wu XM performed the research; Xue JZ and Lu JR contributed new reagents/analytic tools; Wang CL, Liang L and Fu JF analyzed the data; and Wang CL, Liang L and Fu JF wrote the paper.

Supportive foundations: The complete name and number of supportive foundations should be provided, e.g., Supported by National Natural Science Foundation of China, No. 30224801

Correspondence to: Only one corresponding address should be provided. Author names should be given first, then author title, affiliation, the complete name of institution, city, postcode, province, country, and email. All the letters in the email should be in lower case. A space interval should be inserted between country name and email address. For example, Montgomery Bissell, MD, Professor of Medicine, Chief, Liver Center, Gastroenterology Division, University of California, Box 0538, San Francisco, CA 94143, United States. montgomery.bissell@ucsf.edu

Telephone and fax: Telephone and fax should consist of +, country number, district number and telephone or fax number, e.g., Telephone: +86-10-59080039 Fax: +86-10-85381893

Peer reviewers: All articles received are subject to peer review. Normally, three experts are invited for each article. Decision for acceptance is made only when at least two experts recommend an article for publication. Reviewers for accepted manuscripts are acknowledged in each manuscript, and reviewers of articles which were not accepted will be acknowledged at the end of each issue. To ensure the quality of the articles published in *WJR*, reviewers of accepted manuscripts will be announced by publishing the name, title/position and institution of the reviewer in the footnote accompanying the printed article. For example, reviewers: Professor Jing-Yuan Fang, Shanghai Institute of Digestive Disease, Shanghai, Affiliated Renji Hospital, Medical Faculty, Shanghai Jiaotong University, Shanghai, China; Professor Xin-Wei Han, Department of Radiology, The First Affiliated Hospital, Zhengzhou University, Zhengzhou, Henan Province, China; and Professor Anren Kuang, Department of Nuclear Medicine, Huaxi Hospital, Sichuan University, Chengdu, Sichuan Province, China.

Abstract
There are unstructured abstracts (no more than 256 words) and structured abstracts (no more than 480). The specific requirements for structured abstracts are as follows:

An informative, structured abstracts of no more than 480 words should accompany each manuscript. Abstracts for original contributions should be structured into the following sections. AIM (no more than 20 words): Only the purpose should be included. Please write the aim as the form of "To investigate/study/…; MATERIALS AND METHODS (no more than 140 words); RESULTS (no more than 294 words): You should present *P* values where appropriate and must provide relevant data to illustrate how they were obtained, e.g. 6.92 ± 3.86 *vs* 3.61 ± 1.67, $P < 0.001$; CONCLUSION (no more than 26 words).

Key words
Please list 5-10 key words, selected mainly from *Index Medicus*, which reflect the content of the study.

Text
For articles of these sections, original articles, rapid communication and case reports, the main text should be structured into the following sections: INTRODUCTION, MATERIALS AND METHODS, RESULTS and DISCUSSION, and should include appropriate Figures and Tables. Data should be presented in the main text or in Figures and Tables, but not in both. The main text format of these sections, editorial, topic highlight, case report, letters to the editors, can be found at: http://www.wjgnet.com/1949-8470/g_info_20100313183720.htm.

Illustrations
Figures should be numbered as 1, 2, 3, *etc.*, and mentioned clearly in the main text. Provide a brief title for each figure on a separate page. Detailed legends should not be provided under the figures. This part should be added into the text where the figures are applicable. Figures should be either Photoshop or Illustrator files (in tiff, eps, jpeg formats) at high-resolution. Examples can be found at: http://www.wjgnet.com/1007-9327/13/4520.pdf; http://www.wjgnet.com/1007-9327/13/4554.pdf; http://www.wjgnet.com/1007-9327/13/4891.pdf; http://www.wjgnet.com/1007-9327/13/4986.pdf; http://www.wjgnet.com/1007-9327/13/4498.pdf. Keeping all elements compiled is necessary in line-art image. Scale bars should be used rather than magnification factors, with the length of the bar defined in the legend rather than on the bar itself. File names should identify the figure and panel. Avoid layering type directly over shaded or textured areas. Please use uniform legends for the same subjects. For example: Figure 1 Pathological changes in atrophic gastritis after treatment. A: ...; B: ...; C: ...; D: ...; E: ...; F: ...; G: …*etc.* It is our principle to publish high resolution-figures for the printed and E-versions.

Tables
Three-line tables should be numbered 1, 2, 3, *etc.*, and mentioned clearly in the main text. Provide a brief title for each table. Detailed legends should not be included under tables, but rather added into the text where applicable. The information should complement, but not duplicate the text. Use one horizontal line under the title, a second under column heads, and a third below the Table, above any footnotes. Vertical and italic lines should be omitted.

Notes in tables and illustrations
Data that are not statistically significant should not be noted. $^{a}P < 0.05$, $^{b}P < 0.01$ should be noted ($P > 0.05$ should not be noted). If there are other series of *P* values, $^{c}P < 0.05$ and $^{d}P < 0.01$ are used. A third series of *P* values can be expressed as $^{e}P < 0.05$ and $^{f}P < 0.01$. Other notes in tables or under illustrations should be expressed as ^{1}F, ^{2}F, ^{3}F; or sometimes as other symbols with a superscript (Arabic numerals) in the upper left corner. In a multi-curve illustration, each curve should be labeled with ●, ○, ■, □, ▲, △, *etc.*, in a certain sequence.

Acknowledgments
Brief acknowledgments of persons who have made genuine contributions to the manuscript and who endorse the data and conclusions should be included. Authors are responsible for obtaining written permission to use any copyrighted text and/or illustrations.

REFERENCES
Coding system
The author should number the references in Arabic numerals according to the citation order in the text. Put reference numbers in square brackets in superscript at the end of citation content or after the cited author's name. For citation content which is part of the narration, the coding number and square brackets should be typeset normally. For example, "Crohn's disease (CD) is associated with increased intestinal permeability[1,2]". If references are cited directly in the text, they should be put together within the text, for example, "From references[19,22-24], we know that..."

When the authors write the references, please ensure that the order in text is the same as in the references section, and also ensure the spelling accuracy of the first author's name. Do not list the same citation twice.

PMID and DOI
Pleased provide PubMed citation numbers to the reference list, e.g. PMID and DOI, which can be found at http://www.ncbi.nlm.nih.gov/sites/entrez?db=pubmed and http://www.crossref.org/SimpleTextQuery/, respectively. The numbers will be used in E-version of this journal.

Style for journal references
Authors: the name of the first author should be typed in boldfaced letters. The family name of all authors should be typed with the initial letter capitalized, followed by their abbreviated first and middle initials. (For example, Lian-Sheng Ma is abbreviated as Ma LS, Bo-Rong Pan as Pan BR). The title of the cited article and italicized journal title (journal title should be in its abbreviated form as shown in PubMed), publication date, volume number (in black), start page, and end page [PMID: 11819634 DOI: 10.3748/wjg.13.5396].

Style for book references
Authors: the name of the first author should be typed in boldfaced letters. The surname of all authors should be typed with the initial letter capitalized, followed by their abbreviated middle and first initials. (For example, Lian-Sheng Ma is abbreviated as Ma LS, Bo-Rong Pan as Pan BR) Book title. Publication number. Publication place: Publication press, Year: start page and end page.

Format

Journals

English journal article (list all authors and include the PMID where applicable)

1 **Jung EM**, Clevert DA, Schreyer AG, Schmitt S, Rennert J, Kubale R, Feuerbach S, Jung F. Evaluation of quantitative contrast harmonic imaging to assess malignancy of liver tumors: A prospective controlled two-center study. *World J Gastroenterol* 2007; **13**: 6356-6364 [PMID: 18081224 DOI: 10.3748/wjg.13.6356]

Chinese journal article (list all authors and include the PMID where applicable)

2 **Lin GZ**, Wang XZ, Wang P, Lin J, Yang FD. Immunologic effect of Jianpi Yishen decoction in treatment of Pixu-diarrhoea. *Shijie Huaren Xiaohua Zazhi* 1999; **7**: 285-287

In press

3 **Tian D**, Araki H, Stahl E, Bergelson J, Kreitman M. Signature of balancing selection in Arabidopsis. *Proc Natl Acad Sci USA* 2006; In press

Organization as author

4 **Diabetes Prevention Program Research Group**. Hypertension, insulin, and proinsulin in participants with impaired glucose tolerance. *Hypertension* 2002; **40**: 679-686 [PMID: 12411462 PMCID:2516377 DOI:10.1161/01.HYP.0000035706.28494.09]

Both personal authors and an organization as author

5 **Vallancien G**, Emberton M, Harving N, van Moorselaar RJ; Alf-One Study Group. Sexual dysfunction in 1, 274 European men suffering from lower urinary tract symptoms. *J Urol* 2003; **169**: 2257-2261 [PMID: 12771764 DOI:10.1097/01.ju.0000067940.76090.73]

No author given

6 21st century heart solution may have a sting in the tail. *BMJ* 2002; **325**: 184 [PMID: 12142303 DOI:10.1136/bmj.325.7357.184]

Volume with supplement

7 **Geraud G**, Spierings EL, Keywood C. Tolerability and safety of frovatriptan with short- and long-term use for treatment of migraine and in comparison with sumatriptan. *Headache* 2002; **42** Suppl 2: S93-99 [PMID: 12028325 DOI:10.1046/j.1526-4610.42.s2.7.x]

Issue with no volume

8 **Banit DM**, Kaufer H, Hartford JM. Intraoperative frozen section analysis in revision total joint arthroplasty. *Clin Orthop Relat Res* 2002; (**401**): 230-238 [PMID: 12151900 DOI:10.1097/00003086-200208000-00026]

No volume or issue

9 Outreach: Bringing HIV-positive individuals into care. *HRSA Careaction* 2002; 1-6 [PMID: 12154804]

Books

Personal author(s)

10 **Sherlock S**, Dooley J. Diseases of the liver and billiary system. 9th ed. Oxford: Blackwell Sci Pub, 1993: 258-296

Chapter in a book (list all authors)

11 **Lam SK**. Academic investigator's perspectives of medical treatment for peptic ulcer. In: Swabb EA, Azabo S. Ulcer disease: investigation and basis for therapy. New York: Marcel Dekker, 1991: 431-450

Author(s) and editor(s)

12 **Breedlove GK**, Schorfheide AM. Adolescent pregnancy. 2nd ed. Wieczorek RR, editor. White Plains (NY): March of Dimes Education Services, 2001: 20-34

Conference proceedings

13 **Harnden P**, Joffe JK, Jones WG, editors. Germ cell tumours V. Proceedings of the 5th Germ cell tumours Conference; 2001 Sep 13-15; Leeds, UK. New York: Springer, 2002: 30-56

Conference paper

14 **Christensen S**, Oppacher F. An analysis of Koza's computational effort statistic for genetic programming. In: Foster JA, Lutton E, Miller J, Ryan C, Tettamanzi AG, editors. Genetic programming. EuroGP 2002: Proceedings of the 5th European Conference on Genetic Programming; 2002 Apr 3-5; Kinsdale, Ireland. Berlin: Springer, 2002: 182-191

Electronic journal (list all authors)

15 Morse SS. Factors in the emergence of infectious diseases. Emerg Infect Dis serial online, 1995-01-03, cited 1996-06-05; 1(1): 24 screens. Available from: URL: http//www.cdc.gov/ncidod/EID/eid.htm

Patent (list all authors)

16 **Pagedas AC**, inventor; Ancel Surgical R&D Inc., assignee. Flexible endoscopic grasping and cutting device and positioning tool assembly. United States patent US 20020103498. 2002 Aug 1

Statistical data

Write as mean ± SD or mean ± SE.

Statistical expression

Express *t* test as *t* (in italics), *F* test as *F* (in italics), chi square test as χ^2 (in Greek), related coefficient as *r* (in italics), degree of freedom as υ (in Greek), sample number as *n* (in italics), and probability as *P* (in italics).

Units

Use SI units. For example: body mass, m (B) = 78 kg; blood pressure, p (B) = 16.2/12.3 kPa; incubation time, t (incubation) = 96 h, blood glucose concentration, c (glucose) 6.4 ± 2.1 mmol/L; blood CEA mass concentration, p (CEA) = 8.6 24.5 μg/L; CO_2 volume fraction, 50 mL/L CO_2, not 5% CO_2; likewise for 40 g/L formaldehyde, not 10% formalin; and mass fraction, 8 ng/g, *etc.* Arabic numerals such as 23, 243, 641 should be read 23 243 641.

The format for how to accurately write common units and quantums can be found at: http://www.wjgnet.com/1949-8470/g_info_20100313185816.htm.

Abbreviations

Standard abbreviations should be defined in the abstract and on first mention in the text. In general, terms should not be abbreviated unless they are used repeatedly and the abbreviation is helpful to the reader. Permissible abbreviations are listed in Units, Symbols and Abbreviations: A Guide for Biological and Medical Editors and Authors (Ed. Baron DN, 1988) published by The Royal Society of Medicine, London. Certain commonly used abbreviations, such as DNA, RNA, HIV, LD50, PCR, HBV, ECG, WBC, RBC, CT, ESR, CSF, IgG, ELISA, PBS, ATP, EDTA, mAb, can be used directly without further explanation.

Italics

Quantities: *t* time or temperature, *c* concentration, *A* area, *l* length, *m* mass, *V* volume.

Genotypes: *gyrA*, *arg* 1, *c myc*, *c fos*, *etc.*

Restriction enzymes: *Eco*RI, *Hin*dI, *Bam*HI, *Kbo* I, *Kpn* I, *etc.*
Biology: *H. pylori*, *E coli*, *etc.*

RE-SUBMISSION OF THE REVISED PAPER

Please revise your article according to the revision policies of *WJR*. The revised version including manuscript and high-resolution image figures (if any) should be re-submitted or uploaded online. The author should send copyright transfer letter, and responses to the reviewers and science news to us *via* email.

Editorial Office

World Journal of Radiology

Editorial Department: Room 903, Building D,
Ocean International Center,
No. 62 Dongsihuan Zhonglu,
Chaoyang District, Beijing 100025, China
E-mail: wjr@wjgnet.com
http://www.wjgnet.com
Telephone: +86-10-59080036
Fax: +86-10-85381893

Language evaluation

The language of a manuscript will be graded before it is sent for revision. (1) Grade A: priority publishing; (2) Grade B: minor language polishing; (3) Grade C: a great deal of language polishing needed; and (4) Grade D: rejected. Revised articles should reach Grade A or B.

Copyright assignment form

Please download a Copyright assignment form from http://www.wjgnet.com/1949-8470/g_info_20100313185522.htm.

Responses to reviewers

Please revise your article according to the comments/suggestions provided by the reviewers. The format for responses to the reviewers' comments can be found at: http://www.wjgnet.com/1949-8470/g_info_20100313185358.htm.

Proof of financial support

For paper supported by a foundation, authors should provide a copy of the document and serial number of the foundation.

Science news releases

Authors of accepted manuscripts are suggested to write a science news item to promote their articles. The news will be released rapidly at EurekAlert/AAAS (http://www.eurekalert.org). The title for news items should be less than 90 characters; the summary should be less than 75 words; and main body less than 500 words. Science news items should be lawful, ethical, and strictly based on your original content with an attractive title and interesting pictures.

Publication fee

Authors of accepted articles must pay a publication fee.
EDITORIAL, TOPIC HIGHLIGHTS, BOOK REVIEWS and LETTERS TO THE EDITOR are published free of charge.